

## Exploring Ultrasound-Assisted Cementation to Enhance the Recovery of Platinum Group Metals from Process Streams

**Auteur :** Nélissen, Lucie

**Promoteur(s) :** Gaydardzhiev, Stoyan

**Faculté :** Faculté des Sciences appliquées

**Diplôme :** Master en ingénieur civil des mines et géologue, à finalité spécialisée en ressources minérales et recyclage

**Année académique :** 2023-2024

**URI/URL :** <http://hdl.handle.net/2268.2/20858>

---

### Avertissement à l'attention des usagers :

*Tous les documents placés en accès ouvert sur le site le site MatheO sont protégés par le droit d'auteur. Conformément aux principes énoncés par la "Budapest Open Access Initiative"(BOAI, 2002), l'utilisateur du site peut lire, télécharger, copier, transmettre, imprimer, chercher ou faire un lien vers le texte intégral de ces documents, les disséquer pour les indexer, s'en servir de données pour un logiciel, ou s'en servir à toute autre fin légale (ou prévue par la réglementation relative au droit d'auteur). Toute utilisation du document à des fins commerciales est strictement interdite.*

*Par ailleurs, l'utilisateur s'engage à respecter les droits moraux de l'auteur, principalement le droit à l'intégrité de l'oeuvre et le droit de paternité et ce dans toute utilisation que l'utilisateur entreprend. Ainsi, à titre d'exemple, lorsqu'il reproduira un document par extrait ou dans son intégralité, l'utilisateur citera de manière complète les sources telles que mentionnées ci-dessus. Toute utilisation non explicitement autorisée ci-avant (telle que par exemple, la modification du document ou son résumé) nécessite l'autorisation préalable et expresse des auteurs ou de leurs ayants droit.*

---



---

# Exploring Ultrasound-Assisted Cementation to Enhance the Recovery of Platinum-Group Metals from Process Streams

---

Master thesis for the degree Civil Engineer in Mining and Geology, specialising in mineral resources and recycling by NÉLISSEN Lucie

University of Liège - Faculty of Applied Sciences

Academic promoter  
Prof. GAYDARDZHIEV Stoyan

Industrial promoter  
Dr. MOSCHOVI Anastasia-Maria

Comitee member  
Prof. LÉONARD Grégoire  
Ir. AÂTACH Mohamed

Academic year  
2023 - 2024



**MONOLITHOS**  
CATALYSTS - EXHAUSTS - RECYCLING

## Acknowledgements

I would first like to express my deep gratitude to my academic supervisor, Prof. Stoyan Gaydardzhiev, for conceiving this topic and for his support and guidance throughout this semester. I am also very thankful to my industrial supervisor, Dr. Anastasia-Maria Moschovi, and the entire team at Monolithos Catalysts & Recycling Ltd., who welcomed me in Athens, took the time to think through the scientific approach to this work, and provided the necessary materials to advance this project. I would like to warmly thank Engineer Mohamed Aâtach, without whom this work would have been impossible. Thank you for the long hours of discussion, for sharing your vast knowledge, and for your availability during this semester. I am grateful that you completed your secondment at the same time as my internship in Athens and for your invaluable advice.

I also want to thank Sabrina and Sébastien Blastuitig for their expert knowledge of the laboratory and for the hours spent analysing my samples. My thanks also go to Eirini Fotopoulou, who assisted me with my tests in Liège and Athens, and who also dedicated long hours to analysing my samples. I am deeply thankful to the entire GeMMe research group for welcoming me with open arms, for being available to discuss the questions I had regarding this work, and for making me feel at home in the GeMMe laboratory.

My heartfelt thanks go to my family for their unstoppable support and reassurance throughout this semester. Thank you for your trust and encouragement, which have always accompanied me. During moments of doubt, you found the right words to keep me moving forward. I am equally grateful to my close friends, who helped me clear my mind and patiently listened to countless discussions about this work. Special thanks to Guillaume for his unwavering support and belief in me, and for making me a better person every day.

This work has given me the opportunity to gain deeper self-awareness, explore new places, understand the true essence of being a researcher, and connect with remarkable and inspiring individuals. For all of this, I am sincerely grateful.

## Abstract

Catalytic converters, essential for reducing automotive emissions, rely on platinum group metals such as platinum, palladium, and rhodium. The increasing number of end-of-life catalytic converters presents a significant opportunity for PGM recovery, critical due to the scarcity and strategic importance of these metals. Traditional extraction methods are not sufficient to meet the growing demand so in densely populated areas, recycling offers a viable solution for securing PGM supply. This study investigates the removal of PGMs from concentrated process solutions in hydrochloric medium with the cementation of palladium, platinum, and rhodium onto copper. This work focuses on optimizing parameters such as temperature, agitation, Cu/PGM molar ratio, and the use of ultrasound to enhance efficiency.

Three solutions were examined: a synthetic solution to assess the feasibility of cementation, and two process solutions derived from catalytic converter leachates. The synthetic solution demonstrated complete platinum cementation at 65°C, 200 rpm, and a Cu/PGM molar ratio of 16. In the real-life solutions, optimal conditions varied, but a general trend was observed: high temperatures and agitation with a Cu/PGM molar ratio of 15 achieved high removal percentages. Ultrasound significantly improved the results, doubling efficiency in some cases and accelerating reaction kinetics. These findings contribute to developing more effective recycling methods for PGMs, supporting sustainable metal recovery practices.

# Table of Contents

Abstract.....	3
1 Introduction .....	14
2 Catalytic converters .....	14
2.1 Structure and composition.....	14
2.2 Nove catalytic converters design .....	16
2.3 Domains of activities.....	17
3 Cementation .....	18
4 Ultrasound in chemistry.....	20
4.1 Theoretical aspects .....	20
4.1.1 Cavitation and bubble dynamics .....	21
4.1.2 Radicals of H <sub>2</sub> O .....	22
4.1.3 Parameters affecting ultrasound.....	23
4.2 Type of transducers .....	26
5 Extracting PGMs nowadays.....	28
5.1 Primary resources .....	29
5.2 Secondary resources.....	29
5.3 Pre-treatments .....	30
5.4 Pyrometallurgy .....	30
5.4.1 Metal smelting.....	31
5.4.2 Chlorination .....	32
5.4.3 Active metals .....	33
5.4.4 Heating—quenching.....	33
5.5 Hydrometallurgy .....	34
5.5.1 Solvent extraction.....	35
5.5.2 Ion exchange.....	36
5.5.3 Ionic liquids.....	37
5.5.4 Cementation .....	38
5.5.5 Molecular recognition technology .....	39
5.5.6 Cloud point extraction.....	40
6 Experimental context.....	41

7	Materials and reagents .....	42
7.1	Composition of the initial solutions.....	43
8	Experimental Setup.....	44
8.1	Athens Setup.....	44
8.2	Liège Setup .....	44
8.3	Post-experiment filtration.....	45
9	Experimental procedure .....	45
10	Analysis of the experiments.....	47
10.1	Calculations and limitations .....	47
10.1.1	Cementation reactions in the different solutions .....	47
10.1.2	Impact of the pH and $E_h$ .....	48
10.1.3	Mass of the cement.....	48
10.1.4	Platinum or PGMs removal percentage .....	48
10.1.5	Precipitant factor.....	49
10.1.6	Limitations of the ICP .....	49
10.1.7	Filtration at the end of the experiments .....	49
10.2	Conditions for an interesting cement.....	50
10.3	Synthetic solution .....	50
10.3.1	Conditions of the experiment.....	50
10.3.2	Results .....	51
10.4	Pt-DOC solution at Monolithos Catalyst & Recycling Ltd. without sonication.....	52
10.4.1	Conditions of the experiments .....	52
10.4.2	Preliminary results of the solids from the XRF Olympus gun at Athens. ....	53
10.4.3	Results .....	55
10.4.4	Conclusion of the experiments done at Monolithos Catalysts & Recycling Ltd.....	61
10.5	Mixed PGM solution at GEMME laboratory .....	62
10.5.1	Conditions of the experiment.....	62
10.5.2	Presence of iron and aluminium in the GEMME solution .....	64
10.5.3	Results of the experiments without sonication .....	67
10.5.4	Results of the experiments with ultrasounds.....	80
10.5.5	Conclusion of the experiments with ultrasounds on the GEMME solution .....	94

11 Kinetic study of the cementation reactions .....	95
11.1 Theoretical background .....	96
11.1.1 Determination of the rate constant .....	97
11.1.2 Determination of the activation energy of a reaction.....	97
11.1.3 Diffusion coefficient.....	98
11.1.4 Chemically controlled or diffusion-controlled reactions.....	99
11.2 Results for the different experiments .....	99
12 Conclusion .....	101
13 References .....	104

## Table of figures

Figure 1: Contributions to EU Member States' emissions of NH <sub>3</sub> , NO <sub>2</sub> , NMVOCs, SO <sub>2</sub> , primary PM <sub>2.5</sub> , primary PM <sub>10</sub> , BC and CO from the main source sectors in 2021 (European Environment Agency, 2023). .....	15
Figure 2: Three-way catalyst: simultaneous conversion of CO, HC, and NO <sub>x</sub> (Sharma et al., 2015).....	15
Figure 3: Automobile catalytic converter (Kritsanaviparkporn et al., 2021). .....	15
Figure 4: Representation of the key concepts behind ultrasonic scale flow reactors: <b>(a)</b> the different phenomena associated with high and low frequency ultrasound, <b>(b)</b> the ultrasonic frequency (f) and the corresponding wavelength (λ) in water, <b>(c)</b> the cavitation bubble resonance size for low frequency ultrasound (20 kHz – 1MHz) (Dong et al., 2020). .....	21
Figure 5: Principal free radicals produced during ultrasonic irradiation of water and their reactions (Wood et al., 2017; Capote & De Castro, 2007).....	23
Figure 6: Representative examples of four categories of ultrasonic flow reactors. <b>(a)</b> Picture of a piezoelectric plate reactor developed by Dong et al., the reactor consists of a piezoelectric plate glued to the bottom of a silicon plate microreactor <b>(b)</b> Capillary microreactor immersed in an ultrasonic bath <b>(c)</b> Sketch of a Langevin-type transducer indirectly coupled reactor <b>(d)</b> Sketch of a Langevin-type transducer directly coupled reactor (Dong et al., 2020). .....	27
Figure 7: Diagram of the Langevin type transducer (Moreno et al., 2014). .....	28
Figure 8: Hydrometallurgical processing of PGMs (Panda et al., 2018).....	34
Figure 9: Schematic of solvent extraction for PGM recovery (Kinas et al., 2024). .....	35
Figure 10: Cloud point extraction of metal ions and formation of a micelle (Mortada, 2020). .....	42
Figure 1: Roadmap of the internship at Athens at Monolithos Catalyst & Recycling Ltd.....	42
Figure 2: Cumulative mineral mass percentage based on the SEM analysis of the copper powder used for the different experiments .....	43
Figure 3: Experimental setup at the laboratory of Monolithos Catalysts & Recycling Ltd. at Athens. ....	44
Figure 4: Experimental setup at the GEMME laboratory at Liège. ....	45



Figure 5: Experiment on the synthetic solution with 175ppm of Pt, HCl 37% and deionised water to reach a pH of 2. The cementation was done without sonication, at 65°C for 3 hours with a mechanic agitation of 200 rpm. The added copper represents 16 times the stoichiometric amount needed to recover all the PGM. ....	51
Figure 6: Results of the experiment carried out with a synthetic solution containing 175 ppm of Pt at 65°C, using an overhead stirrer set to 200 rpm for agitation. The experiment utilized 16 times the stoichiometric amount of Cu compared to the Pt concentration. The graph illustrates the percentage of platinum removed from the solution over time. ....	52
Figure 7: Pt - DOC solution at 85°C without sonication at 500 rpm with 53 Cu/PGM (mol/mol). The two experiments show a difference in the agitation of the solid. The solid is in movement in the first experiment then it is barely agitated in the second experiment. ....	53
Figure 8: XRF results from the 85°C experiment during 30 minutes of cementation with 53 times the copper stoichiometric amount needed to recover PGM with an agitation of 500rpm. ....	54
Figure 9: XRF results from the 85°C experiment during 2 hours of cementation with 1.6 times the copper stoichiometric amount needed to recover PGM with an agitation of 500rpm. The influence of the container can be seen on the right of the spectrum. ..	55
Figure 10: Results of the experiment conducted on the Pt-DOC solution from Monolithos Catalysts & Recycling Ltd. at 85°C, without sonication, using a magnetic stirrer set to 500 rpm, with 53 times the stoichiometric amount of copper to recover the PGMs. The red-highlighted point indicates a comparable experiment under identical conditions, but with a higher initial platinum concentration (900 ppm instead of 400 ppm). The results represent the platinum removal percentage and the precipitant factor. In the experiments lasting 124 and 134 minutes, the solid was barely agitated compared to the solution, which remained in motion. ....	56
Figure 11: Results of the experiment conducted on the Pt-DOC solution from Monolithos Catalysts & Recycling Ltd. at 65°C, without sonication, at 500 rpm using a magnetic stirrer with the solid barely agitated compared to the solution, with 25 times the stoichiometric amount of copper to recover the PGMs. The results represent the platinum removal percentage and the precipitant factor. ....	57
Figure 12: Results of the experiment conducted on the Pt-DOC solution from Monolithos Catalysts & Recycling Ltd. at 45°C, without sonication, at 500 rpm using a magnetic stirrer with the solid barely agitated compared to the solution, with 16 times the stoichiometric amount of copper to recover the PGMs. The results represent the platinum removal percentage and the precipitant factor. ....	58

Figure 13: Results of the experiment conducted on the Pt-DOC solution from Monolithos Catalysts & Recycling Ltd. at 25°C, without sonication, at 500 rpm using a magnetic stirrer with the solid barely agitated compared to the solution, with 16 times the stoichiometric amount of copper to recover the PGMs. The results represent the platinum removal percentage and the precipitant factor. ....	59
Figure 14: Summary of the experiments done with the same mass of copper powder added to the system at 500 rpm with a magnetic stirrer. ....	60
Figure 15: Results of the experiment on the Pt-DOC solution without sonication at 85°C, 500 rpm with a magnetic stirrer but 1.6 times the stoichiometric amount of copper needed expressed with the platinum removal percentage and the precipitant factor. ....	61
Figure 16: Results of the experiments on the Pt-DOC solution in Athens without sonication at 85°C, with 1.6 times the stoichiometric amount of copper needed to cement the PGMs of the solution. The agitation was step up at 500 rpm and at 0 rpm.....	61
Figure 17: GEMME solution at 65°C without sonication at 400 rpm with 13 Cu/PGM (mol/mol) with the setup of Liège. The Figure shows the initial solution heated, the solution after 2 hours of experiment and the solid after filtration and drying. ....	63
Figure 18: GEMME solution at 65°C with ultrasounds at 20kHz, 10W, at 400 rpm with 13 Cu/PGM (mol/mol) with the setup of Liège. The figure shows the initial solution heated, the solution after 2 hours of experiment and the solid after filtration and drying.....	64
Figure 19: Simplified Pourbaix diagram for the Fe-H <sub>2</sub> O system at 25°C, 1 atm and (Fioravante et al., 2019).....	65
Figure 20: Simplified Pourbaix diagram for the Fe – Cl – H <sub>2</sub> O system at 85°C, 1 atm and a molality of Fe of 10 <sup>-6</sup> . ....	66
Figure 21: Pourbaix diagram for aluminium at 25°C (McCafferty, 2009). ....	67
Figure 22: Palladium removal over time from the GEMME solution under silent conditions at 85°C with a 200 rpm agitation speed and a Cu/PGM molar ratio of 13. The graph compares palladium removal efficiency without the adjustment of the pH and with an adjustment at 1.4 and 1.7. ....	68
Figure 23: Platinum removal over time from the GEMME solution under silent conditions at 85°C with a 200 rpm agitation speed and a Cu/PGM molar ratio of 13. The graph compares platinum removal efficiency without the adjustment of the pH and with an adjustment a ....	69
Figure 24: Rhodium removal over time from the GEMME solution under silent conditions at 85°C with a 200 rpm agitation speed and a Cu/PGM molar ratio of 13. The graph	

compares rhodium removal efficiency without the adjustment of the pH and with an adjustment a .....	69
Figure 25: Palladium removal over time from the GEMME solution under silent conditions at 200 rpm and a Cu/PGM molar ratio of 13. The graph compares palladium removal efficiency at four different temperatures: 25°C, 45°C, 65°C, and 85°C. ....	70
Figure 26: Platinum removal over time from the GEMME solution under silent conditions at 200 rpm and a Cu/PGM molar ratio of 13. The graph compares platinum removal efficiency at four different temperatures: 25°C, 45°C, 65°C, and 85°C. ....	71
Figure 27: Rhodium removal over time from the GEMME solution under silent conditions at 200 rpm and a Cu/PGM molar ratio of 13. The graph compares rhodium removal efficiency at four different temperatures: 25°C, 45°C, 65°C, and 85°C. ....	71
Figure 28: GEMME solution at 85°C without sonication at 200 rpm with a Cu/PGM molar ratio of 13, using the Liège setup. The figure depicts the initial heated solution, the solution after 1 hour of experimentation, the reactor post-filtration, and the solid after filtration and drying. A fine yellowish solid layer is visible in the last two images, indicating challenges in the filtration process. ....	72
Figure 29: Best temperature to achieve high PGMs removal percentage over time from the GEMME solution under silent conditions at 200 rpm and a Cu/PGM molar ratio of 13. ....	73
Figure 30: Palladium removal over time from the GEMME solution under silent conditions at 65°C and a Cu/PGM molar ratio of 13. The graph compares palladium removal efficiency at three different agitations by an overhead stirrer: 0 rpm, 200 rpm and 400 rpm. ....	75
Figure 31: Platinum removal over time from the GEMME solution under silent conditions at 65°C and a Cu/PGM molar ratio of 13. The graph compares platinum removal efficiency at three different agitations by an overhead stirrer: 0 rpm, 200 rpm and 400 rpm. ....	75
Figure 32: Rhodium removal over time from the GEMME solution under silent conditions at 65°C and a Cu/PGM molar ratio of 13. The graph compares rhodium removal efficiency at three different agitations by an overhead stirrer: 0 rpm, 200 rpm and 400 rpm. ....	76
Figure 33: Best agitation with an overhead stirrer to achieve high PGMs removal percentage over time from the GEMME solution under silent conditions at 65°C and a Cu/PGM molar ratio of 13.....	77
Figure 34: Palladium removal over time from the GEMME solution under silent conditions at 65°C and with an overhead stirrer at 400 rpm. The graph compares palladium	

removal efficiency with three different Cu/PGM molar ratios: 5 times, 9 times and 13 times. ....	78
Figure 35: Platinum removal over time from the GEMME solution under silent conditions at 65°C and with an overhead stirrer at 400 rpm. The graph compares platinum removal efficiency with three different Cu/PGM molar ratios: 5 times, 9 times and 13 times. 79	
Figure 36: Rhodium removal over time from the GEMME solution under silent conditions at 65°C and with an overhead stirrer at 400 rpm. The graph compares rhodium removal efficiency with three different Cu/PGM molar ratios: 5 times, 9 times and 13 times. 79	
Figure 37: Image of the residues obtained after filtering the samples through an 8 µm mesh size filter. These samples were associated with an experiment conducted at 65°C with stirring at 400 rpm, using a Cu/PGM molar ratio of 13, and subjected to ultrasound at 20 kHz and 4 W. The sample on the left was taken after 5 minutes and the second sample on the right was taken after 30 minutes. ....	81
Figure 38: Palladium removal over time from the GEMME solution heated at 65°C at 400 rpm and a Cu/PGM molar ratio of 13. The graph compares palladium removal efficiency under silent conditions and with ultrasound at two different frequencies: 20 kHz and 40 kHz with a power consumed by the system of 10 W. ....	82
Figure 39: Platinum removal over time from the GEMME solution heated at 65°C at 400 rpm and a Cu/PGM molar ratio of 13. The graph compares platinum removal efficiency under silent conditions and with ultrasound at two different frequencies: 20 kHz and 40 kHz with a power consumed by the system of 10 W. ....	83
Figure 40: Rhodium removal over time from the GEMME solution heated at 65°C at 400 rpm and a Cu/PGM molar ratio of 13. The graph compares rhodium removal efficiency under silent conditions and with ultrasound at two different frequencies: 20 kHz and 40 kHz with a power consumed by the system of 10 W. ....	83
Figure 41: Best frequency of ultrasounds transmitted to the system to achieve high PGMs removal percentage over time from the GEMME solution at 65°C, with an agitation of 400 rpm, a Cu/PGM molar ratio of 13 and a power consumed by the system of 10 W. ....	84
Figure 42: Palladium removal over time from the GEMME solution heated at 65°C at 400 rpm and a Cu/PGM molar ratio of 13. The graph compares palladium removal efficiency under silent conditions and with ultrasound at 20 kHz with two different powers consumed by the system: 4 W and 10 W. ....	85
Figure 43: Platinum removal over time from the GEMME solution heated at 65°C at 400 rpm and a Cu/PGM molar ratio of 13. The graph compares platinum removal efficiency under silent conditions and with ultrasound at 20 kHz with two different powers consumed by the system: 4W and 10 W. ....	86

Figure 44: Rhodium removal over time from the GEMME solution heated at 65°C at 400 rpm and a Cu/PGM molar ratio of 13. The graph compares rhodium removal efficiency under silent conditions and with ultrasound at 20 kHz with two different powers consumed by the system: 4 W and 10 W.....	86
Figure 45: Palladium removal over time from the GEMME at an agitation of 400 rpm and a Cu/PGM molar ratio of 13. The graph compares palladium removal efficiency under silent conditions and with ultrasound at 20 kHz with a power consumed of 10 W at four different temperatures: 25°C, 45°C, 65°C and 85°C. ....	87
Figure 46: Platinum removal over time from the GEMME at an agitation of 400 rpm and a Cu/PGM molar ratio of 13. The graph compares platinum removal efficiency under silent conditions and with ultrasound at 20 kHz with a power consumed of 10 W at four different temperatures: 25°C, 45°C, 65°C and 85°C. ....	88
Figure 47: Rhodium removal over time from the GEMME at an agitation of 400 rpm and a Cu/PGM molar ratio of 13. The graph compares rhodium removal efficiency under silent conditions and with ultrasound at 20 kHz with a power consumed of 10 W at four different temperatures: 25°C, 45°C, 65°C and 85°C. ....	89
Figure 48: Best temperature to achieve high PGMs removal percentage over time from the GEMME solution at 65°C, at 400 rpm, a Cu/PGM molar ratio of 13 with ultrasound set at 20 kHz and a power consumed by the system of 10 W.....	90
Figure 49: Palladium removal over time from the GEMME at 65°C and a Cu/PGM molar ratio of 13. The graph compares palladium removal efficiency under silent conditions and with ultrasound at 20 kHz with a power consumed of 10 W at three different agitations: 0 rpm, 200 rpm and 400 rpm. ....	91
Figure 50: Platinum removal over time from the GEMME at 65°C and a Cu/PGM molar ratio of 13. The graph compares platinum removal efficiency under silent conditions and with ultrasound at 20 kHz with a power consumed of 10 W at three different agitations: 0 rpm, 200 rpm and 400 rpm. ....	91
Figure 51: Rhodium removal over time from the GEMME at 65°C and a Cu/PGM molar ratio of 13. The graph compares rhodium removal efficiency under silent conditions and with ultrasound at 20 kHz with a power consumed of 10 W at three different agitations: 0 rpm, 200 rpm and 400 rpm. ....	92
Figure 52: Palladium removal over time from the GEMME at 65°C and 400 rpm. The graph compares rhodium removal efficiency under silent conditions and with ultrasound at 20 kHz with a power consumed of 10 W at three different Cu/PGM molar ratio: 5 times, 9 times and 13 times. ....	93
Figure 53: Platinum removal over time from the GEMME at 65°C and 400 rpm. The graph compares platinum removal efficiency under silent conditions and with ultrasound at	

20 kHz with a power consumed of 10 W at three different Cu/PGM molar ratio: 5 times, 9 times and 13 times. .... 93

Figure 54: Rhodium removal over time from the GEMME at 65°C and 400 rpm. The graph compares rhodium removal efficiency under silent conditions and with ultrasound at 20 kHz with a power consumed of 10 W at three different Cu/PGM molar ratio: 5 times, 9 times and 13 times. .... 94

# 1 Introduction

In today's world, catalytic converters are essential components of automotive exhaust systems, designed to reduce harmful emissions and protect air quality. These devices play a critical role in mitigating environmental pollution by converting toxic gases into less harmful substances. The catalytic converters commonly utilize platinum group metals such as platinum, palladium, and rhodium, which are highly effective but also rare and expensive.

The number of end-of-life catalytic converters are increasing. This presents both a challenge and an opportunity for metal recovery. The extraction of PGMs from these spent converters is important not only for resource conservation but also for securing the supply of these critical metals, which are listed as critical raw materials in Europe due to their scarcity and strategic importance. However, the conventional extraction methods used in mining are not sufficient to meet the growing demand, nor are they applicable in all contexts, particularly in densely populated regions where recycling could be a more viable solution.

While the extraction of PGMs from catalytic converters into a solution, such as through leaching, is well-documented in the literature, the challenge today lies in effectively removing these PGMs from the concentrated solution and recovering them in their metallic form. Although various methods have been developed, including solvent extraction, ion exchange, ionic liquids, and molecular recognition technologies, the efficient removal of PGMs from these solutions still faces significant hurdles.

One promising approach under investigation to remove the PGMs from a concentrated solution is cementation, a process where PGMs are selectively deposited onto a sacrificial metal. Different sacrificial metals are studied such as zinc and aluminium but the cementation onto copper is less developed in the literature. This gap presents an opportunity to enhance our understanding and optimize the process. This study aims to address this need by exploring the optimal parameters for cementing PGMs onto copper from real-life solutions. By focusing on achieving high removal percentages, this work seeks to contribute to the development of more effective recycling methods for PGMs. Additionally, the study will investigate the application of ultrasound technology to determine if it can significantly impact the efficiency of the cementation process, potentially offering a novel enhancement to existing methods.

By advancing the field of PGM recovery from end-of-life catalytic converters, this research will help to secure the supply of these critical metals and support sustainable practices in metal recycling and resource management.

## 2 Catalytic converters

### 2.1 Structure and composition

Catalytic converters are an important component in reducing vehicle emissions, relying heavily on Platinum Group Metals. In 2010, autocatalysts accounted for 51% of the total world demand for PGMs (IPA - International Platinum Group Metals Association, n.d.). Catalysts must reduce emissions without significantly affecting performance and fuel economy, particularly for hydrocarbons (HC), carbon monoxide (CO), and nitrogen oxides (NO<sub>x</sub>). NO<sub>x</sub> emissions depend on catalysts for compliance.

There are two main types of catalytic converters: two-way and three-way converters. Two-way catalytic converters are oxidation catalysts that oxidize CO and HC into carbon dioxide (CO<sub>2</sub>) and water but do not reduce NO<sub>x</sub>. Diesel engines typically use these converters due to their effectiveness

with cooler exhausts (Dey & Mehta, 2020). Three-way catalytic converters perform both oxidation and reduction, simultaneously reducing concentrations of CO, NO<sub>x</sub>, and HC. These converters are used with spark-ignition gasoline engines and can reduce pollutant emissions by up to 96% compared to engine-out emission levels (Votsmeier et al., 2019). The effectiveness of these converters hinges on precise control of the air-to-fuel ratio within a narrow window around the stoichiometric ratio of approximately 14.6 (wt basis) as it is shown on the Figure 2 (Farrauto & Heck, 1999).

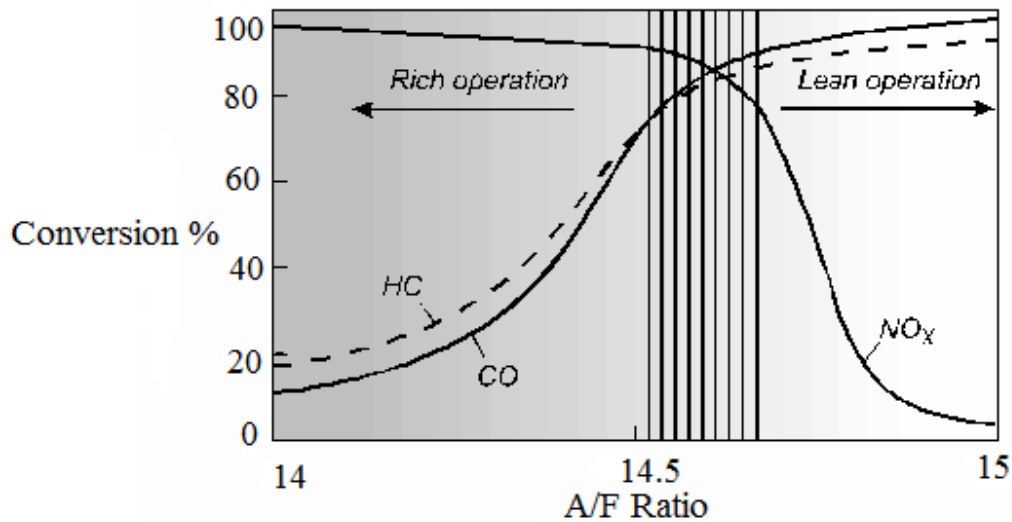


Figure 1: Three-way catalyst: simultaneous conversion of CO, HC, and NO<sub>x</sub> (Sharma et al., 2015).

The honeycomb ceramic structure, known as a monolith, is a common catalyst support. This structure provides a large surface area, enabling efficient redox reactions and facilitating gas flow while controlling pressure drops. Cordierite (2MgO-2Al<sub>2</sub>O<sub>3</sub>-5SiO<sub>2</sub>) is the most used monolith material due to its high surface area, high melting point, mechanical strength, and low thermal expansion coefficient, offering excellent thermal shock resistance. The cordierite is coated with a washcoat solution containing noble metal nitrates such as palladium nitrate, rhodium nitrate, and platinum nitrate. This washcoat, typically made of alumina (γ-Al<sub>2</sub>O<sub>3</sub>), enhances the catalyst's surface area by about 10 000 times. The washcoat also contains catalyst materials, cerium oxide, and stabilizers like barium oxide and rare earth elements. Cerium oxide improves the thermal stability of alumina and can store or release oxygen, enhancing the catalyst's effectiveness. A schema of a catalytic converter is represented on the Figure 3 (Votsmeier et al., 2019; Dey & Mehta, 2020; Kritsanaviparkporn et al., 2021).

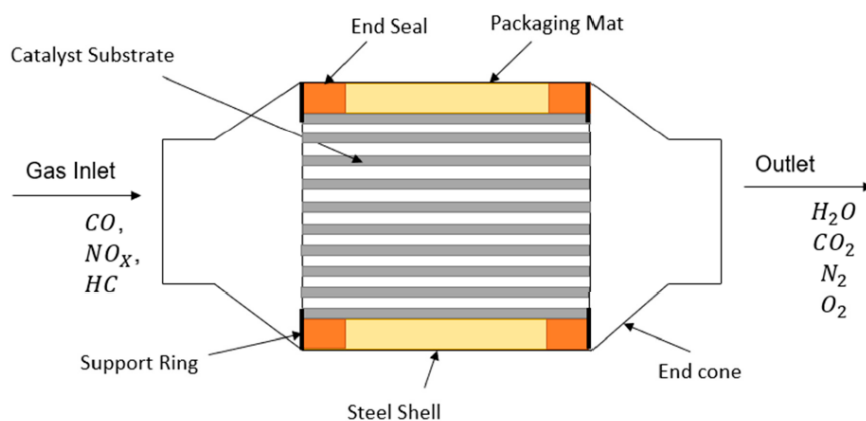


Figure 2: Automobile catalytic converter (Kritsanaviparkporn et al., 2021).



Platinum and palladium are highly effective in oxidizing CO and HC and converting NO to NO<sub>2</sub>, while rhodium reduces NO<sub>x</sub> by lowering the activation barrier for NO<sub>x</sub> reduction by CO. Due to its rarity, rhodium is usually alloyed with platinum or palladium, with typical Pt/Rh and Pd/Rh ratios of 5:1 and 7:1, respectively (Votsmeier et al., 2019; Kritsanaviparkporn et al., 2021). The optimal operating temperature for catalytic converters is between 400°C and 800°C, making the cold-start phase the most polluting, with emissions reaching up to 8 000 ppm for CO and 28 000 ppm for unburned HC (Gao et al., 2019).

The advancement of three-way catalyst technology relies on the development of the O<sub>2</sub> or lambda sensor, which controls the air-to-fuel ratio within a narrow window. This sensor, made of stabilized zirconia with high surface area platinum electrodes, detects oxygen content and adjusts the fuel mixture accordingly. The sensor ensures the catalyst experiences alternating rich and lean conditions, requiring the O<sub>2</sub> storage component to manage unreacted CO and HC. Cerium oxide, often combined with zirconia to form solid solutions, is the most effective OSC due to its ability to adsorb and release oxygen during air-to-fuel perturbations (Farrauto & Heck, 1999).

In an investigation by the Korea Institute of Geoscience and Mineral Resources (KIGAM), over 200 samples of spent auto-catalysts were analysed. Active materials were found to contain ~900 mg/kg Pt, ~1600 mg/kg Pd, and ~120 mg/kg Rh, with Pd showing higher and more variable concentrations. Catalytic converters have a typical lifespan ranging from 70 000 to 100 000 miles, which translates to approximately 10 years under normal driving conditions. Over time, the catalyst materials within the converter can become coated or clogged with contaminants, reducing their effectiveness. Additionally, mechanical damage or thermal shock can also shorten the lifespan of a catalytic converter. Regular maintenance and avoiding prolonged exposure to high temperatures can help in extending its operational life (Trinh et al., 2020).

## 2.2 Novel catalytic converters design

Base metal catalysts, including cobalt, nickel, chromium, iron, manganese, and copper, also play essential roles in catalytic processes. Metal oxides such as Co<sub>3</sub>O<sub>4</sub>, CuO, and MnO<sub>2</sub> exhibit high catalytic activity for CO oxidation. Supported base metal catalysts, especially those involving Cu oxide, are effective for CO and volatile organic compounds (VOCs) oxidation due to their favourable pore structures and surface properties (Dey & Mehta, 2020). Zinc oxide (ZnO) and chromium oxide (Cr<sub>2</sub>O<sub>3</sub>) are well-established for CO oxidation, offering low cost and good thermal activity.

Modifications to these catalysts, such as reducing crystallite size, enhance their specific surface area and catalytic performance, though their effectiveness diminishes at temperatures around 1100°C, necessitating the development of new materials for extreme thermal conditions (Patel et al., 2022).

Perovskite metal oxides, with the general structure ABO<sub>3</sub> where A is a rare earth element and B is a transition metal, are alternative catalysts for automotive exhaust control. These oxides, such as SrCoO<sub>3</sub>, show potential for CO oxidation at ambient conditions and offer a low-cost alternative to noble metals (Dey & Mehta, 2020; Patel et al., 2022). Spinel oxides, formulated as A<sup>2+</sup>B<sub>2</sub><sup>3+</sup>O<sub>4</sub><sup>2+</sup>, crystallize in a cubic system with oxide anions in a close-packed lattice. These include aluminium spinels (e.g., MgAl<sub>2</sub>O<sub>4</sub>), iron spinels (e.g., CuFe<sub>2</sub>O<sub>4</sub>), and chromium spinels (e.g., FeCr<sub>2</sub>O<sub>4</sub>), used in various catalytic applications (Dey & Mehta, 2020). Monel catalysts, composed of about 66.5% nickel, 31.5% copper, and 2% impurities, are used to control emissions of CO, HC, and NO<sub>x</sub>. Despite their lower cost, Monel catalysts have shorter lifespans and lower durability (Dey & Mehta, 2020).

Hopcalite, a mixture of oxides such as CuMnO<sub>x</sub>, is highly effective for CO oxidation at room temperature. Variants include MnO<sub>2</sub> and Ag<sub>2</sub>O mixtures and combinations with CuO, Co<sub>2</sub>O<sub>3</sub>, and Ag<sub>2</sub>O. The addition of elements like gold, silver, cerium, cobalt, iron, and nickel enhances catalytic

performance. CuMnO<sub>x</sub> catalysts prepared by sol–gel methods show better activity than commercial hopcalite, making them well-suited for low-temperature CO oxidation (Dey & Mehta, 2020; Patel et al., 2022).

Monolithos Catalysts & Recycling Limited has launched the Prometheus catalyst, a newly commercialized catalytic converter that marks a significant innovation in automotive emissions control. This catalyst replaces a substantial portion of the platinum group metals, traditionally used in catalytic converters, with copper. The use of copper is particularly notable due to its excellent catalytic properties, such as its ability to facilitate oxidation-reduction reactions crucial for the conversion of harmful exhaust gases into less toxic substances. Copper's abundance and lower cost compared to PGMs make it an attractive alternative, and in the Prometheus catalyst, it achieves up to an 85% reduction in PGM usage while maintaining or even enhancing catalytic performance. This advancement not only reduces the reliance on expensive and scarce PGMs but also represents a more sustainable and cost-effective solution for automotive emissions control (Yakoumis, 2021).

### 2.3 Domains of activities

Catalytic converters play an important role in reducing harmful emissions across a wide range of applications beyond just passenger cars. Their utility extends into industrial processes, marine environments, power generation, and off-road vehicles, each presenting unique challenges and benefits.

In the automotive sector, catalytic converters are essential for reducing emissions of pollutants such as carbon monoxide, hydrocarbons, and nitrogen oxides. These devices are mandated by environmental regulations in many countries to ensure vehicles meet stringent emission standards. Modern vehicles typically use three-way catalytic converters that simultaneously reduce NO<sub>x</sub>, CO, and HC by converting them into nitrogen, carbon dioxide, and water. The widespread adoption of catalytic converters in vehicles has significantly reduced urban air pollution and improved public health.

Industrial applications of catalytic converters are crucial in controlling emissions from chemical plants, refineries, and manufacturing facilities. Industries often emit volatile organic compounds, NO<sub>x</sub>, and other pollutants that can be mitigated using catalytic converters. In chemical plants, these devices are employed to reduce NO<sub>x</sub> emissions during the production of nitric acid. Refineries use catalytic converters to control emissions from various processes, including cracking and reforming. In manufacturing facilities, catalytic converters are used to reduce emissions from furnaces and boilers, helping to meet regulatory standards and reduce the environmental impact of industrial activities.

Marine environments benefit significantly from the use of catalytic converters, particularly in reducing emissions from ships and other marine vessels. Marine engines, which often run on heavy fuels, emit substantial amounts of NO<sub>x</sub>, sulphur oxides, and particulate matter. Catalytic converters help mitigate these emissions, reducing the environmental impact of marine transportation. The International Maritime Organization has established regulations requiring the use of emission control technologies, including catalytic converters, to meet environmental standards. This regulatory push is essential in minimizing the ecological footprint of the shipping industry and protecting marine ecosystems.

In power generation, catalytic converters are used in various types of power plants, including those powered by natural gas, diesel, and biomass. These converters reduce emissions of NO<sub>x</sub>, CO, and VOCs from combustion processes, helping power plants comply with environmental regulations. In natural gas-fired power plants, selective catalytic reduction systems are commonly used to reduce

NOx emissions. Diesel-powered generators also utilize catalytic converters to reduce emissions, making them more environmentally friendly. Biomass power plants, which burn organic materials to generate electricity, use catalytic converters to control emissions of CO and VOCs, ensuring cleaner energy production.

Off-road vehicles, including construction equipment, agricultural machinery, and recreational vehicles, also rely on catalytic converters to reduce their environmental impact. These vehicles often operate in environments where emissions can have a direct impact on local air quality. Catalytic converters in off-road vehicles help reduce emissions of CO, HC, and NOx, contributing to cleaner air and compliance with emission standards set for non-road mobile machinery. This is particularly important in sectors like agriculture and construction, where equipment operates near workers and residential areas, necessitating stringent control of emissions to protect human health and the environment.

Overall, catalytic converters are versatile devices used across different domains to reduce harmful emissions and comply with environmental regulations. Their effectiveness in converting toxic gases into less harmful substances makes them indispensable in efforts to mitigate air pollution and protect environmental and public health.

### 3 Cementation

Cementation is a spontaneous electrochemical process that involves reducing a noble or toxic metal ion ( $M^{m+}$ ) using a more electropositive sacrificial metal (S). This process can be represented by the general heterogeneous reaction:



Cementation is one of the oldest known hydrometallurgical processes. Historically, it was observed in copper mines that iron tools in contact with aqueous mine waters slowly transformed into copper tools. Alchemists saw this as evidence of metal transmutation. Today, cementation is a widely used, efficient, and economical method in industry for electroplating, electrowinning, and waste treatment to remove metal ions from dilute solutions for purification or metal recovery (Casado, 2018; Konsowa, 2010; Sędzimir, 2002; Alemany et al., 2002; Power & Ritchie, 1976).

Cementation reactions are characterized by a significant negative free enthalpy and high equilibrium constants ( $K_{\text{thermo}} > 10^{10}$ ) (Alemany et al., 2002). These reactions are often controlled by diffusion, though chemical reactions or mixed control mechanisms can also be significant (Aâtach et al., 2024; Casado, 2018; Khudenko, 1984; Power & Ritchie, 1976). Diffusion-controlled reactions exhibit mass transport limitations, while the reaction morphology, such as roughness, can enhance mass transport (Casado, 2018).

Power & Ritchie (1976) demonstrated that cementation reactions tend to be chemically controlled if the standard reduction potential  $\Delta E < 0.06$  V and diffusion-controlled if  $\Delta E > 0.36$  V. When  $\Delta E$  falls between these limits, control depends on exchange currents. Practically, a difference in standard reduction potentials greater than 0.36 V usually indicates diffusion control (Power & Ritchie, 1976). The analysis of the energy of activation further supports this assessment by offering a detailed understanding of the underlying mechanisms. The activation energy of a reaction provides insights into whether the reaction is controlled by chemical kinetics, diffusion, or a combination of both. Reactions with low activation energies, typically between 4 and 15 kJ/mol, are generally diffusion-controlled, reflecting limited sensitivity to temperature changes (Zhu et al., 2012; Havlík, 2008; Levenspiel, 1998). In contrast, reactions with high activation energies, usually exceeding 40 kJ/mol,

are chemically controlled and highly sensitive to temperature variations. Reactions governed by a mixed mechanism, with activation energies between 20 and 35 kJ/mol, exhibit characteristics of both diffusion and chemical kinetics (Zhu et al., 2012; Havlík, 2008; Habashi, 1986). Understanding these energy thresholds is important for predicting the impact of various parameters on the system, thereby optimizing reaction conditions for improved efficiency and control.

The presence of hydrogen significantly affects cementation reactions. Gould et al. (1982) and Khudenko (1985) showed that  $H^+$  and intermediate hydride ions ( $H^-$ ) play crucial roles in cementation. Hydride ions, being strong reducing agents, can interact with protons to form  $H_2$ . Casado (2018) emphasized the importance of hydrogen species in acidic media, where the reduction of  $H^+$  to  $H_2$  is a key step. The efficiency of cementation depends on pH, with higher pH leading to reduced efficiency due to hydroxide precipitation, and lower pH causing acid corrosion (Casado, 2018).

Cementation rates and metal recovery are influenced by various parameters, including solution agitation, the specific surface area of the precipitant metal, its roughness, pH, cell potential, and temperature. Agitation generally enhances the rate but can also lead to the dissolution of the recovered metal if prolonged. Larger specific surfaces improve cementation rates (Aâtach et al., 2024; Stefanowicz et al., 1997). The pH of the solution is critical; higher pH levels can reduce efficiency due to the formation of metal hydroxides, while lower pH levels can lead to excessive acid corrosion (Gould, 1982; Sędzimir, 1991, 2002; Luna-Sanchez et al., 2003; Wu et al., 2016). Additionally, the cell potential significantly affects the reaction kinetics and overall efficiency, with optimal cell potentials enhancing the mass transfer and reaction rates. Temperature also plays an important role, as higher temperatures typically increase the reaction rate by providing the necessary activation energy (Reis & Carvalho, 1994).

In some media, agitation may not be crucial, indicating chemically controlled reactions (Alemany et al., 2002). Safarzadeh et al. (2007) identified stoichiometric quantity, size distribution of the less noble metal, cementation time, and temperature as critical parameters in sulfuric media. The concentration of the initial solution also impacts reaction probability (Konsowa, 2010).

While cementing on the precipitant metal, an inhibition or passivation layer could occur through formation of a compact and adherent deposit, acting as a barrier layer, or a tight and impervious oxide film on the precipitant metal stopping the cementation. Powdery non-coherent deposits may enhance the rate of cementation while smooth coherent deposits may inhibit the rate of cementation. The sacrificial metal used in the cementation process can also be found in the final cemented product. This occurs because some of the sacrificial metal dissolves during the reaction and may precipitate out along with the noble metal, leading to impurities in the final product (Konsowa, 2010; Aâtach et al., 2024). If different metals are present in the solution, it is possible to have co-cementation forming a cement with different impurities: the precipitant metal, the other co-cemented metals, and other elements if the conditions in the media lead to their precipitation (Stefanowicz et al., 1997).

Electrochemical studies, particularly Evans' diagrams, have been employed in hydrometallurgy to simulate and explain the redox phenomena that take place at mineral and metal surfaces during operations such as leaching and cementation. However, despite their utility, in some cases, the combination of the cathodic and anodic branches, determined separately, does not reproduce the chemical environment present when both processes occur simultaneously on a specific surface. In the electrochemical studies developed to date, Evans' diagrams have been constructed with voltamperometric data from metal oxidation, on one hand, and oxygen reduction, on the other,

using rotating disks. However, the validity of this technique is questionable considering that the mineral phases of interest are rarely found in metallic form. The use of Evans' diagrams to represent cementation reactions should be avoided or done with a focus on these elements (Casado, 2018; Luna-Sanchez et al., 2003; Sędzimir, 2002).

## 4 Ultrasound in chemistry

Ultrasound, defined as frequencies above 20 kHz extending into the GHz range (Capote & De Castro, 2007), has a multitude of applications across various fields. These include structural testing of materials, underwater ranging and transmissions, imaging and acoustic microscopy, medical treatments, materials processing, cleaning, wireless communications, oxidation processes, material synthesis, extraction, disinfection, and particle aggregation (Wood et al., 2017; Lim et al., 2014). When applied to liquids, ultrasound can break chemical bonds by forming free radicals through nucleation, cavitation, bubble dynamics, and various thermodynamic and chemical interactions. These processes enhance chemical reactions, making ultrasound valuable in wastewater treatment for degrading organic pollutants and destroying pharmaceutical waste. It also aids in synthesizing nanomaterials and biomaterials and has potential applications in producing fuels like ethane, ethylene, and acetylene (Wood et al., 2017).

However, achieving efficient ultrasound processes is challenging. Inefficient energy transfer due to impedance, along with secondary effects such as streaming, sound field attenuation, heating, bulk mixing, emitter erosion, and sound emission, can reduce its effectiveness (Wood et al., 2017).

### 4.1 Theoretical aspects

Being a sound wave, ultrasound is transmitted through any substance, solid, liquid or gas possessing elastic properties. The movement of a vibrating body (the sound source) is communicated to the molecules of the medium, each of which transmits the motion to an adjoining molecule before returning to approximately its original position. In liquids and gases, particle oscillation takes place in the direction of the wave and produces longitudinal waves. Because they additionally possess shear elasticity, solids can also withstand tangential stress and produce transverse waves, where particles move normal to the direction of the wave. Compression cycles push molecules together, whereas expansion cycles pull them apart (Capote & De Castro, 2007).

Ultrasound can be defined based on its frequency. It is classified into low and high frequency ultrasound due to the different physical mechanisms that can be induced. The boundary between low and high frequency ultrasound is not necessarily strict and the transition range is typically recognized within 20 kHz and 1 MHz, as shown in Figure 4. Low frequency ultrasound generates cavitation micro-bubbles, which can intensify mixing, mass transfer, break up agglomerates and detach particles deposited on microchannel surfaces to prevent clogging. High frequency ultrasound, on the other hand, is operated at power levels below the cavitation threshold, therefore cavitation effects are normally not observed (Dong et al., 2020; Capote & De Castro, 2007).

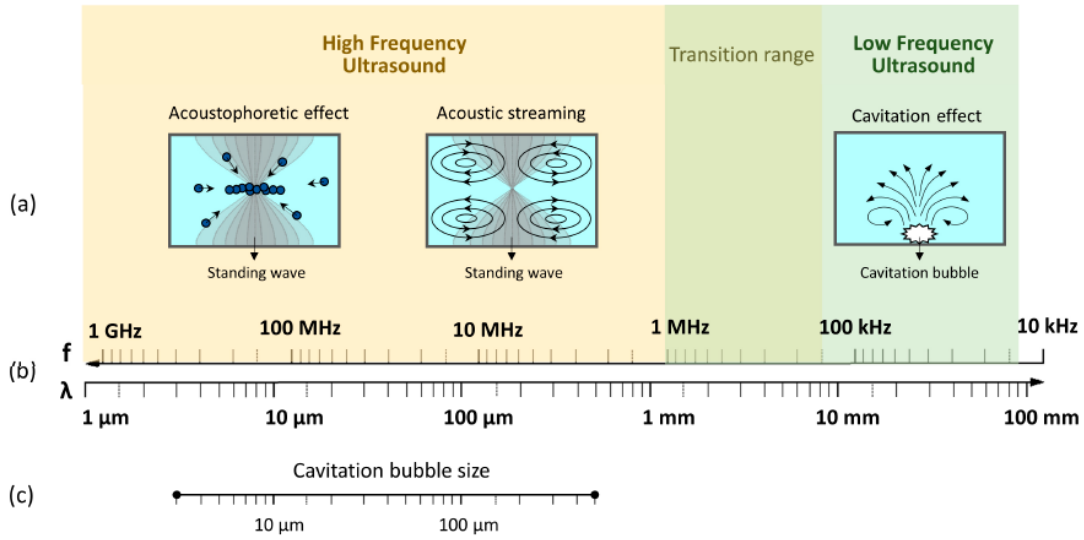


Figure 3: Representation of the key concepts behind ultrasonic scale flow reactors: (a) the different phenomena associated with high and low frequency ultrasound, (b) the ultrasonic frequency ( $f$ ) and the corresponding wavelength ( $\lambda$ ) in water, (c) the cavitation bubble resonance size for low frequency ultrasound (20 kHz – 1 MHz) (Dong et al., 2020).

#### 4.1.1 Cavitation and bubble dynamics

Cavities are formed via nucleation, originating from pre-existing bubbles in the solution called nuclei, which are stabilized against dissolution due to their surface properties. Nucleation sites can be found throughout the solution or at crevices on solid impurities or surfaces. Following nucleation, the sound field causes the liquid to experience cycles of high (compression) and low (rarefaction) pressure. These pressure changes force the bubbles to alternately contract and expand (Dong et al., 2020; Wood et al., 2017; Leighton, 2012). The formation, growth, oscillation, and collapse of these bubbles under the influence of the sound field are termed acoustic cavitation (Dong et al., 2020).

Bubbles radius oscillate around  $R_0$ , with expansion leading to decreased interior pressure and a tendency to restore the original bubble size. Conversely, compression increases gas pressure, leading to a rebound. The bubble volume forms an oscillatory system, and its resonance radius can be derived as:

$$R_{res} = \frac{1}{2\pi f} \left( \frac{3\gamma P_0}{\rho} \right)^{\frac{1}{2}} \quad (3)$$

Where  $f$  is the frequency applied to the cavitation,  $\gamma = \frac{c_p}{c_v}$  is the ratio of the specific heat of the gas at constant pressure to its specific heat at the constant volume,  $\rho$  is the density of liquid and  $P_0$  is the hydrostatic liquid pressure (Dong et al., 2020; Pflieger et al., 2019).

Two types of cavitation are generally considered: stable (non-inertial) and transient (inertial) cavitation. Stable cavitation bubbles last over many cycles and oscillate weakly and symmetrically. In contrast, transient cavitation bubbles grow extensively over a few cycles until the ultrasound energy can no longer be absorbed, leading to instability and violent collapse. This collapse can cause fragmentation into smaller bubbles, which can act as nuclei for further bubbles or dissolve into the bulk solution if their radius is sufficiently small. The concept has been visualized as 'dancing bubbles,' where a larger bubble ejects tiny bubbles and appears to dance by counteraction (Wood et al., 2017; Capote & De Castro, 2007). Transient cavities significantly contribute to sonochemical effects because smaller bubbles, upon dissolution, provide more opportunities for gas products to interact in the liquid and at the bubble surface (Wood et al., 2017).

At some point, a bubble can no longer absorb the energy efficiently from the ultrasound so it implodes. Rapid adiabatic compression of gases and vapours within the bubbles or cavities produces extremely high temperatures (about 5000°C) and pressures (roughly 2000 atm). The size of the bubbles is very small relative to the total liquid volume, so the heat they produce is rapidly dissipated with no appreciable change in the environmental conditions — this is why cavitation is also known as “cold boiling”. The cooling following collapse of a cavitation bubble has been estimated to be in the region of 10 billion °C/s. These high temperature and pressure produce radical or radical-ion intermediates that can react with reactants and thus accelerate some reactions. This process can also generate light, a phenomenon known as sonoluminescence (Dong et al., 2020; Fargassa & Ippoliti, 2016; Capote & De Castro, 2007). The sonoluminescence is a well-known chemical phenomenon linked with ultrasound. Indeed, a tiny light can be emitted in a cool liquid under the influence of ultrasounds. This form of light emission results from the high-temperature formation of reactive chemical species in excited electronic states. Emitted light from such states provides a spectroscopic probe for the cavitation effect (Capote & De Castro, 2007).

When cavitation occurs near a solid surface, the dynamics of cavity collapse change dramatically. In pure liquids, the cavity retains its spherical shape during collapse due to uniform surroundings. Near a solid boundary, however, the cavity collapse is asymmetric, producing high-speed jets of liquid. Liquid jets driving into the surface at speeds close to 400 km/h have been observed. The impact of these jets on the solid surface can cause significant damage to impact zones and produce newly exposed, highly reactive surfaces. The distortions of bubble collapse depend on the surface and are several times larger than the resonant size of the bubble (Pfleiger et al., 2019; Capote & De Castro, 2007).

Another phenomenon observed with high-frequency ultrasound is acoustic streaming. Two major types of streaming result from standing waves: boundary layer streaming and Eckart streaming. Eckart streaming occurs in channels with dimensions on the order of a few centimetres. Boundary layer streaming is the flow generated by the viscous dissipation of acoustic energy in the fluid boundary layer, which plays a significant role in the overall fluid dynamics of the system (Dong et al., 2020).

#### 4.1.2 Radicals of H<sub>2</sub>O

The high temperature and pressure created within a collapsing cavitation bubble produced by ultrasound radiation cause the formation of free radicals and various other reactive species. For instance, sonication of pure water leads to its thermal dissociation into hydrogen (H) and hydroxyl (OH) radicals, with the latter forming hydrogen peroxide (H<sub>2</sub>O<sub>2</sub>) through recombination (Capote & De Castro, 2007). These radicals interact and initiate chemical reactions. Most radicals produced within a repetitive transient bubble are confined to the bubble interior by the bubble surface. However, some direct diffusion of highly soluble products from the bubble can occur. If the lifetime of active bubbles is shorter than the lifetime of the radicals produced, the radicals are released into the liquid through fragmentation or dissolution, where they may trigger further chemical reactions. Conversely, if the bubble lifetime exceeds the radicals' lifetimes, the radicals will mainly recombine, resulting in fewer reactions within the solution. In the case of water, a redox reaction occurs where H<sup>•</sup> and <sup>•</sup>OH radicals are produced inside the compressed bubble due to the dissociation of H<sub>2</sub>O vapor. These radicals may



then recombine to form  $\text{H}_2\text{O}_2$ , while  $\text{H}\cdot$  can react with oxygen to form hydroperoxyl radicals ( $\text{OOH}\cdot$ ) (Wood et al., 2017).

$\text{H}_2\text{O} \rightarrow \text{OH}\cdot + \text{H}\cdot$
$\text{OH}\cdot + \text{H}\cdot \rightarrow \text{H}_2\text{O}$
$2 \text{OH}\cdot \rightarrow \text{H}_2\text{O}_2$
$\text{OH}\cdot + \text{OH}\cdot \rightarrow \text{H}_2 + \text{O}_2$
$2 \text{H}\cdot \rightarrow \text{H}_2$
$2 \text{OH}\cdot \rightleftharpoons \text{O}\cdot + \text{H}_2\text{O}$
$2 \text{O}\cdot \rightleftharpoons \text{O}_2$
$\text{H}_2\text{O}\cdot + 2\text{H}\cdot \rightarrow \text{H}_2\text{O} + \text{H}_2$
$\text{H}_2\text{O}\cdot + \text{H}_2\text{O}\cdot + \text{O}_2 \rightarrow 2\text{H}_2\text{O}_2$
$\text{HO}\cdot + \text{H}_2\text{O} \rightarrow \text{H}_2\text{O}_2 + \text{H}\cdot$
Additional reactions in the presence of oxygen
$\text{O}_2 \rightarrow 2 \text{O}\cdot$
$\text{O}_2 + \text{O}\cdot \rightarrow \text{O}_3$
$\text{O}_2 + \text{H}\cdot \rightarrow \text{OOH}\cdot \text{ (or } \text{OH}\cdot + \text{O)}$
$\text{O}\cdot + \text{OOH}\cdot \rightleftharpoons \text{OH}\cdot + \text{O}_2$
$\text{O}\cdot + \text{H}_2\text{O} \rightarrow 2 \text{OH}\cdot$

Figure 4: Principal free radicals produced during ultrasonic irradiation of water and their reactions (Wood et al., 2017; Capote & De Castro, 2007)

Sonochemistry encompasses both homogeneous and heterogeneous processes, with specific effects on chemical reactions based on the nature of intermediates involved. In homogeneous systems, reactions that proceed via radical or radical-ion intermediates are particularly sensitive to sonochemical effects, while purely ionic reactions are less likely to be influenced by sonication. In heterogeneous systems, mechanical agitation from cavitation can stimulate reactions involving ionic intermediates, a phenomenon sometimes referred to as "false sonochemistry." Although some argue this term is misleading, the principle is that similar results might be achieved with efficient mixing instead of sonication. Heterogeneous reactions with mixed mechanisms (both radical and ionic) will have their radical components enhanced by sonication. In such systems, if the pathways converge to the same product, sonication increases the overall reaction rate. However, if the pathways diverge to different products, sonication can favour the radical pathway, altering the reaction products. Additionally, high-speed stirring can mimic the effects of sonication in heterogeneous systems, particularly in processes driven by hydrodynamic cavitation rather than acoustic cavitation (Capote & De Castro, 2007).

The interaction of radicals generated through cavitation has profound implications for sonochemical processes. These high-energy intermediates drive a wide range of chemical reactions, enhancing reaction rates and enabling transformations that may not occur under standard conditions. By understanding and harnessing the dynamics of radical formation and behaviour within cavitation bubbles, researchers can optimize sonochemical processes for desired outcomes, paving the way for innovative solutions in various scientific and industrial fields.

#### 4.1.3 Parameters affecting ultrasound

Factors such as pressure, frequency, intensity, signal type, temperature, and flow dynamics have an important effect on the ultrasound. These parameters determine the efficiency of bubble formation, collapse, and energy transfer, influencing the outcomes of ultrasonic applications. Understanding and optimizing these factors is necessary for maximizing the performance and efficiency of ultrasonic processes.



#### 4.1.3.1 Pressure

Pressure amplitude significantly influences the power transferred to the liquid in sonochemical processes. Within an optimal range, increasing pressure amplitude enhances the number of cavitation bubbles, the temperature during collapse, and the overall sonochemical yield. There are both upper and lower limits to this effect. Above the upper limit, coalescence and degassing occur, leading to reduced active cavitation. Below the lower limit, the sound field's amplitude is too small to induce nucleation or bubble growth, causing bubbles to dissolve due to surface tension effects. Within the optimal range, higher pressure amplitudes result in larger bubbles and more intense compression and rarefaction forces, leading to more violent collapses and higher temperatures. This increases the dissociation or ionization of gases within the bubbles (Wood et al., 2017; Leighton, 2012).

Non-linear oscillations at high pressure amplitudes can cause bubbles to fragment, creating new bubbles and enhancing sonochemical activity. High pressure amplitudes also promote structural instability in bubbles, leading to increased acoustic streaming. This motion reduces coalescence, increases bubble instabilities, and enhances rectified diffusion of species into the bubbles. However, at very high powers, coalescence can still occur due to agglomeration in antinode regions, which can attenuate the sound field and reduce its effectiveness. Instabilities may also cause liquid jets (Wood et al., 2017; Leighton, 2012; Capote & De Castro, 2007).

Regarding sonochemical reactions, higher pressure amplitudes generally increase the number of active cavitation bubbles, thus boosting sonochemical yield. However, beyond a certain point, excessive power leads to a decrease in active bubbles per unit volume due to coalescence, degassing, and increased liquid agitation, ultimately reducing the sonochemical yield (Wood et al., 2017).

#### 4.1.3.2 Frequency

The frequency of the ultrasound field significantly impacts the behaviour and characteristics of cavitation bubbles, influencing their number, size, distribution, and chemical activity. These effects are also dependent on reactor geometry, ambient pressure, temperature, viscosity, and the gas composition of the liquid (Wood et al., 2017). Generally, higher frequencies lead to increased nucleation and the formation of smaller bubbles, as the resonance size of a bubble is inversely related to the applied frequency (Leighton, 2012). Higher frequencies reduce the amount of vapor entering the bubble due to shorter expansion phases, allowing small bubbles to reach resonance size more efficiently. However, higher frequencies also raise the cavitation threshold, necessitating more power to achieve cavitation. For instance, ten times more power is needed to cavitate water at 400 kHz compared to 10 kHz (Capote & De Castro, 2007).

Frequency also affects coalescence and bubble size. At low frequencies, coalescence leads to the formation of larger degassing bubbles, while at high frequencies, it helps small inactive bubbles grow to active sizes. The distance between antinode regions decreases at higher frequencies, which can increase coalescence. Smaller bubbles have shorter film drainage times, enhancing the likelihood of coalescence. Higher frequencies produce more active bubbles and reactive species, as bubbles collapse and fragment more quickly due to shorter oscillation periods. However, bubbles at higher frequencies are smaller and more stabilized against fragmentation, which affects the overall sonochemical yield (Wood et al., 2017).

Frequency also influences reaction pathways within the bubble. At lower frequencies, radicals inside the bubbles have more time to follow pathways similar to flame reactions, whereas at high frequencies, diffusion into the bulk solution increases, releasing more hydroxyl radicals into the liquid (Rooze et al., 2011). Although increasing frequency reduces bubble growth time and sonochemical

yield, there is an upper limit beyond which active cavitation decreases. Smaller bubbles result in less severe collapses and fewer radicals produced (Wood et al., 2017).

The influence of frequency on bubble surface instabilities and the degree of sonochemistry can be understood by considering two limits. At low frequencies, bubbles are larger, collapse more vigorously, and exhibit greater surface instability, but increased coalescence due to bubble size is also observed. At high frequencies, antinode regions are closer, leading to increased coalescence, yet smaller bubbles experience more intense quasi-acoustic streaming, causing nonlinear bubble motion and surface instabilities. High frequencies also reduce reactive species production due to shorter growth times and less intense collapses. Therefore, mid-range frequencies are generally more effective for sonochemical activity, as bubble surface instability effects are more pronounced between an upper and lower frequency limit (Pflieger et al., 2019; Wood et al., 2017).

#### 4.1.3.3 *Intensity*

The sonication intensity is directly proportional to the square of the vibration amplitude of the ultrasonic source. Typically, increasing the intensity enhances sonochemical effects; however, the amount of ultrasonic energy a system can handle is limited. At higher frequencies, where cavitation bubbles are initially difficult to create due to shorter rarefaction cycles, increased intensity allows for effective cavitation by improving collapse time, temperature, and pressure. Despite this, intensity cannot be increased indefinitely because the maximum bubble size is constrained by pressure amplitude. If the pressure amplitude is too high, bubbles may grow excessively during rarefaction, leaving insufficient time for collapse (Capote & De Castro, 2007).

It is established that a minimum sonication intensity is necessary to reach the cavitation threshold. When a substantial amount of ultrasonic power is applied, the solution generates numerous cavitation bubbles, which can coalesce into larger, longer-lived bubbles that impede the transport of acoustic energy through the liquid. At high vibrational amplitudes, the ultrasonic source may not maintain consistent contact with the liquid throughout the cycle, a phenomenon known as decoupling. This significantly reduces the efficiency of power transfer from the source to the medium, particularly when many cavitation bubbles accumulate near the transducer's emitting surface. Additionally, excessive intensity can cause the transducer material to degrade and fracture due to the large size changes in the transducer (Capote & De Castro, 2007).

Overall, while higher power inputs generally improve system efficiency, this efficiency tends to plateau or reach a maximum at power levels ranging from 10 to 100 W, depending on the frequency used (Rooze et al., 2011).

#### 4.1.3.4 *Signal types*

Pulsed, sweeping, and bi-modal ultrasound signals can enhance active cavitation more effectively than continuous wave output. Continuous wave ultrasound often suffers from inefficiencies due to limited spatial distribution, coalescence-induced loss of applied pressure amplitude, and bubble growth beyond the active cavitation region (Wood et al., 2017).

Pulsed wave ultrasound, characterized by alternating periods of power on time (PONT) and power off time (POFFT), can increase the sonochemically active region, enhance sonochemical effects, and reduce bubble growth and associated degassing. The effectiveness of pulsed wave ultrasound depends on the duration of PONT and POFFT. Optimizing the PONT to POFFT ratio is essential to enhance bubble activity and radical production while minimizing coalescence and degassing. Sweeping frequencies, either upward or downward, can significantly influence cavitation. Frequency sweeps affect inertial cavitation by altering the resonance bubble size, which in turn impacts the sonochemical yield. Bi-modal or dual-frequency signals, where two frequencies are used

simultaneously, can significantly boost sonoluminescence intensity. This method enhances bubble oscillation, potentially altering the active bubble population and increasing bubble collapse temperatures. The dual-frequency approach reduces standing wave effects, leading to more distributed cavitation activity and improved energy transfer efficiency (Wood et al., 2017).

#### 4.1.3.5 *Liquid flow and temperature*

The influence of flow on the cavitation environment can be applied through mechanical stirring, circulation pumping, or frequency-dependent quasi-acoustic streaming. Flow helps prevent cavitation bubbles from coalescing and clustering by counteracting the natural tendency for bubbles to merge and grow. Properly managed flow can minimize coalescence, thereby enhancing sonochemical activity. Additionally, increased flow refreshes the solution around the bubbles, improving gas concentration and mass transfer. The movement of the liquid can disperse bubbles from stagnant regions into more active areas within the sound field, further increasing overall activity. The nonlinear motion induced by fluid flow can also cause structural instability and asymmetric collapse of bubbles, contributing to enhanced sonochemical effects (Wood et al., 2017).

Increasing the temperature of the liquid lowers the cavitation threshold due to a rise in vapor pressure, decreased surface tension, or reduced viscosity. While higher temperatures facilitate cavitation by lowering the acoustic intensity needed, they also decrease gas solubility, reducing the number of available cavitation nuclei. Elevated temperatures lead to a higher vapor pressure, which can diminish peak cavitation temperatures and slow sonochemical reactions by cushioning bubble collapse with more vapor. Additionally, increased temperature can alter other parameters, such as frequency. Consequently, to optimize sonochemical effects, experiments should be conducted at the lowest feasible temperature or with solvents of low vapor pressure (Wood et al., 2017; Capote & De Castro, 2007).

#### 4.1.3.6 *Solid addition*

The influence of solids in cavitation environments has been a topic of study since the late 19th century, initially focusing on cavitation damage to ship propellers. Modern research investigates how solids affect reaction rates in both stoichiometric and catalytic reactions. Solids larger than 150  $\mu\text{m}$  in the liquid can cause nearby bubbles to collapse non-spherically, generating high-speed jets that impact the surface, potentially leading to surface perforation and exposing reactive sites. Smaller particles, such as powders, experience high-velocity collisions and melting due to bubble collapse shockwaves. Metal powders can act as sonochemical catalysts, enhancing reaction rates by removing surface oxides or through mechano-chemical effects. For instance, micron-sized particles at 20 kHz improve hydrogen yields by contributing to water splitting, while nanoparticles at 362 kHz increase nucleation and ultrasonic attenuation. Despite these effects, studies on the impact of powders on sonochemical activity remain limited (Wood et al., 2017).

## 4.2 *Category of transducers*

Ultrasonic flow reactors usually consist of an ultrasonic transducer and a microfluidic device. The transducer, typically based on piezoelectric materials, converts alternating current into ultrasonic vibrations. It is normally actuated by a power amplifier driven with a sine wave from a signal generator. Based on the type of transducer used, ultrasonic reactors can be classified as piezoelectric plate-based reactors or Langevin-type transducer-based reactors.

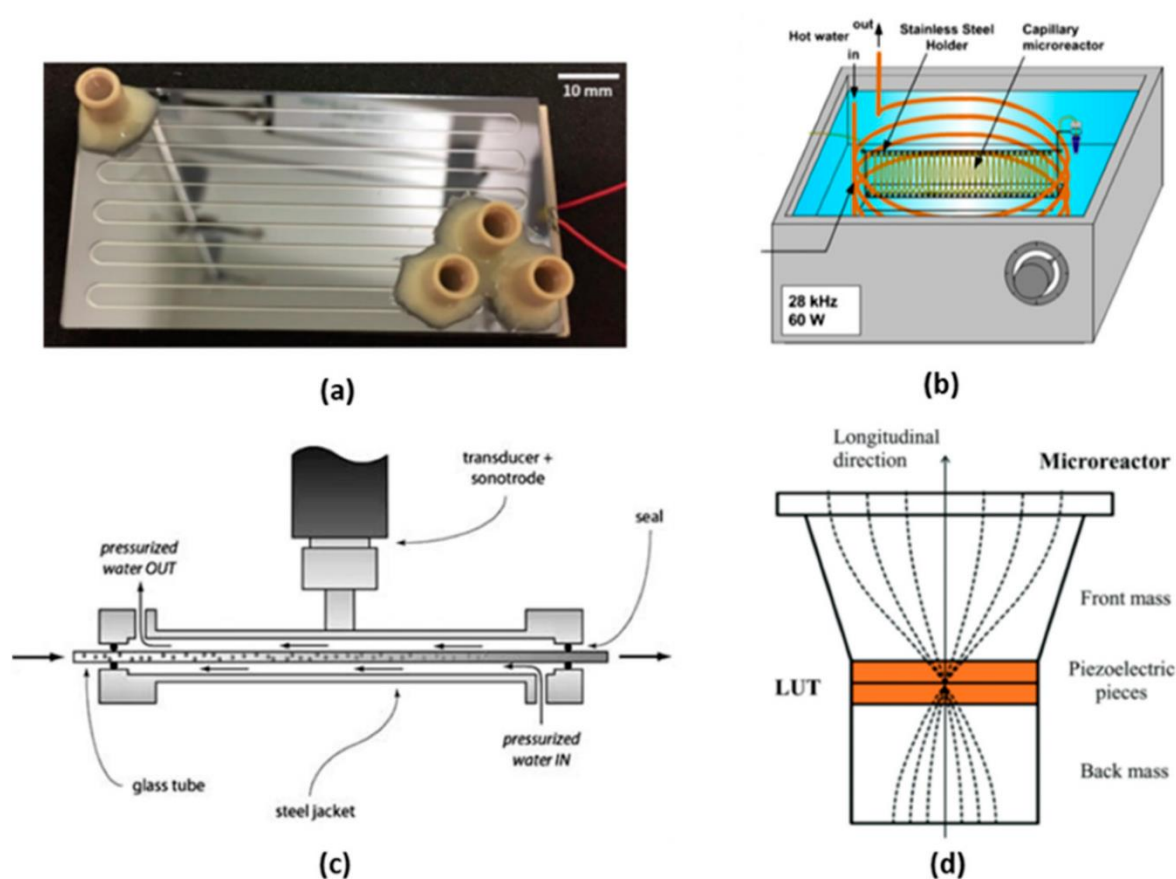


Figure 5: Representative examples of four categories of ultrasonic flow reactors. (a) Picture of a piezoelectric plate reactor developed by Dong et al., the reactor consists of a piezoelectric plate glued to the bottom of a silicon plate microreactor (b) Capillary microreactor immersed in an ultrasonic bath (c) Sketch of a Langevin-type transducer indirectly coupled reactor (d) Sketch of a Langevin-type transducer directly coupled reactor (Dong et al., 2020).

Piezoelectric plate reactors are favoured in laboratories for their versatility and ease of fabrication. Langevin-type reactors are preferred for both large and small-scale applications due to their higher efficiency and broader power range. Ultrasonic bath reactors are widely used in organic synthesis due to their availability, ease of use, and flexibility (Dong et al., 2020).

Piezoelectric plate reactors are often constructed by bonding a piezoelectric plate to a microreactor using epoxy glue, or by clamping them with transmission grease at low ultrasonic power to allow disassembly and reuse. These reactors operate efficiently at various resonance frequencies and can function at both low and high frequencies. Their versatility, ease of fabrication, and operation make them the most common ultrasonic flow reactors in academic research (Dong et al., 2020).

Langevin-type transducers are cost-effective for high ultrasonic power applications, especially at low frequencies. They consist of piezoelectric ceramic rings sandwiched between metal masses, which help protect the ceramics from overheating and improve ultrasound transmission efficiency as it is shown on the Figure 7. The front mass, typically light metal, radiates the ultrasound, often through a sonotrode. For large reactors requiring high power, these transducers are preferred (Dong et al., 2020). Ultrasonic flow reactors are categorized into directly and indirectly coupled types. Direct coupling uses epoxy or clamps to attach the transducer directly to the microreactor, offering efficient energy transfer but reducing flexibility and complicating temperature control. Indirect coupling uses a transmission medium, like a liquid, to transfer ultrasound, which can dissipate energy and reduce efficiency but allows modularity and better temperature control. Recent designs improve efficiency

by matching the transducer and microreactor structure to form a half-wavelength resonator, generating a strong, uniform acoustic field. Direct coupling, however, can lead to heat management issues, mitigated by methods such as pulsed ultrasound or combining direct and indirect coupling (Dong et al., 2020).

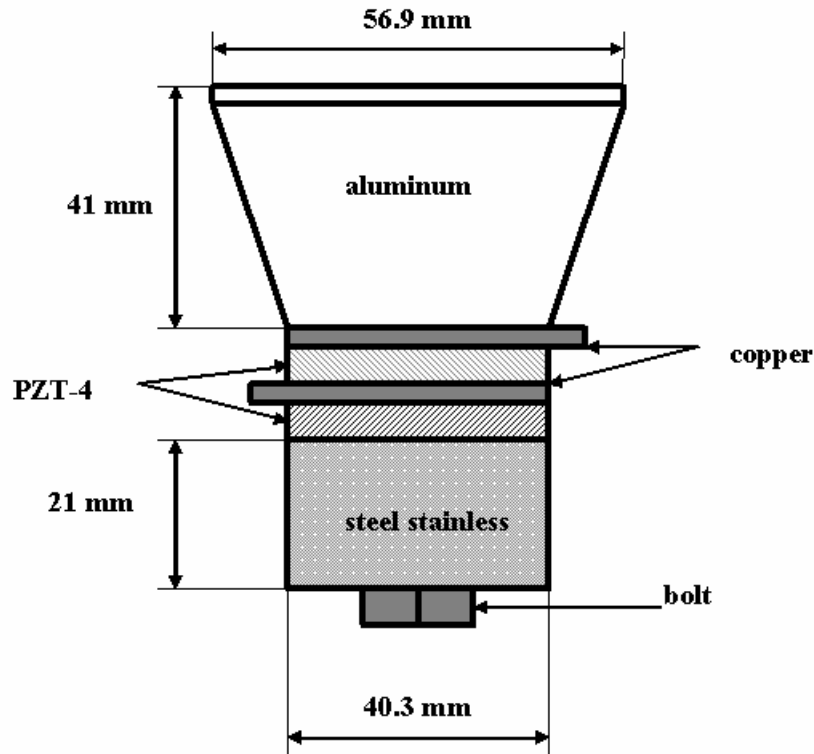


Figure 6: Diagram of the Langevin type transducer (Moreno et al., 2014).

## 5 Extracting PGMs nowadays

Platinum Group Metals, including platinum, palladium, and rhodium, are indispensable to the European economy due to their critical role in industries such as automotive, electronics, and chemical manufacturing. The European Union has classified PGMs as critical raw materials, emphasizing their strategic importance and the vulnerabilities associated with their supply. Given that the majority of PGM production is concentrated in a few regions, particularly South Africa and Russia, the supply chain is susceptible to geopolitical and economic disruptions. Moreover, the rarity of these metals and the increasing global demand further intensify the need for sustainable supply solutions. Recycling PGMs from end-of-life products, such as catalytic converters, emerges as a vital strategy to address these challenges. By enhancing recycling efforts, the EU can reduce its dependency on primary sources, secure a steady supply of these essential materials, and contribute to environmental sustainability by reducing the need for environmentally damaging mining operations (European Commission, 2023). As of August 21, 2024, the daily prices of PGMs reflect their continued high demand. Platinum and palladium are both trading at approximately \$975 per troy ounce, highlighting their near parity in value. Rhodium, however, stands out with a significantly higher price of \$4 750 per troy ounce, underscoring its scarcity and critical importance in industrial applications (Umicore, 2024).

Platinum Group Metals can be extracted from both primary and secondary sources, with catalytic converters being a major secondary source. The extraction method chosen depends on various

factors such as physical and chemical properties, impurities, granulometry, and the grade of the PGM. The three main recovery processing routes are pyrometallurgy, hydrometallurgy, and biometallurgy. Often, a combination of these methods is employed to optimize efficiency, considering economic, environmental, and technical factors.

### 5.1 Primary resources

Primary resources for PGM extraction typically involve mining ores using conventional underground or open-pit techniques followed by grinding. Gravity-based separation and flotation are used to produce PGM-rich concentrates. The common extraction process combines pyrometallurgy and hydrometallurgy, where ores are mined, ground, and subjected to gravity separation and flotation. Achieving optimal recovery depends on the level of liberation of PGM minerals, which informs the choice of the grinding process. Sulfide minerals containing PGMs are enriched through gravity and flotation techniques. In cases of low-grade PGM ores, advanced gravity separation techniques are used due to the finely dispersed nature of PGM minerals. Enhanced gravity separators are developed to manage these fine particles effectively (Chidunchi et al., 2024; Yakoumis et al., 2021; Panda et al., 2018).

The PGM concentrate is melted at high temperatures ( $>1500^{\circ}\text{C}$ ), and PGMs are refined via hydrometallurgy. In the hydrometallurgical process, PGM concentrate is leached in an autoclave under high pressure conditions to oxidize sulfates, leading to low impurity content. However, considerable PGM losses occur during ore treatments, with 27% lost during mining, 15% during overall processing, and 13% during the concentration stage (Yakoumis et al., 2021).

### 5.2 Secondary resources

The demand for platinum, palladium, and rhodium has been steadily increasing due to their use in autocatalytic converters. Recycling PGMs from spent auto-catalysts offers several advantages over primary resources, including significantly higher concentrations of PGMs. One automotive catalytic converter can contain up to 2000 g/t of PGMs, compared to less than 10 g/t in primary ores. Other secondary sources include computer motherboards, mobile phones, and jewelry. Road dust has also been identified as a potential raw material with PGM concentrations up to 2.252 g/t for Pt and 1 g/t for Pd. Secondary sources typically have lower impurities than primary ores, making them more efficient and cost-effective to process (Panda et al., 2018; Saguru et al., 2018).

Spent automotive catalysts are the richest PGM secondary resource, widely exploited for PGM recovery. They primarily contain Al-Mg-Si based ceramics and several additives, which result in much lower impurities compared to primary ores. Consequently, recycling PGMs from spent auto-catalysts leads to lower operating costs and environmental impact due to reduced energy consumption and emissions. For instance, producing 1 kg of platinum from primary ores in South African mines requires 20 times more energy and results in significantly higher greenhouse gas emissions than recycling from secondary resources in European refining plants (Yakoumis et al., 2021; Trinh et al., 2020).

In 2014, the recycling of spent automotive catalytic converters accounted for 60% of total platinum recovery, though only over 5% of palladium and ruthenium from electronic devices was recovered. Recycling from secondary sources is preferred due to higher PGM concentrations, significantly lower energy consumption (70–100 times less), higher recovery yields, and a reduced environmental footprint compared to primary production. Recycling PGMs from spent auto-catalysts involves separating, drying, crushing, and grinding the waste catalysts, followed by hydrometallurgical or pyrometallurgical methods to recover the metals (Kinas et al., 2024).



Prominent companies like Umicore (Belgium), Johnson Matthey (United Kingdom), Hereaus (Germany), and Nippon (Japan) employ various techniques to recover PGMs. For example, Johnson Matthey uses smelting, leaching, and refining, while Umicore combines waste catalysts with e-waste, smelts them in a high-temperature furnace, and then uses hydrometallurgical processes to produce high-purity platinum. The choice of processing methods depends on the concentration of PGMs, metallic constituents, and other materials (Liu et al., 2020).

### 5.3 Pre-treatments

Regardless of the chosen processing route, whether pyrometallurgical, hydrometallurgical, or a combination of both, the preparation of catalytic converter material follows a similar path. Initially, the ceramic PGM carrier-monolith is decanned, delaminated, cut, shredded, and ground to remove residues. For the pyrometallurgical route, the prepared material is then fed into a furnace with fluxes and collector metals. In the hydrometallurgical route, the material undergoes pre-treatment steps before direct leaching (Zupanc et al., 2023; Saguru et al., 2018).

In hydrometallurgical processes, PGMs are extracted using aqueous media with suitable leachants. This can be done directly on spent auto-catalysts or after enrichment stages, and it is also used for PGM alloys obtained post-smelting. Pre-reduction of PGM oxides with reducing agents before dissolution is beneficial, as thermodynamic calculations show that Pt, Pd, and Rh oxides form spontaneously at high temperatures. Therefore, PGMs are likely transformed into oxides and exist in solid or gaseous forms during the operation of a mobile auto-catalyst since the temperature can exceed 1150°C. Rh<sub>2</sub>O<sub>3</sub> can form a protective layer on the surface, decreasing the dissolution of Rh and other PGMs. Consequently, pre-treatment to convert PGM oxides to metals ensures efficient recovery during leaching, which can be treated with certain reductants (Trinh et al., 2020).

Pre-treatment steps in the hydrometallurgical process involve substrate calcining to convert alumina into a form which is not amenable to leaching, to reduce solubilising alumina which would contaminate the PGM solution (Saguru et al., 2018). In the hydrometallurgical process, pre-treatment of catalytic waste is required to eliminate organic residues and carbon deposition (Chidunchi et al., 2024; Kinas et al., 2024; Yakoumis et al., 2021; Liu et al., 2020; Panda et al., 2018; Dong et al., 2015). Reduction roasting removes passivation layers on PGMs, and oxidative roasting converts base metal sulphides to oxides and forms PGM metallic phases. Calcination with salts like Na, Li, or K at temperatures above 800°C accelerates leaching kinetics. Mechanochemical activation combines milling and leaching, reducing process costs by shortening steps. For rhodium, reductive heating under hydrogen yields nearly 80% recovery. Otherwise, Rh kinetics are very low, requiring stronger leaching conditions (Yakoumis et al., 2021).

Magnetic separation is used to eliminate iron contaminants introduced during decanning (Saguru et al., 2018). Ultrasound pre-treatment enhances PGM cyanide-complex formation by removing base metals, influenced by factors such as ultrasound power, frequency, acid concentration, pulp density, and duration (Grilli et al., 2023; Yakoumis et al., 2021). Through these comprehensive pre-treatment processes, the recovery of PGMs from spent auto-catalysts can be optimized, ensuring efficient and environmentally friendly extraction of these valuable metals.

### 5.4 Pyrometallurgy

Pyrometallurgical processes involve the high-temperature physical or chemical transformation of PGMs, often with additives such as collectors and fluxes. This includes smelting, chlorination, metal vapor treatment, and heating-quenching processes (Trinh et al., 2020). The traditional method for recovering PGMs from spent catalysts encompasses steps like crushing, batching, granulation, smelting, and separation (Panda et al., 2018; Dong et al., 2015).

Despite their widespread use, pyrometallurgical processes face several challenges. These high-temperature operations are energy-intensive and produce toxic emissions. The need for specialized equipment can make these processes impractical for small-scale recycling. Additionally, recovering additives like Ce, Zr, and Al, which have economic value, can be technically challenging as they often end up in the slag phase (Yakoumis et al., 2021; Saguru et al., 2018).

Several well-known facilities, including Umicore and Johnson Matthey, utilize pyrometallurgy to recover PGMs. Umicore operates an integrated metal smelter and refinery that recovers PGMs along with other metals from auto-catalysts, printed circuit boards, and electronic components. Their PGM-Fe collection process mainly involves plasma arc smelting, a technology that was popular in the 1980s for its high energy density, high temperatures, and flexibility in plasma gases. However, the short lifespan of the plasma gun accessory limited its industrial application. The Johnson Matthey process involves smelting crushed catalysts with flux materials in a crucible containing molten collector metal (Fe or Cu) using a plasma torch. This operation, conducted at temperatures between 1500–1650°C, allows for the tapping off the collector metal alloy, with 95% of PGMs being recovered through conventional refining methods (Panda et al., 2018).

#### 5.4.1 Metal smelting

Metal smelting is the most mature technique used for PGM recovery from both primary ores and spent auto-catalysts. This process involves melting the crushed catalyst, mixed with fluxes, in a crucible containing a collector metal at temperatures exceeding 1600°C. Collectors used include Cu, Fe, Pb, Ni, matters (Ni<sub>2</sub>Se<sub>3</sub>–CuS) or waste printed circuit boards. The catalyst is melted with flux, an auxiliary metal, and a reducing agent, forming an auxiliary metal-PGM alloy that undergoes purification to isolate the PGMs. Matte separation, used for metal-bearing sulphide ores in primary PGM production, involves collecting PGMs with metal base-rich matte in an electric furnace. Melting point, rheological behaviour, solubility, droplet size, and environmental factors must be controlled. Moreover, impurities can form complexes with PGMs during the calcination stage (Chidunchi et al., 2024; Yakoumis et al., 2021; Liu et al., 2020; Trinh et al., 2020; Ghodrat et al., 2018).

Collector selection is essential for an efficient smelting process, which includes choice of fluxes, smelting equipment, operating system, and the subsequent PGM separation process. The collector is selected based on the miscibility of PGMs in the liquid phase, melting temperature, chemical properties between collector and PGMs, as well as the loss of PGMs in the slag. The low-viscosity and low melting temperature of smelting slag is the base principle in the selection process for high-efficiency recovery of PGMs. Common collectors are lead, copper, iron, and nickel (Chidunchi et al., 2024; Yakoumis et al., 2021; Trinh et al., 2020; Liu et al., 2020; Ghodrat et al., 2018; Panda et al., 2018).

Lead has been used since the 1980s in developed countries (Inco, Johnson Matthey, or Impala Platinum) for recycling PGMs from spent auto-catalysts with some associated advantages, such as simplicity of operation, a simple subsequent oxidation to separate PGMs from lead, low smelting temperature in a minor furnace, and lower investment. However, the recovery of Rh is relatively low (70–80%) and the environmental issues due to the formation of toxic PbO should be a concern. To use an iron collector (iron or iron oxide), the spent auto-catalysts along with fluxes and reductants are smelted at ~2000 °C via plasma arc smelting. The resulting iron alloy is dissolved using H<sub>2</sub>SO<sub>4</sub> or H<sub>2</sub>SO<sub>4</sub>/air, with PGMs concentrated in the residue. However, the short plasma gun lifespan and high-temperature reduction of silica if carbon is present can create silicon-iron alloys that complicate PGM separation. Copper (CuO or CuCO<sub>3</sub>) offers an alternative method for extracting PGMs from spent auto-catalysts, allowing for lower smelting temperatures. A conventional electric furnace can be utilized to streamline operations and improve slag chemistry control. The resulting alloy from



smelting can be dissolved using  $\text{H}_2\text{SO}_4$ /air, and the copper in the solution can be recovered and recycled by converting it back to  $\text{CuCO}_3$  with soda ash (Chidunchi et al., 2024; Yakoumis et al., 2021; Trinh et al., 2020; Liu et al., 2020; Panda et al., 2018).

Matte collection is an emerging technique for recovering PGMs from waste catalysts, offering an advantageous affinity of matte for PGMs compared to traditional methods such as lead, copper, and iron collection. This process involves concentrating PGMs in the matte phase at smelting temperatures between  $1000^\circ\text{C}$  and  $1450^\circ\text{C}$ . The procedure includes the addition of metallic nickel and nickel sulphides ( $\text{NiS}$  and  $\text{Ni}_2\text{S}_3$ ), along with fluxes such as  $\text{CaO}$ ,  $\text{Na}_2\text{CO}_3$ ,  $\text{Na}_2\text{B}_4\text{O}_7$ , or a combination thereof. The smelting slag typically comprises  $\text{SiO}_2$ ,  $\text{CaO}$ ,  $\text{MgO}$ , and  $\text{FeO}$ , which significantly affects the distribution of PGMs between the slag and metallic phases. The basicity of the slag, defined as the mass ratio of basic oxides to  $\text{SiO}_2$ , influences this distribution by promoting desulfurization reactions that form  $\text{Na}_2\text{S}$ , potentially enriching PGMs in the slag. Increased solubility of PGMs in the slag can thus reduce the recovery rate. However, excessively low basicity results in higher slag viscosity, which can hinder the separation of slag and matte. Additionally, the introduction of sulphur in this process may generate sulphur and its oxides, posing health and environmental risks to workers (Chidunchi et al., 2024; Yakoumis et al., 2021; Trinh et al., 2020; Liu et al., 2020; Panda et al., 2018).

Other materials containing PGMs, such as waste printed circuit boards (WPCBs) or their metallic oxides, can serve as effective collectors due to their strong affinity for PGMs. WPCBs contain numerous base metals, including tin, iron, and copper, which can act as metal collectors for PGMs. Additionally, the carrier materials in waste catalysts can be used as slag formers, enabling the simultaneous recovery of precious metals such as gold, platinum, and palladium from WPCBs without the need for an added metal collector. The process begins with the pretreatment of WPCBs and waste catalysts through crushing and incineration, followed by smelting with fluxes and a reducing agent. The metal oxides in WPCBs, such as  $\text{CuO}$ ,  $\text{FeO}$ , and  $\text{SnO}$ , are reduced to their metallic phases. Precious metals, including gold, platinum, palladium, copper, and tin, are primarily enriched in the alloy phase ( $\text{Cu-Sn}$  alloy), while iron and lead are distributed between the alloy and slag phases. In this collection process, the distribution ratios of precious metals between the alloy and slag phases are notably high. This method is simpler than conventional processes and allows for the recovery of valuable metals like copper, tin, iron, and lead from WPCBs. However, the application of this process is limited by the complex composition of WPCBs and the emission of volatile heavy metals, such as  $\text{Pb}$  and  $\text{As}$ , which pose health and environmental risks (Yakoumis et al., 2021; Liu et al., 2020; Ghodrat et al., 2018).

Metal smelting for PGM recovery is widely applied in industrial production by corporations such as Umicore, Johnson Matthey, and Badische Anilin-und-Soda-Fabrik. These processes underscore the importance of metal smelting as an efficient method for PGM recovery, leveraging advancements in technology and collector materials to optimize recovery rates and minimize environmental impact (Liu et al., 2020; Dong et al., 2015).

#### 5.4.2 Chlorination

Chlorination, also known as the carbochlorination process, involves selectively converting PGMs into volatile chloride compounds at high temperatures. These compounds are then condensed in a cooler zone, separated by repulp washing, or absorbed using activated carbon, while the unreacted substrate remains with the chloride sources. This process can achieve high PGM recovery rates (80–90%) by roasting spent autocatalysts at  $600\text{--}1200^\circ\text{C}$  in chlorine gas. The recovery rates can reach 96% for platinum and 93% for rhodium when using a mixture of chlorine and carbon monoxide. Despite the high recovery efficiencies, chlorination has drawbacks, including the need for high

temperatures, strong corrosion, high equipment requirements, and the production of toxic gases (CO, Cl<sub>2</sub>) (Grilli et al., 2023; Yakoumis et al., 2021; Trinh et al., 2020; Dong et al., 2015).

An alternative chlorination method using molten salts as the reaction medium shows promise for selective PGM recovery. In this method, insoluble substances dissolve in the molten salts, forming products that are looser and more disordered than those in the crystalline phase. This enhances reaction kinetics and conversion efficiency at high temperatures, overcoming the limitations of conventional chlorination, which is hindered by solid-gas phase interactions. The chlorination reactions involve the solvation interaction between oxide anions (O<sup>2-</sup>) and the molten salts, dissolving metal oxides and converting insoluble metal oxides into stable, soluble chloride complexes. Selective recovery is achievable by optimizing the choice of salt mixtures, temperatures, and chlorinating agents (Trinh et al., 2020).

#### 5.4.3 Active metals

Active metals such as magnesium, calcium, and zinc possess significant physicochemical properties due to their strong affinity for PGMs (platinum and rhodium). At high temperatures, these metals can react with PGMs to form reactive metal-PGM compounds or their oxidized products, which dissolve more readily in aqua regia compared to pure PGMs. Consequently, Mg, Ca, and Zn in vapor form are used to extract Pt and Rh from spent auto-catalysts. These vapors effectively deposit and react not only with the PGMs on the washcoat but also with the metal oxides in the cordierite substrate, owing to the high porosity of both layers (Trinh et al., 2020).

In this process, crushed spent auto-catalysts (30–50 mm) are placed above the reactive metal (Mg, Ca, or Zn) in a sealed vessel and heated in an electric furnace at 900 °C. The products from Mg vapor treatment dissolve more effectively in aqua regia than those from Ca treatment. Zn vapor also promotes the dissolution of PGMs in acidic solutions, reducing the need for chemical agents and processing time. Additionally, Zn vapor is easier to handle and may react more selectively with PGMs than Ca and Mg. Approximately 100% of Pt and Pd, and 20 to 40% of Rh, dissolve in Ca and Mg vapor, compared to more than 60% in Zn vapor. This process allows for high-efficiency recovery of PGMs with reduced reactant consumption and processing time. However, it has only been tested on simulated spent auto-catalysts, and further procedural modifications are needed for practical applications (Liu et al., 2020; Trinh et al., 2020).

The reactive metal vapor can also interact with the surface layer and substrate. SiO<sub>2</sub>, Al<sub>2</sub>O<sub>3</sub>, and CeO<sub>2</sub> in the catalyst substrate can be thermodynamically reduced by Ca or Mg, decreasing the available reactive metal vapor for PGM reactions, and increasing the impurity content in the resulting alloy. Moreover, this process typically achieves unsatisfactory PGM recovery (less than 80%), despite improving the dissolution ratio of PGMs in aqueous solutions. Additionally, the alloy obtained from reactive metal treatment requires dissolution in aqua regia for PGM purification, generating large amounts of waste acid and wastewater, which have significant environmental impacts (Liu et al., 2020).

#### 5.4.4 Heating—quenching

The heating—quenching process, followed by grinding, has been investigated as an alternative thermal method to enrich PGMs in the washcoat and separate them from the cordierite substrate. This process begins with pre-treating the spent auto-catalyst sample to decompose unburned carbon. The sample is then heated to a high temperature (>600 °C) for a short duration before being rapidly cooled in water (20 °C) during the quenching step. The thermal stress induced by this rapid temperature change affects the washcoat and substrate differently due to their unique structures (Trinh et al., 2020).

Heating–quenching generates micro-cracks in the coating layer and larger cracks at the interface between the washcoat and the substrate, without damaging the cordierite substrate. This causes the washcoat to break into a fine powder containing PGM particles, while the cordierite substrate remains in larger lumps. However, the thicker washcoat layer at the corners of the cell holes is not efficiently removed, necessitating further separation techniques such as surface grinding or flotation to fully liberate the washcoat from the substrate (Trinh et al., 2020).

Despite these challenges, the combination of heating–quenching, selective grinding, and screening can concentrate 45.8% of the PGMs in the washcoat phase into fine fractions, achieving a recovery ratio of 85.7%. Although this is not as efficient as smelting, it offers a viable alternative that can significantly reduce energy consumption during processing (Trinh et al., 2020).

### 5.5 Hydrometallurgy

A hydrometallurgical process for recovering PGMs typically involves homogenizing old catalytic converters, followed by pretreatments, leaching, concentration, extraction, stripping, and recovery of the metal in metallic form or as a salt as it is shown on the Figure 8 The noble metals Pt, Pd, and Rh require acidic, highly oxidizing environments for dissolution. The presence of a complexing agent significantly reduces the potential energy barrier needed for this process (Saguru et al., 2018). The selective dissolution can be done through different methods.

One method is the direct transfer of PGMs from a raw material into a solution and etching them out. Another method involves precipitating the already dissolved PGMs by forming complex compounds under acidic or alkaline conditions in the presence of complexing agents (e.g., iodides, bromides, and chlorides) or additional compounds, elements, or ions (e.g., oxygen, iodine, chlorine, and hydrogen peroxide) (Kinas et al., 2024; Zupanc et al., 2023).

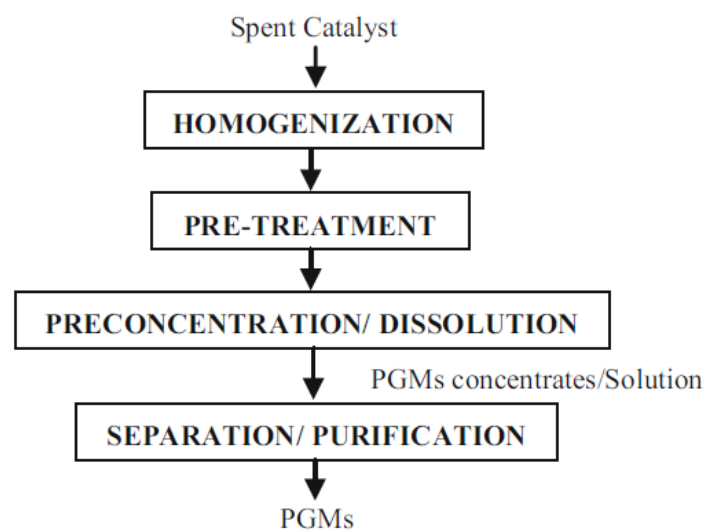


Figure 7: Hydrometallurgical processing of PGMs (Panda et al., 2018).

Hydrometallurgy, under specific conditions, can contribute to the sustainability of PGMs in a more environmentally friendly manner than pyrometallurgy. Compared to pyrometallurgy, hydrometallurgy offers several advantages, such as higher purification yields, scalability, milder process temperatures, minimized energy consumption, better process control, and promising recovery yields. However, waste management (liquid wastes, gas emissions), process duration, as well as the cost and nature of reagents must be considered (Yakoumis et al., 2021). Companies such as Platinum Lake Technology Inc., Canada, have successfully developed hydrometallurgical processes

for recovering PGMs, achieving 95% recovery of Pt and 98% of Pd from spent automotive catalysts. Nippon PGM Co. has reported commercial-scale PGM production from various resources. Heraeus, Germany, has reported the recovery of PGMs from spent materials using hydrometallurgical processes involving HCl leaching with an oxidant, followed by selective precipitation and ion exchange. BASF Catalysts LLC, USA, developed a novel process for recovering PGMs from membrane electrode assemblies (MEAs) that eliminates the release of highly toxic HF gas generated during current combustion recycling processes. Additionally, studies at the Mining and Materials Processing Institute of Japan have shown high leaching efficiency in recycling PGMs from automobile catalyst residues (Panda et al., 2018).

The hydrometallurgical route offers a faster rate of metal recovery at lower capital costs compared to pyrometallurgy, which requires high temperatures to melt raw materials. Furthermore, the energy consumption is lower, and the wastewater generated can be treated in effluent treatment plants, with possibilities for further recovery of value-added products (Grilli et al., 2023).

However, established techniques often use potent oxidizing acidic solutions, such as aqua regia and hydrochloric acid with chlorine gas, which have adverse ecological consequences. Recently, there has been a growing focus on developing alternative methodologies that are both environmentally friendly and economically viable for recovering PGMs from spent catalysts (Chidunchi et al., 2024).

Therefore, in the following sections, we will focus solely on the extraction of PGMs. Extraction techniques will be discussed without delving into the details of PGM dissolution from secondary resources.

### 5.5.1 Solvent extraction

Hydrometallurgical solvent extraction (SX) is a technique utilized to separate platinum group metals from aqueous leaching solutions using organic solvents. This process is typically divided into three key stages: first is the extraction stage, where a specific metal is selectively transferred from the aqueous phase to the organic phase. The second stage is the scrubbing stage, which involves removing co-extracted metals to enhance the purity of the target metal. The final stage is the stripping stage, where the metal is recovered from the organic phase (Kinas et al., 2024).

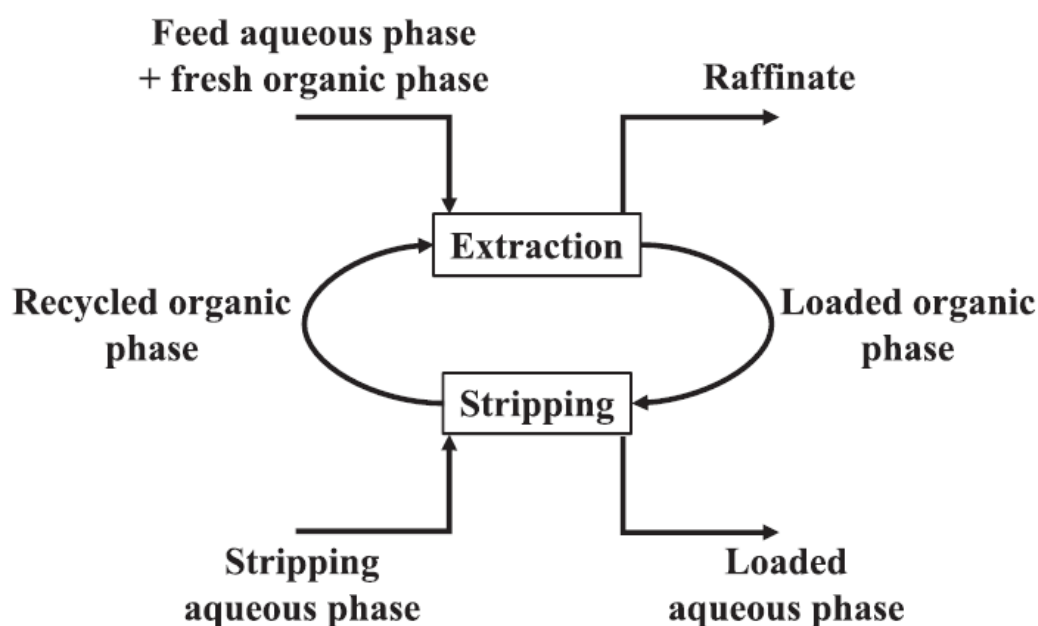


Figure 8: Schematic of solvent extraction for PGM recovery (Kinas et al., 2024).

The extraction mechanisms for platinum group metals are generally classified into three main types, each employing different organic solvents. The first mechanism is ion-pair formation, which uses amines and ammonium salts. The second involves compound formation, utilizing substances such as alkyl sulphides, dialkyl sulphides, dialkyl sulfoxides, phosphine sulphides, hydroxyoximes, and hydroxyquinolines. The third mechanism is solvation, which incorporates solvents like ketones, ethers, phosphine oxides, and tributyl phosphate (Trinh et al., 2020; Saguru et al., 2018).

This technique offers high selectivity compared to conventional precipitation methods. The use of a multi-stage counter-current system enhances the efficient removal of metals and allows for effective purification through the scrubbing stage. However, solvent extraction is associated with several challenges. The organic solvents used are often toxic and can create environmental hazards due to their interactions with concentrated acids and strong oxidants. Solvent volatility is also a concern, as it contributes significantly to greenhouse gas emissions. Additionally, the mixing of solvents with acids and oxidants can produce harmful gases such as CO, CO<sub>2</sub>, NO<sub>x</sub>, and HCl (Kinas et al., 2024). To address these issues, measures like air-scrubbing equipment and reducing the acidity of the PGM-bearing phase are employed. The selection of solvents is crucial, as different solvents offer varying efficiencies and sustainability for PGM extraction. The process typically achieves a recovery rate of 90-95% for PGMs, although Rhodium extraction often shows lower recovery percentages (Kinas et al., 2024).

Despite its advantages, such as high operational efficiency and effectiveness, the major drawbacks of solvent extraction include its complexity, the need for multiple stages, and safety concerns due to solvent toxicity. While most organic solvents used are relatively stable and not carcinogenic, they are incompatible with oxidants and acids, which can generate toxic gases. As a result, ionic liquids are emerging as viable alternatives or complements to traditional organic solvents (Saguru et al., 2018). Solvent extraction remains a widely used technique in commercial refining processes, including operations at Hartley Platinum, Anglo Platinum Rustenburg Base Metals Refinery, and Impala Platinum Base Metal Refinery (Trinh et al., 2020; Saguru et al., 2018).

### 5.5.2 Ion exchange

Ion exchange is a solid-phase extraction technique where metal ions in a liquid phase are exchanged with ions on a solid-phase ion exchanger. These ion exchangers can be inorganic materials, such as aluminosilicate minerals and zeolites, or organic materials like resins, membranes, and coal. Commercially, ion exchange resins are widely used across various industries, including water treatment, petroleum refining, chemical processing, food production, biotechnology, and drug delivery (Trinh et al., 2020).

In hydrometallurgy, ion exchange resins are particularly valued for their high selectivity, loading capacity, mechanical stability, and exchange rate, making them effective for separating PGMs from diverse media (Hosseinzadeh & Petersen, 2024; Trinh et al., 2020).

The separation of PGMs using ion exchange resins generally involves two key steps. The first step, known as metals loading or adsorption, involves the transfer of PGMs onto the solid support through ion association or chelation mechanisms, depending on the type of extractants used. This process involves the interaction of metal ions with the ion exchange resin, which can occur through ion exchange or the formation of coordination complexes. The second step is elution, where metal ions are released back into the liquid phase using suitable eluents. Following elution, the metals may be subjected to either individual precipitation or stripping from the liquid phase (Hosseinzadeh & Petersen, 2024; Yakoumis et al., 2021; Trinh et al., 2020).

Ion exchange resins can achieve high recovery efficiencies, particularly in environments with low concentrations of PGMs, such as chloride, bromide, or cyanide media. This method is often more efficient than solvent extraction for these applications. However, the process can be costly due to expenses related to the preparation and synthesis of solvent-impregnated and chelating resins, the loss of organic extractants, and the complexities involved in the elution and reactivation stages. Additionally, environmental impacts related to the use of organic extractants and other chemical reagents during metal loading and elution should be carefully considered (Trinh et al., 2020; Green et al., 2014).

Different types of resins exist:

- Strong Acid Cation Resins: These resins contain sulfonic acid groups that strongly attract and exchange cations, making them effective for cation removal.
- Weak Acid Cation Resins: Featuring carboxylic acid groups, these resins have a lower affinity for cations, making them suitable for selective cation exchange.
- Strong Base Anion (SBA) Resins: These utilize a polystyrene matrix with quaternary ammonium groups to exchange anions at low acidity levels.
- Weak Base Anion (WBA) Resins: Made from polystyrene and dimethylamine, these resins are effective only in high-acidity media due to their lower affinity for anions (Hosseinzadeh & Petersen, 2024).

Ion exchange resins are versatile and offer high loading capacity, mechanical stability, and effective separation of PGMs from low-leach solutions. Their performance varies depending on the type of resin and the specific PGMs targeted. For instance, strong base anion resins are efficient for platinum and palladium, achieving high recovery rates, but they are less effective for rhodium due to its lower charge density. Separating Pt and Pd can be challenging because of their similar charge densities and geometric configurations (Hosseinzadeh & Petersen, 2024).

Resins come in gel or macroporous forms, with porosity influencing their absorption rates, capacity, and selectivity. Higher cross-linkage results in macroporous structures, which have better ion exchange capabilities for larger ions but reduced moisture content. Although conventional ion exchange resins may not be ideal for the individual separation of PGMs, they are useful for simultaneous recovery from bulk leach liquor. Enhanced effectiveness can be achieved by combining them with selective elution techniques or using modified resins for more targeted separations. Due to their cost, ion exchange resins are typically employed in the final refining stages and for the extraction of low-concentration target metals (Hosseinzadeh & Petersen, 2024; Green et al., 2014).

### 5.5.3 Ionic liquids

Ionic liquids (ILs) are molten salts composed of organic cations and organic or inorganic anions, with melting points below 100 °C. They are increasingly researched for various applications, including reaction catalysis, energy storage, lubrication, and particularly hydrometallurgical metal extraction. ILs are known for their unique properties such as nonflammability, nonvolatility, high conductivity, and excellent chemical, electrochemical, and thermal stability. They offer a diverse range of cation-anion combinations, which can be specifically synthesized to meet particular operational needs. Notable advantages of ILs include their resistance to highly acidic conditions, potential for enhanced selectivity in PGM extraction over traditional organic solvents, and their high capacity for metal extraction (Kinas et al., 2024; Trinh et al., 2020).



In hydrometallurgical processes, ILs are utilized either to supplement or replace the organic phase in liquid-liquid extraction of PGMs. They can significantly improve the efficiency of metal extraction from leach liquors and present a more environmentally friendly alternative to conventional solvents. Despite these benefits, the widespread industrial adoption of ILs faces several challenges. The integration of ILs into existing processes introduces additional complexity, which may necessitate costly modifications. The high production costs of ILs further exacerbates this issue. Additionally, ILs are generally more viscous than conventional organic solvents, which complicates their regeneration and circulation. This increased viscosity also negatively impacts mass transfer rates, leading to slower extraction kinetics. Moreover, the regeneration and circulation of ILs are more energy-intensive compared to those of organic solvents, contributing to higher operational costs. Although ILs are often considered more environmentally friendly, their high production costs and the complexities involved in incorporating them into established systems hinder their broader acceptance (Saguru et al., 2018).

Recent research underscores the potential of ILs to serve as a greener and safer alternative to traditional solvent extraction and ion exchange systems in hydrometallurgy. They have shown promise in extracting PGMs from chloride solutions, suggesting that they could offer a more sustainable and efficient extraction process compared to conventional methods (Kinas et al., 2024; Trinh et al., 2020; Saguru et al., 2018).

#### 5.5.4 Cementation

Cementation, which was detailed in the section 3, is a method used in hydrometallurgy for extracting PGMs from rich leachate solutions by removing metals through reactions with sacrificial metals. This technique can efficiently recover PGMs from leach solutions and is particularly useful when other processing methods have not achieved high recovery rates (Reis & Carvalho, 1994). Commonly used sacrificial metals in cementation include aluminium, zinc, and copper. However, to my knowledge, very few articles discuss cementation using copper (Nguyen & Lee, 2023; Aktas, 2012).

Cementation onto zinc is frequently employed for the recovery of rhodium, especially when other methods have not reached satisfactory recovery levels. For instance, T.H. Nguyen et al. (2016) demonstrated that using zinc for cementation increased Rh recovery from 56% to 83% after a solvent extraction step. Aktas (2011) also showed that zinc cementation is effective for Rh recovery, highlighting its utility in improving extraction efficiency.

Aluminium is the most used sacrificial metal in the industry due to its presence in the washcoat of catalytic converters, which is primarily composed of alumina. Using aluminium as a sacrificial metal helps avoid introducing new impurities into the solution (Chidunchi et al., 2024; Kinas et al., 2024; Liu et al., 2020; Trinh et al., 2019; Dong et al., 2015; Kim et al., 2011; Dragulovic et al., 2008). However, aluminium has some drawbacks, including its susceptibility to oxidation when exposed to air, high flammability, and difficulty in recovery, as it often turns into a gel. Additionally, the cementation reaction produces hydrogen gas, which is flammable. The high electrochemical potential difference between aluminium and hydrogen, coupled with the low hydrogen overvoltage, can lead to uncontrollable reactions if the aluminium is too fine. Conversely, coarse particles increase the cementation time. Therefore, aluminium should be used with an optimal grain size to ensure effective cementation conditions. The cementation process results in significant hydrogen formation, leading to high aluminium consumption (Rumpold & Antrekowitsch, 2012).

Cementation with copper is less well-documented, with only a few papers discussing this process. The acidity of the solution plays a significant role in the cementation reaction when hydrogen ions are involved. Since the reduction potential of Cu(II) is higher than that of hydrogen ions, hydrogen

evolution does not occur during cementation with copper metal powder. The amount of copper added to the solution significantly affects the cementation of palladium (Pd). The acidity and side reactions in the media necessitate adding copper in excess (Nguyen & Lee, 2023; Aktas, 2012). Furthermore, cementation can produce toxic gases such as NO<sub>x</sub>, so careful monitoring is required to optimize recovery rates and minimize the generation of these hazardous gases (Nguyen & Lee, 2023).

#### 5.5.5 Molecular recognition technology

Molecular Recognition Technology (MRT) represents an advanced approach for achieving highly selective metal separation. This technique involves bonding metal-specific ligands to solid matrices, such as polymer substrates or silica gel, followed by solid-phase extraction, which eliminates the need for organic solvents. MRT offers several key advantages over traditional methods. It operates with high reaction speeds, allowing for efficient and rapid metal separation, and exhibits remarkable selectivity, enabling the precise binding of target metals. Additionally, the technology features strong binding energies between the ligands and target metals, ensuring effective extraction, and is environmentally friendly due to the elimination of organic solvents. The high selectivity of MRT is achieved through several mechanisms. It uses recognition molecules with specific shapes and functional groups tailored to the target metal, facilitating strong interactions. The three-dimensional alignment of atoms and complementary functional groups enhances this selectivity, while parameters such as temperature and pH can be controlled to optimize the extraction process (Chidunchi et al., 2024).

The principles underlying MRT trace back to 1987, when Pedersen's research on selective binding of alkali metal ions using cyclic polyesters earned him the Nobel Prize (Izatt, 2007). MRT employs custom-designed ligands chemically attached to solid supports for precise metal separations. An example of this is SuperLig<sup>®</sup> resins, which consist of ligands pre-designed using supramolecular chemistry principles to achieve high target metal selectivity. These ligands are covalently bound to silica gel or other solid supports and used in solid bead form within a packed column. The high selectivity of SuperLig<sup>®</sup> resins for target PGMs, combined with the non-use of organic solvents, allows for the design of low-complexity operating systems. The selective and complete separation of the target PGM during the loading step ensures that traces of the target PGM do not pass into the raffinate, which would otherwise require further separation steps downstream. High metal selectivity and binding strength enable high-capacity loading of the target PGM on the SuperLig<sup>®</sup> resin, as competing metals either do not bind or are displaced due to the stronger binding of the target PGM. This results in the complete separation of the target PGM from other PGMs and base metals, which proceed to the raffinate. Subsequent use of other SuperLig<sup>®</sup> resins can further separate the remaining PGMs, leading to comprehensive recovery and conservation of valuable resources while avoiding significant waste generation (Izatt et al., 2023).

SuperLig<sup>®</sup> resins are utilized particularly for exclusive palladium separations at Impala Platinum's Germiston refinery in South Africa and are also applied in Japanese and Chinese PGM refineries. It addresses the need to isolate harmful elements from PGM-containing solutions, preventing their incorporation into waste products. However, the resins used in MRT are proprietary and not available on the general market. Their highly customized manufacture incurs considerable costs, which justifies their use primarily in niche applications such as large-scale PGM recovery (Hosseinzadeh & Petersen, 2024).

Despite these benefits, MRT faces certain challenges. The concentration of PGMs in primary refinery liquors is substantially higher than in typical catalyst leach liquors. Even with high adsorption rates, residual PGMs may remain at levels similar to those found in catalyst leach solutions. Additionally, MRT is most effective for selectively separating individual metals from specific solutions. Its efficiency



may decrease when handling complex mixtures with a broad range of elements. Developing ligands capable of selectively recognizing multiple metals simultaneously, or creating process sequences involving multiple MRT resins, remains a significant challenge (Hosseinzadeh & Petersen, 2024).

#### 5.5.6 Cloud point extraction

Cloud point extraction (CPE) is an eco-friendly method for the preconcentration and separation of various analytes, offering significant advantages over traditional liquid-liquid extraction. This technique is fast, inexpensive, accurate, selective, and precise, and is considered a green extraction procedure due to its minimal use of toxic organic solvents. CPE relies on the property of non-ionic surfactants to form micelles in aqueous media when heated above a certain temperature, known as the cloud point (Samaddar & Sen, 2014), or by adding salt to induce the salting-out phenomenon. The separation into two phases—an aqueous phase and a surfactant-rich phase—occurs through centrifugation, with the analyte typically partitioning into the surfactant-rich phase (Mortada, 2020; Pocurull et al., 2020; Suoranta et al., 2015).

The first application of CPE was in 1976 by extracting  $\text{Ni}^{2+}$  from aqueous solutions after complexation with 1-(2-Thiazolylazo)-2-naphthol (TAN) and Triton X-100 as the micelle-mediated extracting agent. Since then, CPE has been used for the preconcentration of various metal ions and other analytes, such as albumin, persistent organic pollutants (POPs), fluoroquinolone antimicrobial agents, pesticides, and insecticides (Mortada, 2020; Makua et al., 2019).

CPE operates on the principle that non-ionic surfactants, when heated above their cloud point, exceed their critical micellar concentration (CMC) and form micelles as it is shown on the Figure 10. These micelles consist of hydrophobic tails that orient inward to minimize contact with water, and hydrophilic heads that face outward. Alternatively, micelle formation can occur at room temperature with the addition of salts, known as the salting-out effect. Phase separation, accelerated by centrifugation, results in a surfactant-rich phase containing most of the surfactant molecules and the hydrophobic analytes, and an aqueous phase containing molecules or ions that do not incorporate into the micelles. For CPE to be effective, the substance to be separated must be hydrophobic or convertible to a hydrophobic form, ensuring incorporation into the micellar system. Surfactants are crucial in CPE, classified into non-ionic, anionic, cationic, and zwitterionic types based on their hydrophilic group. Non-ionic surfactants are most widely used due to their high stability and minimal effect from added salts, acids, or bases. The concentration of surfactants is critical, with a narrow range required for effective phase separation—too much surfactant reduces extraction efficiency, while too little results in insufficient analyte uptake (Mortada, 2020; Makua et al., 2019; Suoranta et al., 2015).

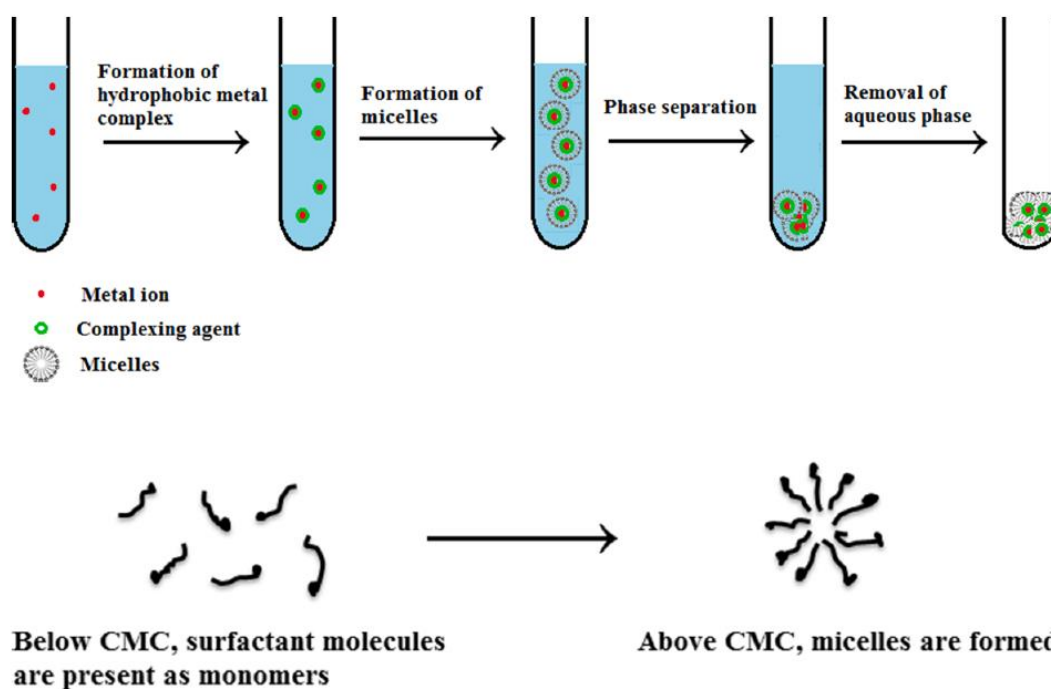


Figure 9: Cloud point extraction of metal ions and formation of a micelle (Mortada, 2020).

The pH of the medium significantly influences CPE, particularly for ionizable species such as metal ions, amines, and phenols. Each CPE procedure has an optimal pH range where the extraction of the analyte is quantitative, with the uncharged form of the analyte being incorporated into the micelles. The stability constant of metal complexes, affected by pH, plays a critical role in the separation of metal ions. For instance,  $\text{Pt}^{2+}$  and  $\text{Pt}^{4+}$  can be separated by CPE based on their stability constants at different pH levels. At pH 7,  $\text{Pt}^{2+}$  forms a stable complex with a thiosemicarbazide derivative, allowing its extraction into the surfactant-rich phase, while  $\text{Pt}^{4+}$  does not form a stable complex under these conditions (Mortada, 2020; Suoranta et al., 2015). Temperature is another vital factor in CPE, with increasing temperatures above the cloud point leading to micelle dehydration, forming a turbid solution, and resulting in phase separation. This property of CPE makes it a versatile and efficient technique for the separation and preconcentration of various analytes in different fields, maintaining its relevance and application since its inception (Mortada, 2020; Suoranta et al., 2015; Samaddar & Sen, 2014). The recovery of PGM through CPE is still studied but according to Suoranta et al. (2015), this process can achieve  $91 \pm 6\%$  for Pd,  $91 \pm 5\%$  for Pt,  $85 \pm 6\%$  for Rh, and  $66 \pm 11\%$  for Ru.

## 6 Experimental context

The primary objective of this research is to identify optimal parameters for recycling platinum group metals from a leaching solution through cementation onto copper and to study the kinetics of this reaction. Additionally, the study explores the effects of ultrasound on the cementation process to gain a comprehensive understanding of this system. Cementation onto copper for PGM recovery is a relatively unexplored area in the literature, making this research a significant contribution to future recycling initiatives.

This research aligns with the goals of Monolithos Catalysts & Recycling Ltd., an Athens-based company where I completed a six-week internship. Together, we established objectives that focused on the real-life application of recovering PGMs from the leachate of spent catalysts via cementation onto copper, with the goal of directly reusing the recovered PGMs in new catalytic converters. The

experimental roadmap for the work conducted in Athens is depicted in Figure 10. The study of ultrasound's impact on cementation will be conducted at the GEMME laboratory in Liège.

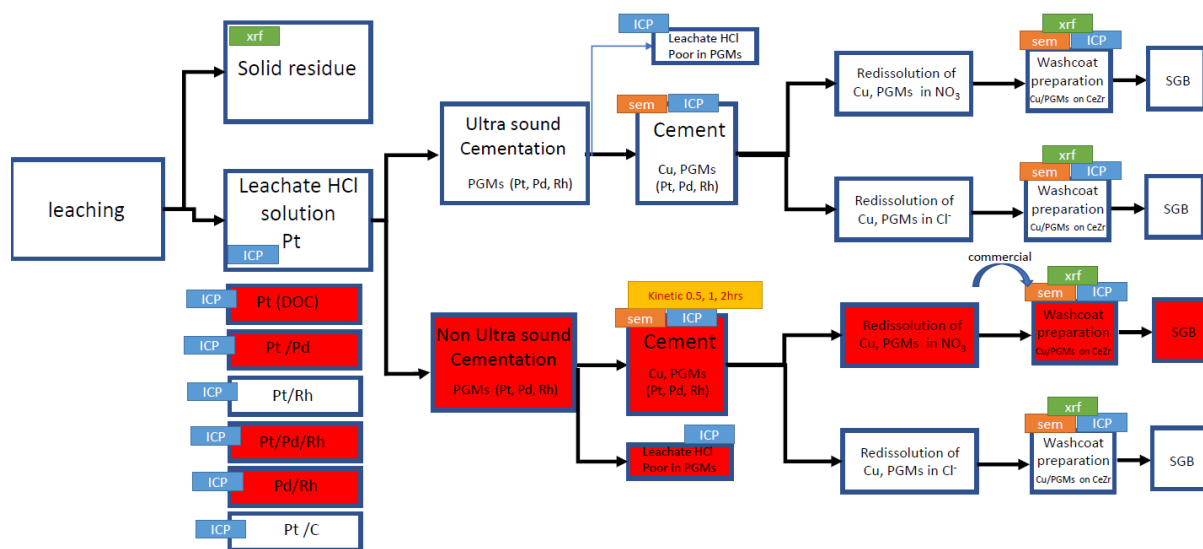


Figure 10: Roadmap of the internship at Athens at Monolithos Catalyst & Recycling Ltd.

This research was conducted as part of the European project CHemPGM, which aims to exploit Platinum Group Metals from secondary materials to enhance and secure the PGMs value chain. The CHemPGM project focuses on improving existing processes and developing new ones, all in alignment with sustainable principles, to establish a circular operation model for the relevant industries.

## 7 Materials and reagents

The materials and reagents used in the experiments were consistent across all trials. The copper powder employed was 99.69% pure, as verified by a certificate of analysis from ThermoFisher Scientific. Scanning Electron Microscopy (SEM) analysis determined that the copper powder particles

had a mean diameter of 58  $\mu\text{m}$ . The particle size distribution, expressed as cumulative mineral mass percentage, is illustrated in Figure 11.

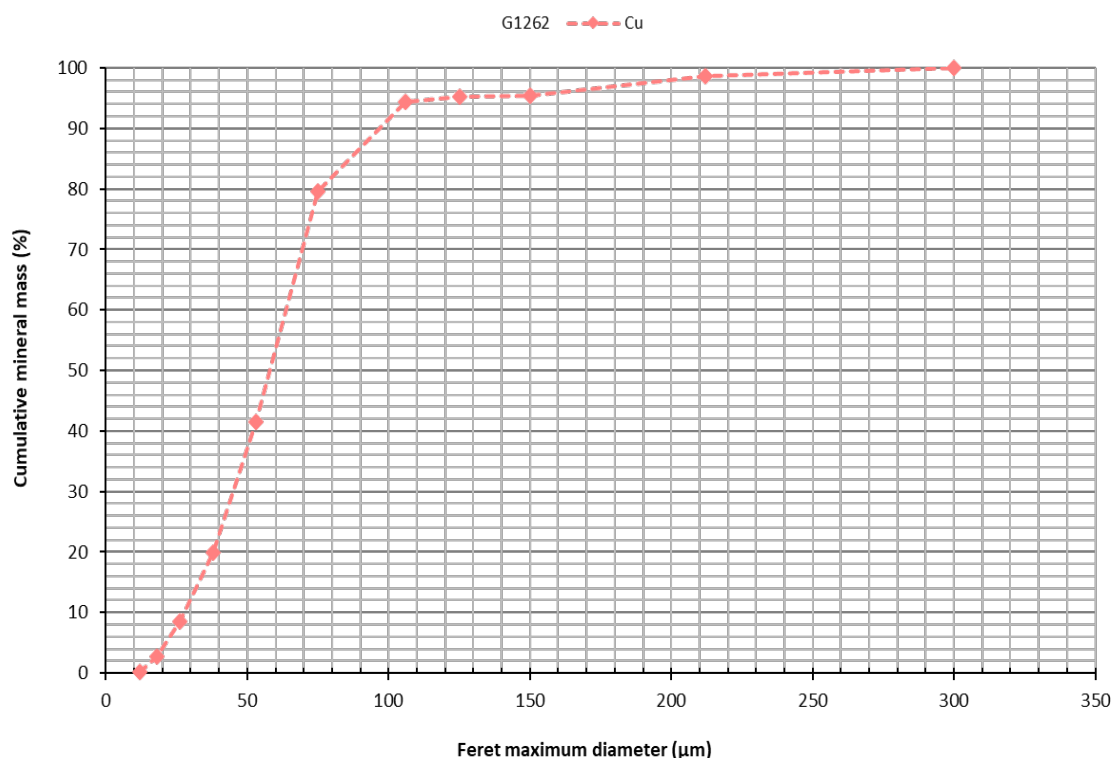


Figure 11: Cumulative mineral mass percentage based on the SEM analysis of the copper powder used for the different experiments

Analytical-grade hydrochloric acid (37% HCl), branded as "AnalaR NORMAPUR" from VWR Chemicals, was used in all experiments. For experiments requiring a synthetic platinum solution, platinum (IV) chloride, sourced from ThermoFisher Scientific, was dissolved in deionized water with 37% HCl.

Two distinct leachate solutions were used: one derived from Diesel Oxidation Catalysts (DOC) prepared at Monolithos Catalysts & Recycling Ltd. in Athens, and the other from a mix of various catalytic converters prepared at the GEMME laboratory.

### 7.1 Composition of the initial solutions

A synthetic solution was used during the experiments with a concentration of 175 ppm of Platinum, an initial pH of 1.5 and a redox potential of 800 mV vs. SHE. It was only composed of platinum chloride, deionised water and HCl 37%.

The Pt-DOC solution from Athens, derived from diesel catalytic converters, primarily contained platinum, with occasional trace amounts of palladium. The solution had a negative pH, a redox potential of 750 mV vs. SHE, and platinum concentrations that varied from 400 ppm to 1300 ppm, depending on storage conditions and aging. This solution was stored in various containers, referred to as "batches," and analysed by inductively coupled plasma optical emission spectrometry (ICP-OES, Varian Liberty Series II) at the GEMME laboratory.

The leachate solution from the GEMME laboratory contained 410 ppm of palladium, 219 ppm of platinum, and 60 ppm of rhodium. It had a pH of 1.6 and a redox potential of around 720 mV vs. SHE. Additionally, this solution contained 30 ppm of copper and 3500 ppm of iron.

## 8 Experimental Setup

Two distinct experimental setups were employed, tailored to the equipment availability in each laboratory.

### 8.1 Athens Setup

The experimental arrangement in Athens consisted of a 600 mL beaker placed on a heating plate equipped with a magnetic stirrer. The stirring of the hot plate was controllable with a dial. A thermometer mounted on a stand was used to monitor the temperature, and the beaker was covered with a watch glass to minimize evaporation and contamination. Two types of magnetic stirrers were utilized: one measuring 3 cm and another 4 cm in length, both featuring a central ridge to reduce friction and enhance mixing efficiency.



Figure 12: Experimental setup at the laboratory of Monolithos Catalysts & Recycling Ltd. at Athens.

### 8.2 Liège Setup

At the GEMME laboratory, a different apparatus was utilized. The core of the setup was a custom-made, double-walled, flat-bottomed cylindrical glass reactor with an inner diameter of 65 mm, an outer diameter of 90 mm, and a height of 110 mm. This reactor featured four necks for various attachments. The reactor's bottom incorporated a 5 mm thick borosilicate glass disk affixed to a bolt-clamped Langevin-type transducer with a contact surface area of 50.3 cm<sup>2</sup> (MPI-7850D-20\_40\_60H, Ultrasonics World). A custom stainless-steel frame coupled with EPDM gaskets ensured a secure and sealed assembly.

Temperature control was achieved by connecting the reactor to a thermostatic water bath (Polystat 36, Fisher Scientific), maintaining the process temperature within  $\pm 1$  °C. Ultrasonic waves generated by the transducer were regulated using a radio frequency amplifier (E&I 2100L, Electronics and Innovation) in conjunction with a waveform generator (DG1032z, Rigol).

Mechanical stirring was provided by an overhead stirrer (Eurostar 60 Control, IKA) equipped with a PTFE-jacketed stainless-steel shaft of 6 mm diameter and a PTFE propeller featuring four 45° angled blades (axial flow type) with a diameter of 40 mm. The impeller blades were positioned 3 cm above the reactor bottom to optimize mixing. To prevent overheating, an axial fan (DP201AT2122HST,

Sunon) was directed at the transducer during operation. Notably, the transducer was arranged to avoid direct contact with the solution, thereby mitigating potential contamination from corrosion or erosion of its surface.

The samples taken during the experiments were filtered by a Whatman prepleated qualitative filter paper, grade 2V filter with a mesh size of 8 $\mu$ m.

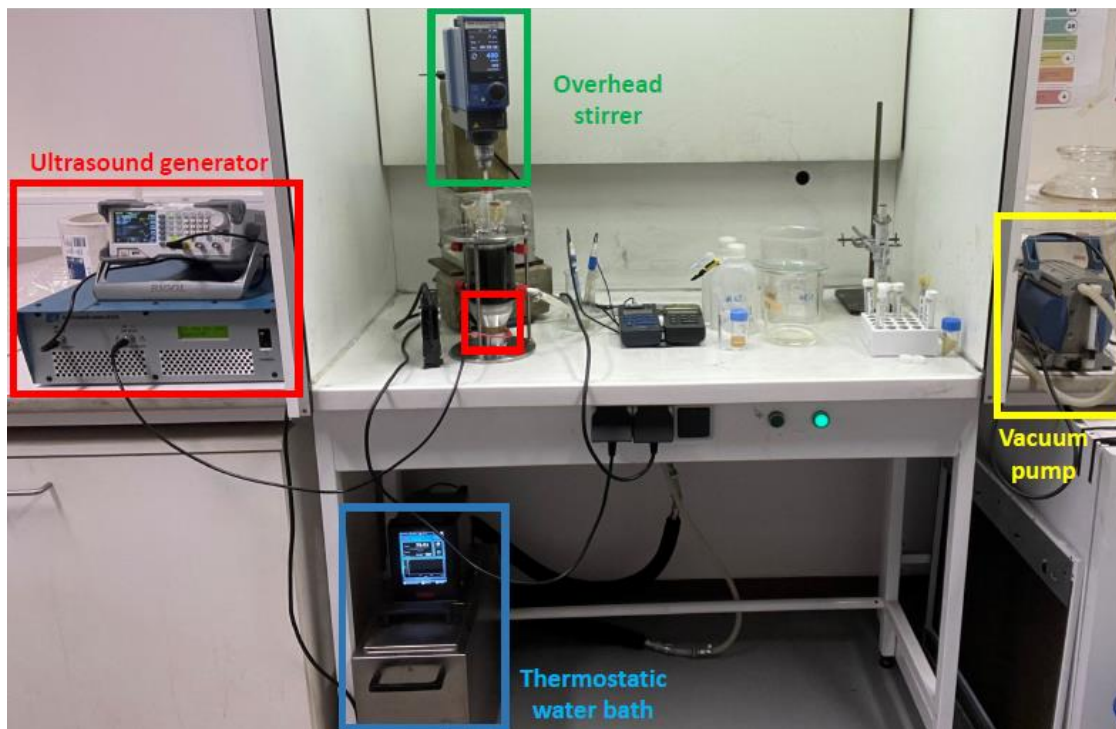


Figure 13: Experimental setup at the GEMME laboratory at Liège.

### 8.3 Post-experiment filtration

At the end of each experiment, vacuum filtration was employed to separate the solid precipitates from the liquid phase. A cellulose filter from AHLSTROM called ReliaDisc™ Membrane Filters with a mesh size of 0.45  $\mu$ m and a diameter of 5 cm was used for this purpose. The vacuum filtration setup ensured a more efficient and rapid separation process by applying reduced pressure, which pulled the liquid through the filter while retaining the solid particles on its surface. This method was particularly useful for collecting the fine cemented materials formed during the reaction. The cellulose filter was chosen because it can be easily dissolved later, allowing for the recovery of the majority of the cemented material for further analysis. This step ensured minimal loss of the precious metal content and provided a clean separation of solids from the liquid, facilitating accurate downstream processing and characterization.

## 9 Experimental procedure

The experimental procedure was structured into several distinct phases to evaluate the cementation of PGMs onto copper and to explore the impact of ultrasound on this process.

The initial phase involved assessing the feasibility of PGMs cementation using a synthetic solution containing only platinum. This preliminary step was designed to confirm whether the cementation reaction could occur under controlled conditions without interference from other elements. Following this, in the Monolithos Catalyst & Recycling Ltd. laboratory at Athens, a series of general experiments were conducted with a real-life leachate solution to understand the overall behaviour of

the system. At this stage, ultrasound effects were not considered; the focus was on determining effective parameters such as temperature, agitation, and copper amount to globally understand the system respond to the addition of the copper powder. Upon returning to Liège, additional experiments were carried out using a new solution, incorporating insights from previous tests. These experiments were conducted under more controlled conditions, with precise monitoring of temperature, pH, and redox potential, reduced evaporation, and mechanical stirring. This phase provided a baseline for comparing results with and without ultrasound.

The experiments investigated various parameters including temperature (25°C, 45°C, 65°C, and 85°C), agitation (0 to 500 rpm), and the amount of copper added (5 to 15 times the stoichiometric amount needed to recover PGMs in the initial solution). Additionally, the effect of ultrasound was studied using different frequencies (20 kHz and 40 kHz) and power levels (4W, 10W). At Athens, cementation times ranged from 30 minutes to 3 hours. Based on these results, experiments at Liège were conducted over two hours, with samples taken at 5 minutes, 30 minutes, 1 hour, and 2 hours.

At Athens, the experiments were carried out with a 250 mL solution, which was measured using a graduated cylinder. The solution was brought to the desired temperature before the copper was added, marking the start of the experiment. Depending on the target temperature, some evaporation occurred, occasionally reducing the volume by up to 50 mL. While the heating system and vessel setup differed from a heating bath and sealed system, efforts were made to minimize evaporation by covering the vessel with a glass watch. To conduct a kinetic study, different reaction times are generally required. However, at Athens, it was not possible to sample during the experiment, meaning that each experiment corresponded to a single reaction time. This approach necessitated performing separate experiments for each reaction time of 30 minutes, 1 hour, 2 hours, and 3 hours. Due to equipment availability, each experiment was conducted on a different day, resulting in a complete set of parameters taking about a week. In contrast, at Liège, sampling during the experiments allowed for monitoring different reaction times within a single experiment. Additionally, the availability of equipment enabled the performance of up to two experiments per day, making the process more efficient and reducing the overall time required for data collection. A significant advantage of the procedure conducted at Monolithos Catalysts & Recycling Ltd. was the larger volume of filtrates available for each cementation time, which allowed cross-checking results between the two laboratories.

In the laboratory at Liège, experiments were conducted using 300 mL of leachate solution from old catalytic converters, freshly sampled from a main stock solution. The solution was homogenized before being stirred at a fixed speed, with the temperature pre-set and regulated. Copper powder was then added to the solution, and if sonication was studied, ultrasound was simultaneously applied, marking the beginning of the experiment. At each sampling point, if sonication was in use, it was temporarily stopped to monitor pH, Eh, and temperature. The sample was then taken, filtered with a mesh size of 8  $\mu\text{m}$ , and replaced by an equal volume of stock solution. At the conclusion of the experiment, the reactor's contents were vacuum filtered, and the solid part was gently washed. The first wash was done with an HCl solution at pH 1.5 to match the solution's pH, followed by a final rinse with deionized water to prevent any reaction of the solid with the HCl wash solution in the drying oven. The solid was then dried overnight at 65°C.

The analysis of samples from both Athens and Liège involved several steps. After each experiment, the filtrate and wash solutions were analysed using ICP-OES to determine the concentrations of PGMs, allowing for the construction of a metallurgical balance. The cemented solid could be also analysed by ICP-OES and Scanning Electron Microscopy – Energy-Dispersive X-ray Spectroscopy (SEM-EDS) to understand the distribution of metals and particle size. Before ICP-OES analysis, tellurium



precipitation was required to remove sodium from the solution, as sodium can damage the plasma torch of the machine and interfere with the detection of PGMs. This standardized analysis protocol was developed in the GEMME laboratory in collaboration with Bachelet laboratories, and adjustments were made to analyse smaller sample volumes, minimizing the quantity required for accurate analysis. Indeed, initial protocol required 10mL of solution but after adjustments, 3 to 5mL would be enough.

## 10 Analysis of the experiments

Mohamed Aâtach, a member of the thesis committee who was on secondment at Monolithos Catalysts & Recycling Ltd. during my internship, demonstrated theoretically that the cementation of PGMs onto copper is feasible both thermochemically and kinetically using synthetic solutions. This study aimed to verify the feasibility of high recovery rates in real-life solutions and assess the impact of sonication on the cementation process.

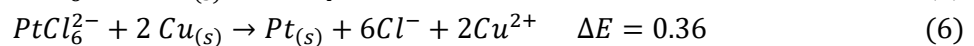
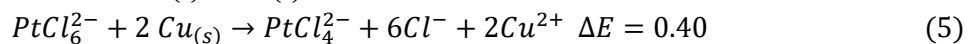
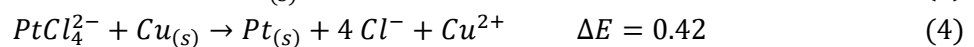
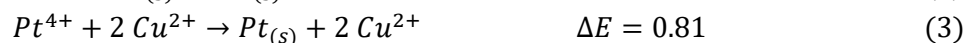
### 10.1 Calculations and limitations

The kinetics of cementation are characterized by the progression of the PGM conversion rate, which is defined as the difference between the PGM concentration measured at time  $t$  and the total PGM available for cementation at that time. This includes adjustments for the stock solution volumes used to maintain the level and accounts for all liquid samples taken for monitoring. Consequently, the PGM cementation rate is initially equated to the degree of PGM removal, thereby disregarding the potential impact of any other PGM dissipation processes.

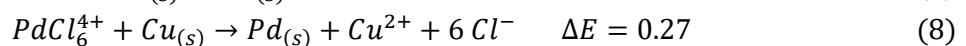
#### 10.1.1 Cementation reactions in the different solutions

Understanding the reactions that could occur in the studied system is important. This study specifically investigates the cementation of platinum group metals onto copper. The reactions involved in this system can be broadly described by redox processes, where PGMs are reduced and deposited onto the copper surface. The reactions happen in a hydrochloric solution. The Pt-DOC solution is mainly composed of platinum while the GEMME solution is composed of palladium, platinum, and rhodium. The different reactions studied are based on these three elements, the hydrochloric solution and the sacrificial metal added to the system which is the copper.

Focusing on the platinum reactions:

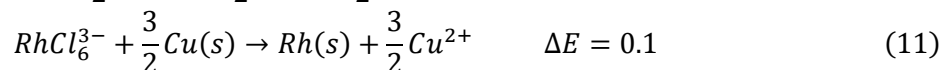
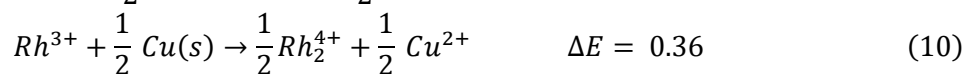


Focusing on the palladium reactions:





Focusing on the rhodium reactions:



In these reactions, the  $\Delta E$  is a critical factor. It represents the difference in the electrochemical potentials of the reactants and products, which drives the reaction forward. A positive  $\Delta E$  indicates a favourable reaction where energy is released as the PGMs are reduced and deposited. These equations detail the system in a hydrochloric medium and give an idea of the stoichiometric factor between each element and the solid copper. The higher stoichiometric factor was chosen for each element to know how much copper should be added to the system to have specific Cu/PGM molar ratio.

The metal copper can also dissolve in the solution as  $Cu^+$  which only liberates 1 electron. This would consume two times the stoichiometric amount of copper needed. Copper complexes can also be formed in hydrochloric solution which is another consumption of copper by the system. The copper added to the system should therefore be in excess to be able to cement all the PGMs in the different solutions even if side reactions also occur.

#### 10.1.2 Impact of the pH and $E_h$

During the experiments, key parameters such as pH and  $E_h$  were continuously monitored when possible. A drop in redox potential was observed to be important for achieving high PGM removal percentages. Both real-life solutions initially had an  $E_h$  of approximately 750 mV vs. SHE. In the Pt-DOC solution,  $E_h$  dropped to negative values when high removal rates were achieved, while in the GEMME solution, it decreased to around 350 mV vs. SHE. Monitoring  $E_h$  provided a useful indication of successful PGM cementation. The pH also increased during the experiments, with the GEMME solution it goes from 1.4 to approximately 2, but no clear trend could be identified.

#### 10.1.3 Mass of the cement

The mass of cement recovered after filtration and drying serves as an indicator of the experiment's effectiveness. By comparing this mass with the initial concentration of PGMs in the solution, one can estimate the minimum mass required to confirm substantial PGMs removal. However, some solids may be lost during manipulation, so this mass provides only an approximate indication of efficiency. If the element is not in its metallic form, it will weigh more, so estimating the minimum mass required for an effective experiment provides a useful approximation. This can quickly give an idea of the overall efficiency of the process while awaiting more comprehensive results.

#### 10.1.4 Platinum or PGMs removal percentage

The percentage of PGMs removed reflects the quantity of PGMs extracted from the solution. Ideally, if PGMs are not present in the solution, they should be in the cement. However, quantification errors or discrepancies in mass balances can affect accuracy. Although detailed analysis of the cements was not performed within this study, future work by Mohamed Aâtach could provide validation. Removal percentage is calculated by comparing the initial concentration of the element to its concentration in the filtrate, adjusting for added quantities after sample compensation. Recovery rates higher than 95-96% are generally considered as completely recovered, given the small quantities involved in the initial solution and the significant impact of even minor manipulation errors.

### 10.1.5 Precipitant factor

The precipitant factor measures the quantity of the copper present in the solution compared to the quantity of PGMs recovered. The goal is to minimise this indicator. However, this indicator is not perfect. If copper precipitates after being dissolved without cementing the PGMs, the precipitant factor will be underestimated. To the best of my knowledge, no other indicators provide a precise understanding of the system and its reactions. Therefore, while the precipitant factor serves as a useful general indicator, its limitations should be carefully considered.

$$\text{Precipitant factor} = \frac{\text{mass of Cu in the final solution}}{\text{mass of PGMs recovered}} \quad (11)$$

### 10.1.6 Limitations of the ICP

The analysis using Inductively Coupled Plasma Optical Emission Spectroscopy (ICP-OES) encountered several limitations, primarily due to sample volume constraints and dilution effects. The initial procedure aimed for a 5-fold dilution of samples for analysis. However, due to the small volumes available for analysis (3 to 4 mL after accounting for sample retention in filters), the actual dilution often approached 20 to 25 times. This substantial dilution increased the detection limits. Indeed, the ICP-OES instrument has inherent detection limits, which are exacerbated by higher dilution factors. As the sample is diluted more, the effective concentration of elements decreases, pushing the results closer to or below the instrument's lower detection thresholds. Consequently, this can lead to inaccurately high readings for elements at low concentrations, as the raw results are multiplied by the dilution factor. For instance, during experiments at Liège, the machine reported imprecise results for Rhodium concentrations below 40 ppm, even though the initial concentration was 60 ppm.

To address these challenges, it was decided to analyse larger volumes of filtrates and wash solutions to enhance measurement precision. When results fell below reliable detection levels, the values were adjusted by dividing the reported concentrations by two to provide a more realistic estimate. Despite these adjustments, the inherent limitations of ICP-OES and the effects of high dilution factors highlight a particular attention to these lower detection limits.

### 10.1.7 Filtration at the end of the experiments

At the conclusion of the cementation period, filtration was performed to separate the solid cement from the liquid filtrate. The start of the filtration process could be delayed by a few minutes depending on the availability of the necessary materials. The experimental conditions were only concluded once all equipment was prepared for filtration. In some cases, the filtration process was prolonged due to factors such as the temperature of the filtrate, the distribution of particle sizes, and the precipitation of salts. The final cementation time was defined as the moment when the filtrate was fully separated from the solid, ensuring that no further reactions could occur. These filtration delays were accounted for in the subsequent calculations to ensure accurate results.

The formation of white crystals after significant evaporation in experiments with the Pt-DOC solution posed challenges during the final filtration step. It is hypothesized that this precipitate consists of sodium chloride crystals, as it dissolves upon washing. Additionally, a yellowish fine precipitate was observed during experiments with the GEMME solution at 85°C, further complicating filtration. This precipitate is likely a result of iron hydrolysis, as discussed in Section 10.5.4.1, which aligns with the expected behaviour of iron under these conditions. Both precipitates hindered the filtration process, highlighting the importance of optimizing experimental conditions to ensure efficient filtration.

## 10.2 Conditions for an interesting cement

In cementation processes, the sacrificial metal inevitably becomes part of the final cement. It is essential to select a sacrificial metal that does not introduce impurities or complicate the future use of the noble metals. Copper is an advantageous choice as a sacrificial metal for several reasons. It is increasingly used as a substitute in new catalytic converters to reduce the quantity of PGMs required. For instance, Monolithos has recently begun commercializing a new catalytic converter primarily composed of copper (Yakoumis, 2021). Therefore, using copper as the sacrificial metal minimizes the risk of future impurities.

Discussions at Monolithos have highlighted that other elements are not considered as impurities for the reuse of recovered PGMs. The primary objective is to achieve high recovery rates to avoid losing valuable metals in the solution. It is important to minimize the ratio of copper to PGMs in the cement. Although copper can be used as a substitute, there is a threshold beyond which its presence becomes problematic. If the copper content exceeds this limit, additional PGMs can be introduced into the cement to achieve the desired composition. Moreover, achieving a small particle size for copper is beneficial as nanoparticles possess exceptional catalytic properties. This enhances the overall effectiveness of the cementation process and ensures better performance in applications where the cemented material is used.

The presence of other metals in the solid after the cementation of PGMs onto copper does not pose an issue for Monolithos Catalyst and Recycling Ltd, as they are not regarded as impurities. Consequently, the presence of iron and aluminium is not problematic. If the concentrations of these elements exceed the permissible limits for use in a new catalytic converter, supplementary PGMs can be introduced to correct the ratios. Therefore, these metals do not present a challenge in the process.

## 10.3 Synthetic solution

### 10.3.1 Conditions of the experiment

The initial experiment was conducted using a synthetic solution to assess the kinetical feasibility of cementing platinum onto copper. This approach was chosen to establish a baseline and determine whether high recovery rates could be achieved with this method in suitable timing. Synthetic solutions offer a controlled environment and the ability to avoid complications associated with real-life solutions, such as the presence of sodium, which requires additional tellurium precipitation—a time-consuming process that limits sample throughput to about four per day.

Synthetic solution, silent, 200 rpm, 65°C, 16 Cu/PGM (mol/mol), 3 hours

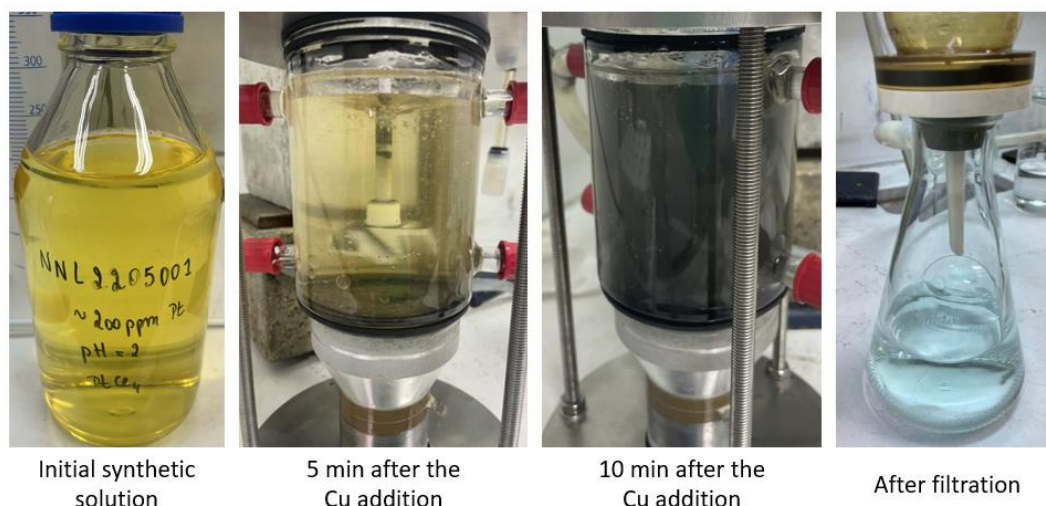


Figure 14: Experiment on the synthetic solution with 175ppm of Pt, HCl 37% and deionised water to reach a pH of 2. The cementation was done without sonication, at 65°C for 3 hours with a mechanic agitation of 200 rpm. The added copper represents 16 times the stoichiometric amount needed to recover all the PGM.

The synthetic solution used in this experiment contained approximately 200 ppm of platinum, with an initial pH of 1.5 and a redox potential of 800 mV vs SHE. The colour of the initial solution was yellowish. The setup for the experiment was conducted in the GEMME laboratory, as depicted in Figure 14. The copper amount added to the system was 16 times the stoichiometric amount required to recover all the platinum.

#### 10.3.2 Results of the experiment on the synthetic solution

The results, illustrated in Figure 15, demonstrate the effectiveness of the cementation process. Within 30 minutes, over 95% of the platinum was removed from the solution, and by 2 hours, nearly 100% of the platinum had been removed. These findings indicate that the selected parameters—65°C, 200 rpm agitation, and 16 times the stoichiometric amount of copper, without sonication—are effective for cementing all the platinum from the chloride solution within an acceptable timeframe.

The next step is to evaluate whether this method can be applied to more complex solutions that contain a greater variety of metals and have a lower initial pH.

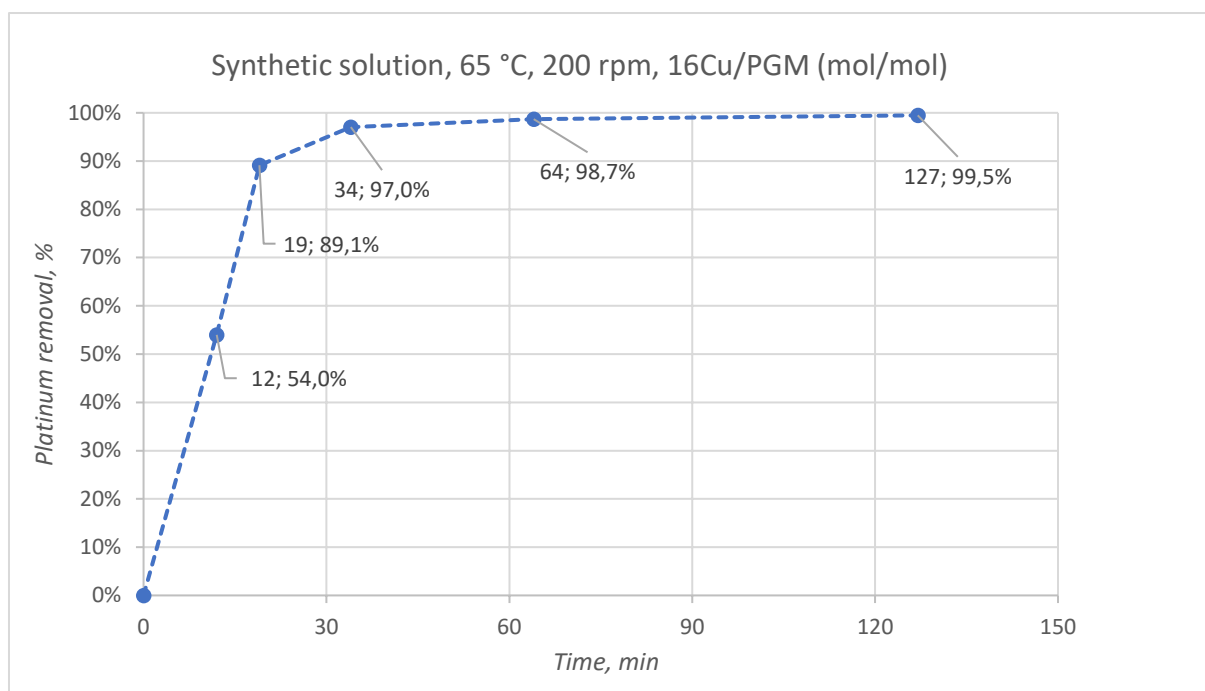


Figure 15: Results of the experiment carried out with a synthetic solution containing 175 ppm of Pt at 65°C, using an overhead stirrer set to 200 rpm for agitation. The experiment utilized 16 times the stoichiometric amount of Cu compared to the Pt concentration. The graph illustrates the percentage of platinum removed from the solution over time.

## 10.4 Pt-DOC solution at Monolithos Catalyst & Recycling Ltd. without sonication

### 10.4.1 Conditions of the experiments

The experiments conducted in Athens aimed to provide an overview of how a real-life solution behaves in the cementation of PGMs onto copper. Various tests were performed using the same set of parameters to examine the influence of temperature on the system. The solution used was highly acidic, with a negative pH, making pH monitoring during the experiments impractical because the equipment was not designed to handle such low acidity.

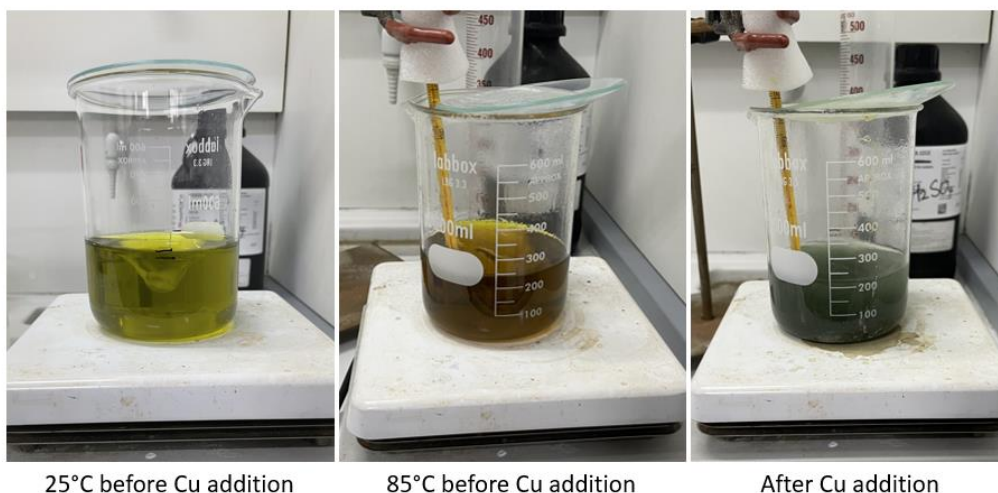
The temperatures studied were 25°C, 45°C, 65°C, and 85°C, with cementation times ranging from 30 minutes to 1, 2, or 3 hours. Agitation was maintained at 500 rpm using a magnetic stirrer, and the copper amount was initially set at 15 times the stoichiometric amount based on the 1400 ppm of platinum reported by Monolithos. However, it was only after the internship that the actual initial platinum concentration was confirmed to range from 400 ppm to 1300 ppm, leading to copper amounts varying from 16 times to 53 times the stoichiometric amount required.

Once the results for all temperatures were unavailable, I selected the temperature of 85°C as it initially appeared to be the most promising. Experiments were then conducted with reduced copper amounts, specifically five times the stoichiometric amount, which corresponded to 1.6 times the stoichiometric amount needed based on the actual concentration. Additionally, an experiment was carried out for two hours without agitation.

These experiments provided a general understanding of the system's efficiency and helped identify the optimal set of parameters. This information will be valuable for guiding the subsequent experiments conducted in Liège.



Pt (DOC), silent, 500 rpm, 85°C, 53 Cu/PGM (mol/mol)



Pt (DOC), silent, 500 rpm, 85°C, 53 Cu/PGM (mol/mol), solid barely agitated

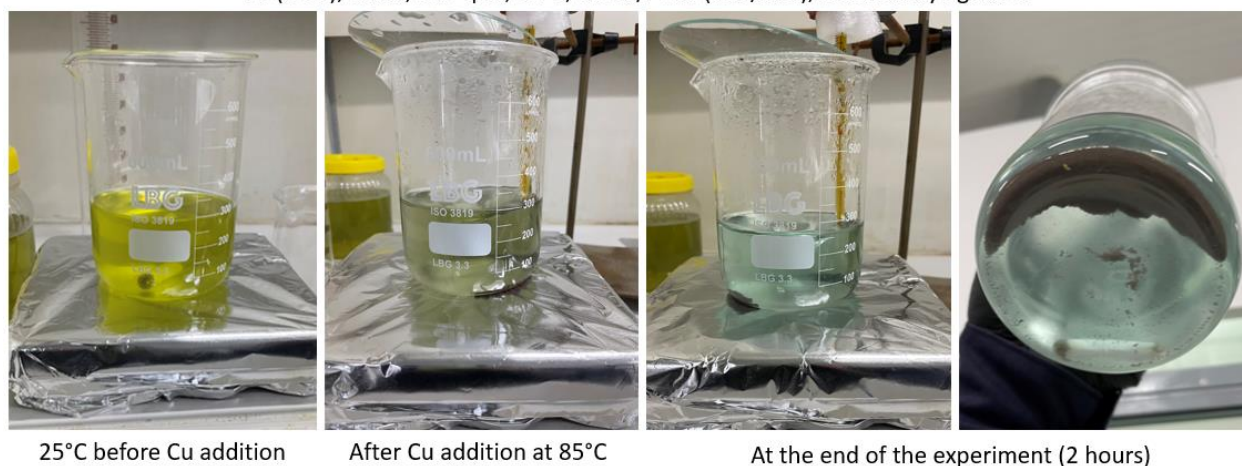


Figure 16: Pt - DOC solution at 85°C without sonication at 500 rpm with 53 Cu/PGM (mol/mol). The two experiments show a difference in the agitation of the solid. The solid is in movement in the first experiment then it is barely agitated in the second experiment.

It is important to note that the behaviour of the solid changed during the experiments at 85°C, as shown in Figure 16. Initially, the solid was in motion, but during the two-hour experiments, it was barely agitated at the bottom of the beaker compared to previous experiments. Despite using the same amount of copper, with identical magnetic stirrers, stirring speeds, and magnetic plates, the solid did not move as it had before. The colour of the final solution also differed, indicating a change in the system's behaviour linked to the agitation of the solid. The only noticeable change during the experiments was the batch of the initial solution; a new container was used.

#### 10.4.2 Preliminary results of the solids from the XRF Olympus gun at Athens.

XRF analysis was performed using an Olympus gun at Monolithos to qualitatively assess the composition of several solids. A calibration method called "Ceramic," developed by the Monolithos laboratory, was used to ensure precise identification of PGMs. The analysis, conducted on five solid samples, confirmed the presence of platinum in experiments conducted at 85°C and 65°C, regardless of the cementation duration.

To maintain sample integrity and improve analysis accuracy, tests were also conducted directly through the falcon tube, which allowed the solid samples to be analysed without removal from their

storage container. These tests showed that the falcon tube's signature could be distinguished without affecting the results, confirming that analysis through the storage container is feasible.

The solids analysed included samples from experiments at 85°C with cementation durations of 30 minutes, 2 hours, and 3 hours, as well as a sample from a 65°C experiment with a 3-hour cementation period. Each of these experiments involved adding 3.47 g of copper to a 250 mL solution containing 400 ppm or 900 ppm of platinum, representing 53 or 25 times the stoichiometric value. Additionally, a separate analysis was conducted on a solid from an 85°C experiment with a 2-hour duration, where only 0.33 g of copper (5 times the stoichiometric amount) was added.

Figures 17 and 18 illustrate the XRF results, showing the presence of copper, platinum, palladium, and tin, along with traces of bismuth, which were ultimately dismissed due to non-corresponding peaks. The exact composition will be verified through ICP-OES analysis of the initial solutions. The results indicate that platinum can be recovered even with low copper input, though the analysis is qualitative and cannot provide quantitative data. However, these rapid XRF analyses effectively verify the success of the platinum cementation process.

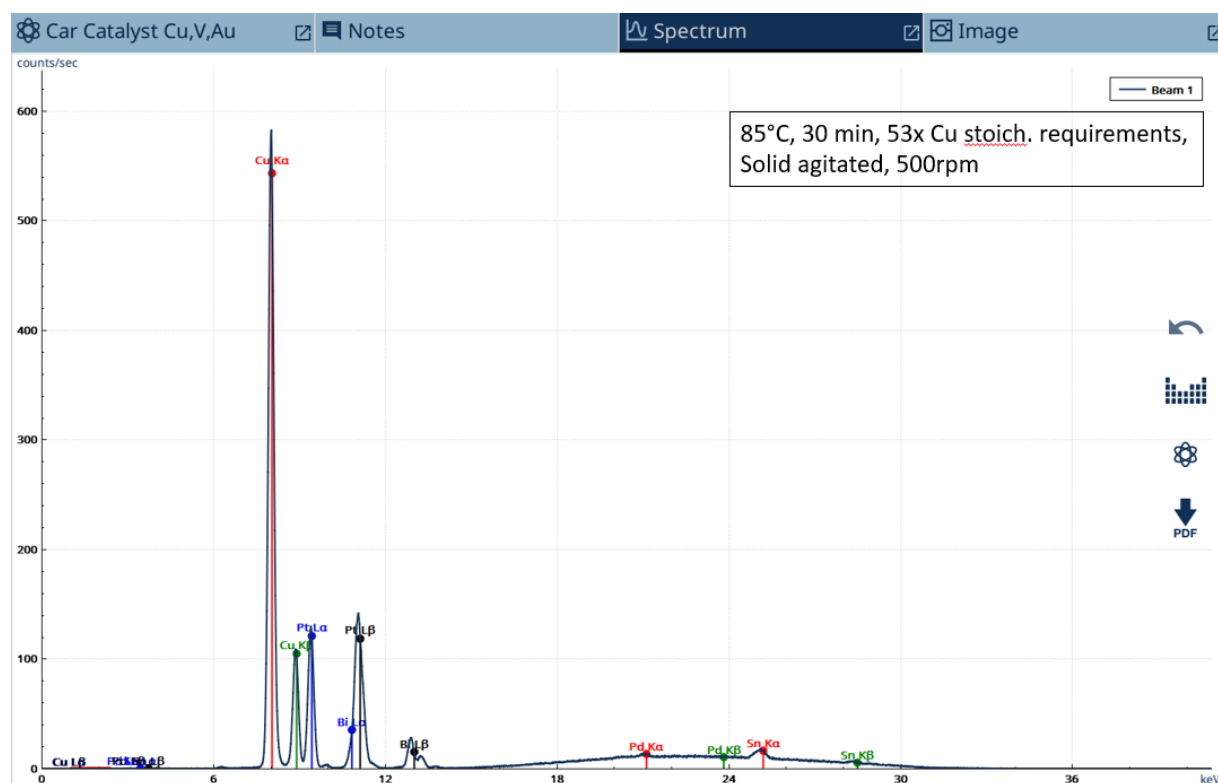


Figure 17: XRF results from the 85°C experiment during 30 minutes of cementation with 53 times the copper stoichiometric amount needed to recover PGM with an agitation of 500rpm.

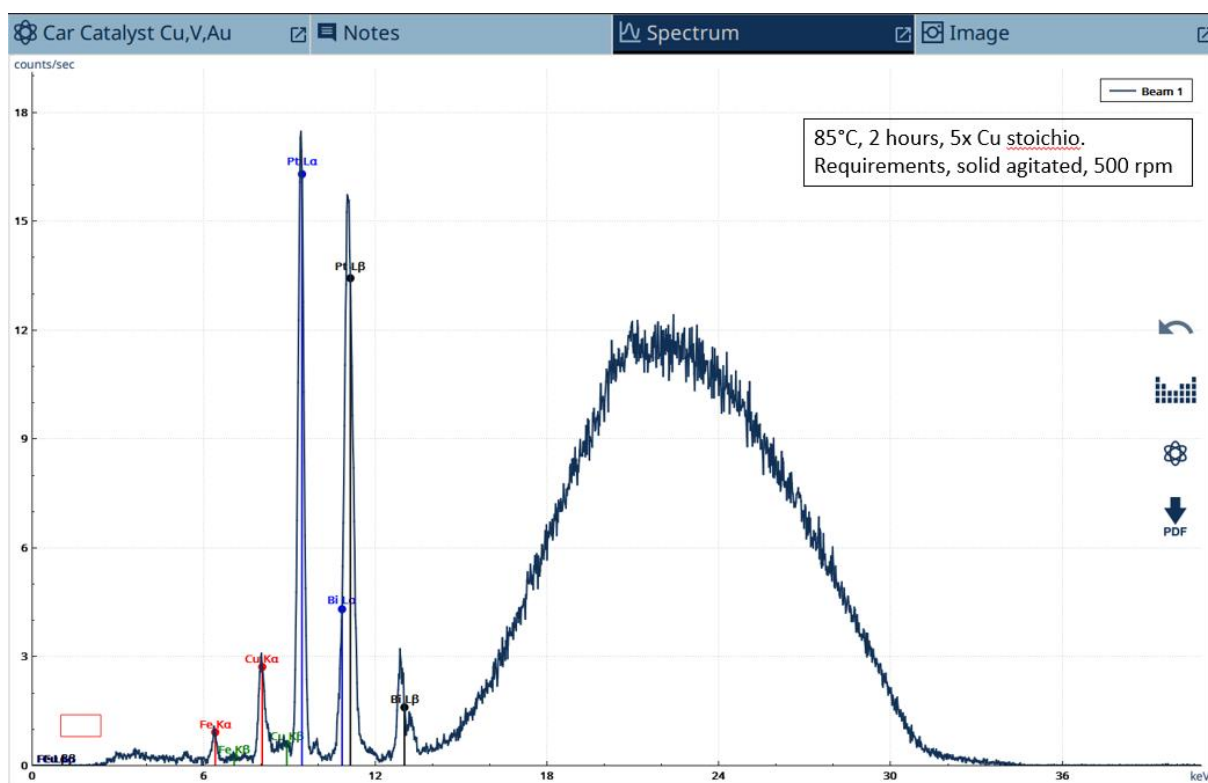


Figure 18: XRF results from the 85°C experiment during 2 hours of cementation with 1.6 times the copper stoichiometric amount needed to recover PGM with an agitation of 500rpm. The influence of the container can be seen on the right of the spectrum.

#### 10.4.3 Results of the experiments on the Pt-DOC solution

In subsequent experiments, the solid exhibited the same reduced movement and did not fully agitate. This change in behaviour can be attributed to the variations in the initial Pt-DOC solution, likely due to aging, storage conditions, or other factors affecting its composition because other parameters stayed unchanged.

The precipitant factor was monitored in the results to provide a general idea of copper powder consumption in the system. While the primary objective was to achieve high recovery rates of PGMs, once these were attained, efforts were focused on minimizing the precipitant factor to maximize overall efficiency. Various temperatures and copper-to-platinum ratios were investigated in the following figures. The variation in copper amounts is due to the fluctuating concentration of the initial solution; however, in each case, the copper quantity exceeded the stoichiometric amount required.



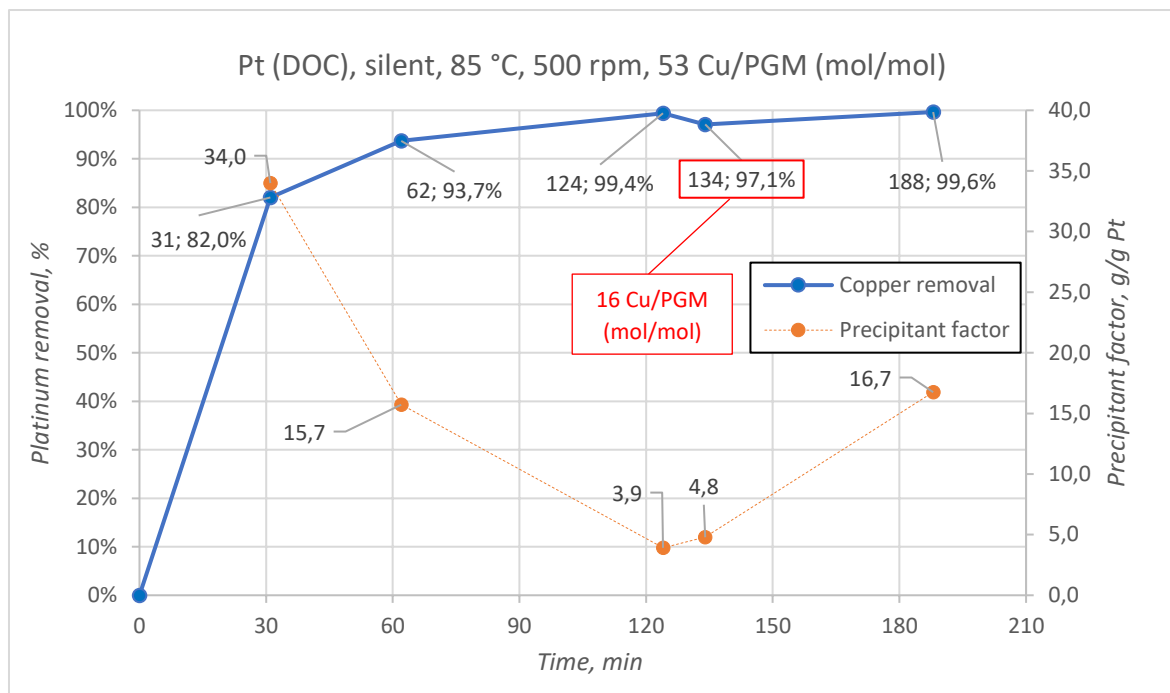


Figure 19: Results of the experiment conducted on the Pt-DOC solution from Monolithos Catalysts & Recycling Ltd. at 85°C, without sonication, using a magnetic stirrer set to 500 rpm, with 53 times the stoichiometric amount of copper to recover the PGMs. The red-highlighted point indicates a comparable experiment under identical conditions, but with a higher initial platinum concentration (900 ppm instead of 400 ppm). The results represent the platinum removal percentage and the precipitant factor. In the experiments lasting 124 and 134 minutes, the solid was barely agitated compared to the solution, which remained in motion.

Figure 19 shows the results of the experiments conducted at 85°C, where high platinum recovery was achieved. The kinetics of the cementation reaction is rapid, with 82% of the platinum being removed from the solution within the first 30 minutes. After 2 hours, platinum removal is nearly 100%, indicating that extending the experiment beyond this time is unnecessary. This finding suggests that focusing on the initial stages of the reaction is important for understanding the kinetics, and that waiting more than two hours does not yield additional benefits. Consequently, in subsequent experiments conducted in Liège, samples will be taken at 5 minutes, 30 minutes, 1 hour, and 2 hours.

During the experiments, a significant change in the agitation of the solid was observed. With a new stock solution containing 900 ppm of Pt, compared to the previous solution with 400 ppm, the solid in the two-hour experiments mostly settled at the bottom of the beaker, showing minimal agitation, unlike in other experiments where it was fully agitated. While platinum recovery followed the general trend of the graph, the precipitant factor was affected. Increased solid agitation seemed to lead to greater consumption of the copper through side reactions, which reduced the overall efficiency of the process. The high acidity of the solution might be responsible for this behaviour, as discussed by Grilli et al. (2023), who mention the use of  $H_2O_2$  during leaching. The negative pH of the solution suggests that excess  $H_2O_2$  should have been present in the Pt-DOC solution. Although it was not possible to closely monitor the pH due to equipment limitations, the precipitant factor indicates that copper agitation likely enhanced side reactions, consuming more copper and lowering process efficiency. This is one of the reasons why an excess amount of copper powder was initially added compared to the stoichiometric amount required.

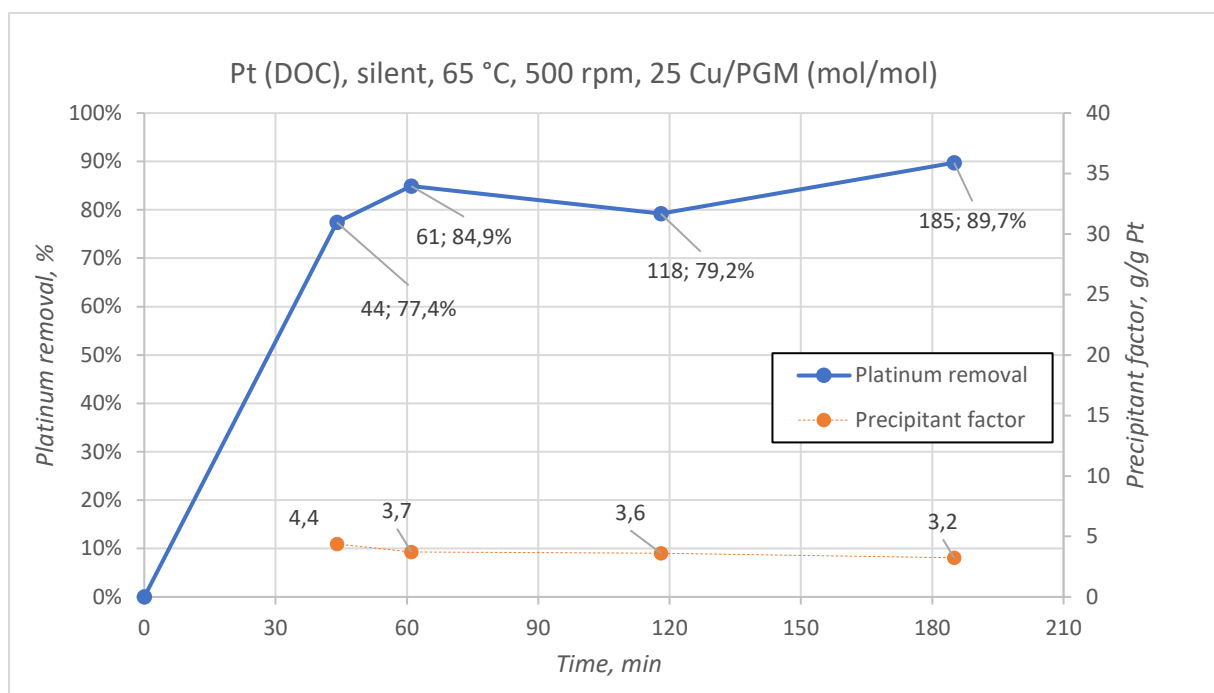


Figure 20: Results of the experiment conducted on the Pt-DOC solution from Monolithos Catalysts & Recycling Ltd. at 65°C, without sonication, at 500 rpm using a magnetic stirrer with the solid barely agitated compared to the solution, with 25 times the stoichiometric amount of copper to recover the PGMs. The results represent the platinum removal percentage and the precipitant factor.

The influence of temperature is observable on the Figure 20 when comparing the results at 85°C and 65°C. At 65°C, platinum removal reaches 90% after 3 hours, which is a high recovery rate but still lower than the results at 85°C. This suggests that while cementation onto copper is feasible at 65°C, optimal conditions must be identified to minimize the loss of valuable elements. Specifically, at 65°C, 85% of the platinum is removed after 1 hour, with a modest increase to 90% after 3 hours. In contrast, at 85°C, 94% of the platinum is removed within 1 hour, and 100% is removed after 2 hours.

The precipitant factor remains stable and close to the value observed at 85°C, where the solid was barely agitated during the two-hour experiments. However, it decreases with longer cementation times, suggesting either that the copper amount in the solution is stable while the amount of PGMs recovered increases or that some copper might be precipitating. The slight decrease in the precipitant factor indicates that this is not a significant issue. It is essential to pay close attention at the beginning of future experiment, as 78% of the platinum is already removed within just 30 minutes.

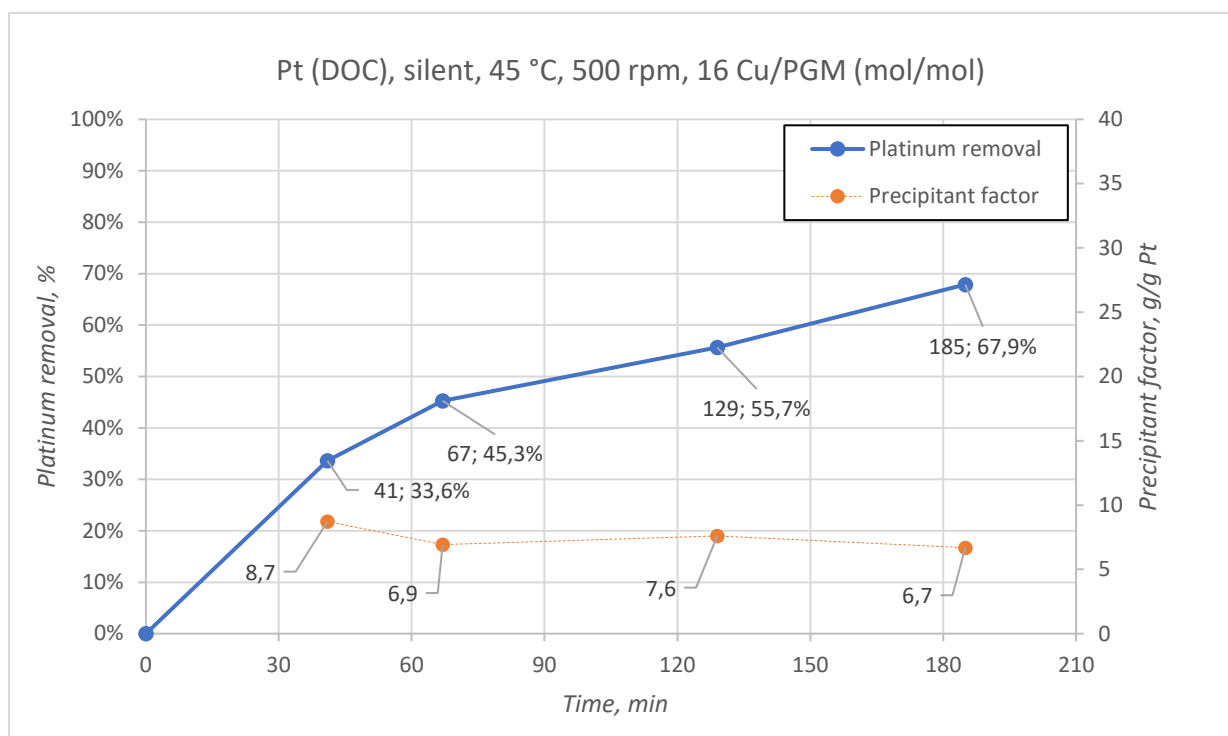


Figure 21: Results of the experiment conducted on the Pt-DOC solution from Monolithos Catalysts & Recycling Ltd. at 45°C, without sonication, at 500 rpm using a magnetic stirrer with the solid barely agitated compared to the solution, with 16 times the stoichiometric amount of copper to recover the PGMs. The results represent the platinum removal percentage and the precipitant factor.

Figure 21 illustrates that at 45°C, high recovery of PGMs is not achieved. After 3 hours, only 68% of the platinum is removed from the initial solution, and after 30 minutes, just 34% is removed. The kinetics of cementation at this temperature are slower compared to previous experiments, indicating that higher temperatures facilitate quicker cementation. The typical plateau observed in earlier tests is not reached under these conditions. Waiting more than 3 hours could be an option to increase the platinum removal percentage. However, due to laboratory constraints such as equipment and personnel limitations, it would be more efficient to select a different set of parameters that allows for better results in a shorter time. The precipitant factor remains stable but is higher than in Figure 20, indicating that more copper is required to achieve the cementation of PGMs.

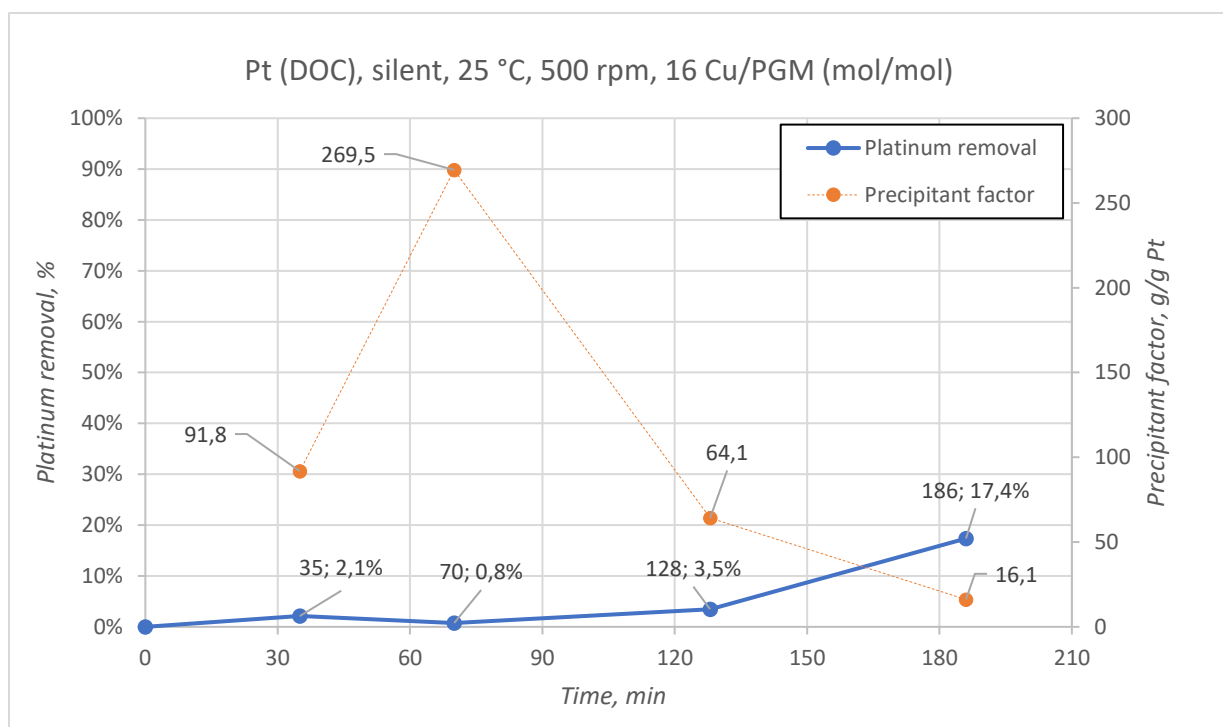


Figure 22: Results of the experiment conducted on the Pt-DOC solution from Monolithos Catalysts & Recycling Ltd. at 25°C, without sonication, at 500 rpm using a magnetic stirrer with the solid barely agitated compared to the solution, with 16 times the stoichiometric amount of copper to recover the PGMs. The results represent the platinum removal percentage and the precipitant factor.

At 25°C, the cementation process is significantly hindered. After 3 hours, only 15% of the platinum was removed from the solution, indicating that side reactions proceed at a faster rate than the cementation reaction. The precipitant factor reveals that a substantial portion of copper remains in the solution, rendering it unavailable for the cementation process. The high acidity of the solution contributes to the dilution of the copper powder, while the slow cementation rate fails to outpace the dilution of the copper. After two hours, the side reactions appear to diminish in intensity, likely due to the depletion of one or more reactants, allowing cementation to proceed if sufficient copper remains. The minimal recovery of PGMs can also be attributed to these side reactions, as indicated by the large discrepancies observed in the data.

Based on these findings, Figure 22 illustrates the experimental outcomes in relation to the temperature of the cementation reaction. The optimal conditions for this leachate, without the application of sonication, are 85°C with a barely agitation of the solid for a cementation duration of two hours. This experimental setup is depicted in Figure 13. By introducing an excess of copper to the system, a high recovery rate can be achieved. Therefore, future experiments should focus on

reducing this excess parameter to identify the most efficient conditions. Additionally, the impact of solution agitation will be explored in greater detail in subsequent experiments.

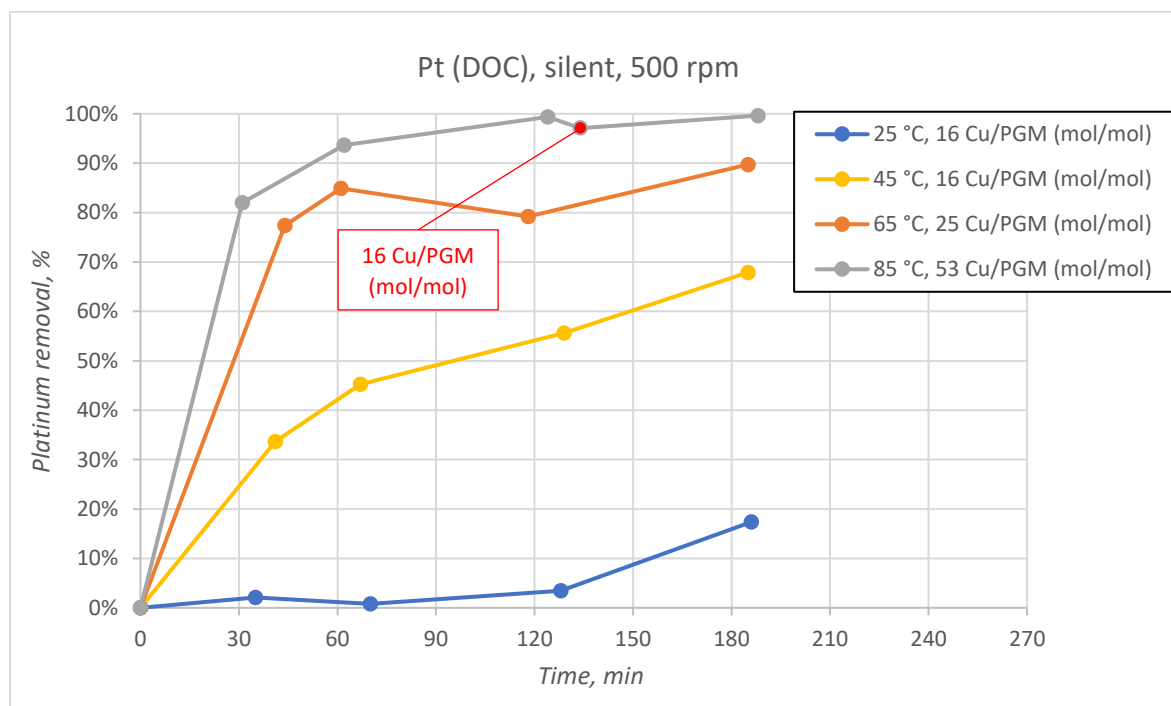


Figure 23: Summary of the experiments done with the same mass of copper powder added to the system at 500 rpm with a magnetic stirrer.

The next experiments on the Pt-DOC solution were conducted to assess the influence of agitation and the quantity of copper added to the system. In Figure 24, the system was maintained at 85°C with 1.6 times the stoichiometric amount of copper and a magnetic stirring rate of 500 rpm. The results show that recovery is insufficient; less than 5% of the platinum was removed from the initial solution within two hours. This suggests that a higher amount of copper is necessary to achieve significant recovery, as indicated by the precipitant factor which really high. This is an indicator that all the copper added to the system is dissolved in the solution with no PGMs removed. This behaviour of the system is depicted with a high value of the precipitant factor. The addition of 1.6 times the stoichiometric amount proved inadequate, highlighting the impact of side reactions on the system. The presence of dissolved copper, as indicated by the precipitant factor, suggests that these side reactions consume copper before cementation can start, leaving insufficient copper available for the process. Consequently, the reduced copper amount in this experiment led to inhibited cementation due to the depletion of copper powder. This underscores the need for a detailed examination of the cementing agent to identify the optimal parameters.

Figure 25 illustrates the impact of agitation on the system. After two hours of agitation at 500 rpm, 5% of the platinum was removed from the solution, compared to only 2% without agitation, even though both experiments were conducted at 85°C. Agitation enhances cementation, as discussed in section 3, although it is still possible to achieve some degree of cementation without movement, albeit with significantly lower efficiency. Therefore, agitation will be a critical parameter in the forthcoming experiments at Liège.

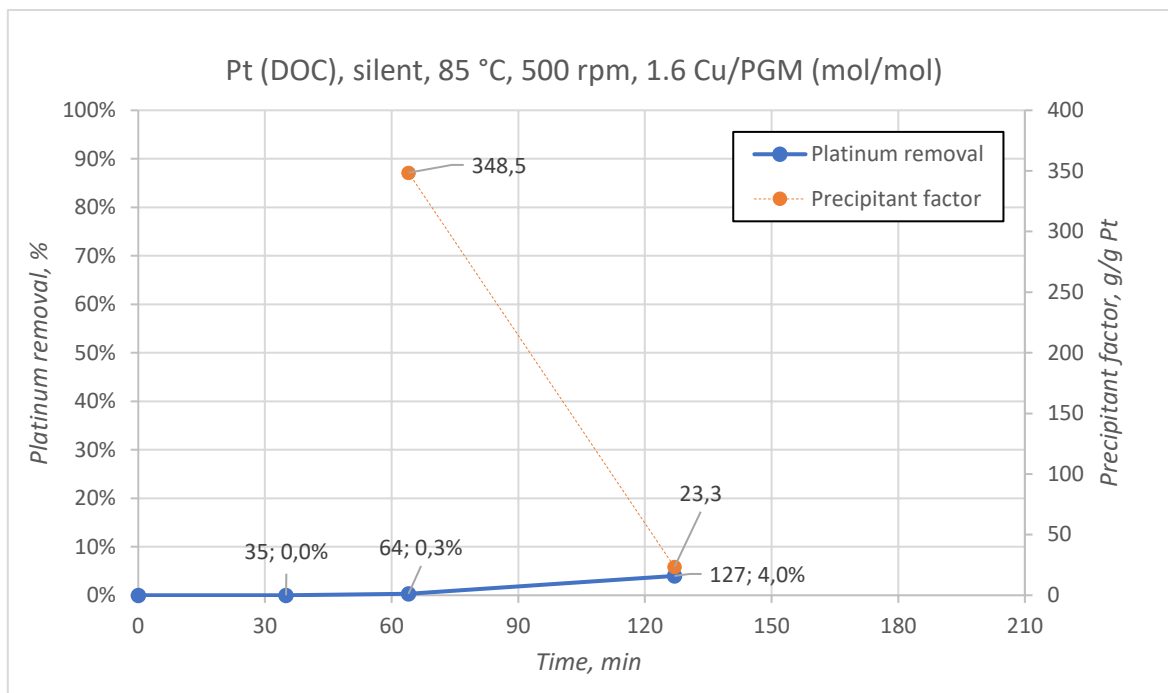


Figure 24: Results of the experiment on the Pt-DOC solution without sonication at 85°C, 500 rpm with a magnetic stirrer but 1.6 times the stoichiometric amount of copper needed expressed with the platinum removal percentage and the precipitant factor.

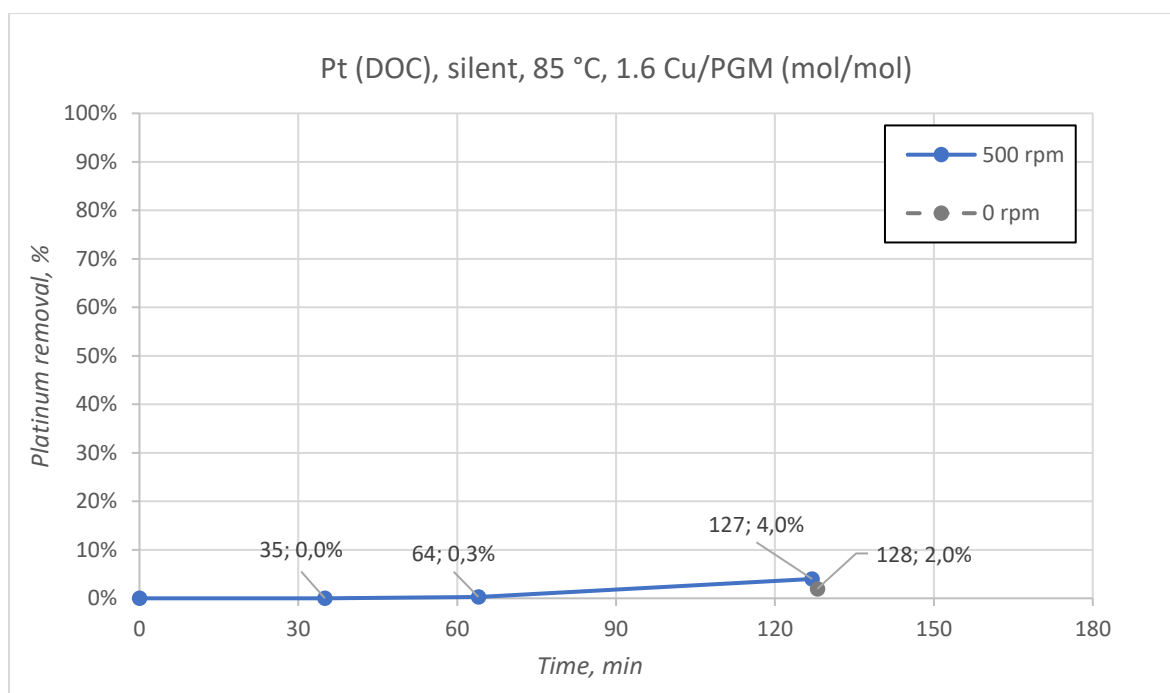


Figure 25: Results of the experiments on the Pt-DOC solution in Athens without sonication at 85°C, with 1.6 times the stoichiometric amount of copper needed to cement the PGMs of the solution. The agitation was step up at 500 rpm and at 0 rpm.

#### 10.4.4 Conclusion of the experiments done at Monolithos Catalysts & Recycling Ltd.

The series of experiments conducted at temperatures ranging from 25°C to 85°C indicate that 85°C is the most efficient for a two-hour cementation process. Trials of varying durations, from 30 minutes to three hours, consistently demonstrated that elevated temperatures enhance cementation efficiency. Agitation also plays a critical role; notably, barely agitated solids appear more efficient

according to the precipitant factor. However, this could be attributed to the solution's acidity, suggesting that further detailed investigation into the effects of agitation and acidity is necessary for future experiments.

Similarly, the amount of copper used is a key factor, as excess is necessary for successful cementation. While 53 times the stoichiometric amount proved excessive, 1.6 times was insufficient, highlighting the presence of side reactions and the highly corrosive nature of the Pt-DOC solution on the cementing agent. Additionally, the solution's acidity and composition differences require exploration, especially as subsequent studies will involve solutions containing not only platinum but also palladium and rhodium. Understanding the system's response to these compositional variations will be essential for optimizing the cementation process in diverse conditions.

In these experiments, temperature was thoroughly investigated, providing conclusions about its impact on the cementation process. However, for the amount of copper and the level of agitation, only a limited number of experiments were conducted with variations in these parameters. As a result, we can only make preliminary hypotheses about their effects and suggest possible trends. To draw definitive conclusions about the system, additional experiments focusing on these variables are required.

## 10.5 Mixed PGM solution at GEMME laboratory

### 10.5.1 Conditions of the experiment

A series of experiments were conducted at the laboratory in Liège to determine the optimal parameters for cementing PGMs onto copper powder from the GEMME solution, which contains 410 ppm of palladium, 220 ppm of platinum, and 60 ppm of rhodium at a pH of 1.5. The study also aimed to assess the impact of ultrasound on this system. The initial redox potential of the solution was approximately 750 mV vs. SHE. Additionally, analyses were performed on the concentrations of copper, iron, and aluminium within the solution, which initially comprised 1000 ppm of aluminium, 30 ppm of copper, and 3400 ppm of iron.

The experiments were conducted using a specialized setup at Liège, designed to minimize evaporation, precisely control temperature, and using overhead stirring for solution agitation. This setup also allowed for the application of ultrasound. An initial solution volume of 300 mL was selected for the reactor. pH and redox potential were measured before each sampling, and a 5 mL sample was taken at specified intervals. Each sample was immediately replaced with 5 mL of stock solution to maintain consistent volume, ensuring that the ultrasound effects were not influenced by volume variations. Sampling occurred at 5 minutes, 30 minutes, 1 hour, and 2 hours, after which the solution was vacuum filtered. The data from the filtrate and wash solution represents an additional data point collected at the end of the filtration process. These time intervals were chosen based on previous experiments conducted in Athens on the Pt-DOC solution, which suggested that significant kinetic events occur within the first 30 minutes, while extending the experiments beyond 2 hours provided limited additional insights. Additionally, ending the experiments after 2 hours allowed for two experiments to be completed per day. The experiments were conducted at four different temperatures: 25°C, 45°C, 65°C, and 85°C.

Agitation was provided by an overhead stirrer set to 0 rpm, 200 rpm, and 400 rpm. Different agitation speeds affected the distribution of solids within the reactor, similar to previous experiments in Athens where agitation resulted in solids settling at the bottom. At 400 rpm, although some solid still concentrated at the bottom, more particles were suspended in the solution, creating manageable vortices that allowed for accurate sampling and monitoring of pH and Eh. The influence of the copper powder amount added to the system was also examined, with 5 times, 10 times, and



15 times the stoichiometric molar amount of copper required to recover the PGMs in the solution being tested. Due to slight variations in the solution's aging and storage, the actual copper amounts used were 5 times, 9 times, and 13 times the stoichiometric molar amount.

After completing these experiments, the same conditions were replicated with the addition of sonication to assess its influence on the system. Two ultrasound parameters were investigated: frequency and power, with an amplitude close to 2 V. Frequencies of 20 kHz and 40 kHz were tested, along with power levels of 4 W and 10 W. An experiment was also conducted at 40 kHz to maximize the power transmitted to the system, reaching up to 40 W but the results are not available before the date of the deadline of this work. This experiment was notably noisy for researchers in the laboratory.

Figures 26 and 27 illustrate two of the experiments conducted at GEMME. The first figure shows a test without sonication using one of the optimal parameter sets—65°C, 400 rpm, and a Cu/PGM molar ratio of 13. The colour change of the solution provides an initial indication of the reaction's efficiency, with detailed results discussed in the next section. The second figure depicts the same parameters, but with the application of ultrasound at a frequency of 20 kHz and a power of 10 W. In this case, the solution cleared more rapidly and turned black during the final hour of the experiment. The filtrate was translucent at the experiment's conclusion, demonstrating that ultrasound had a significant impact on the system in just one trial. Notably, ultrasound led to a marked reduction in particle size, enhanced PGM removal, and accelerated reaction kinetics. A more detailed analysis will be presented in the following sections.

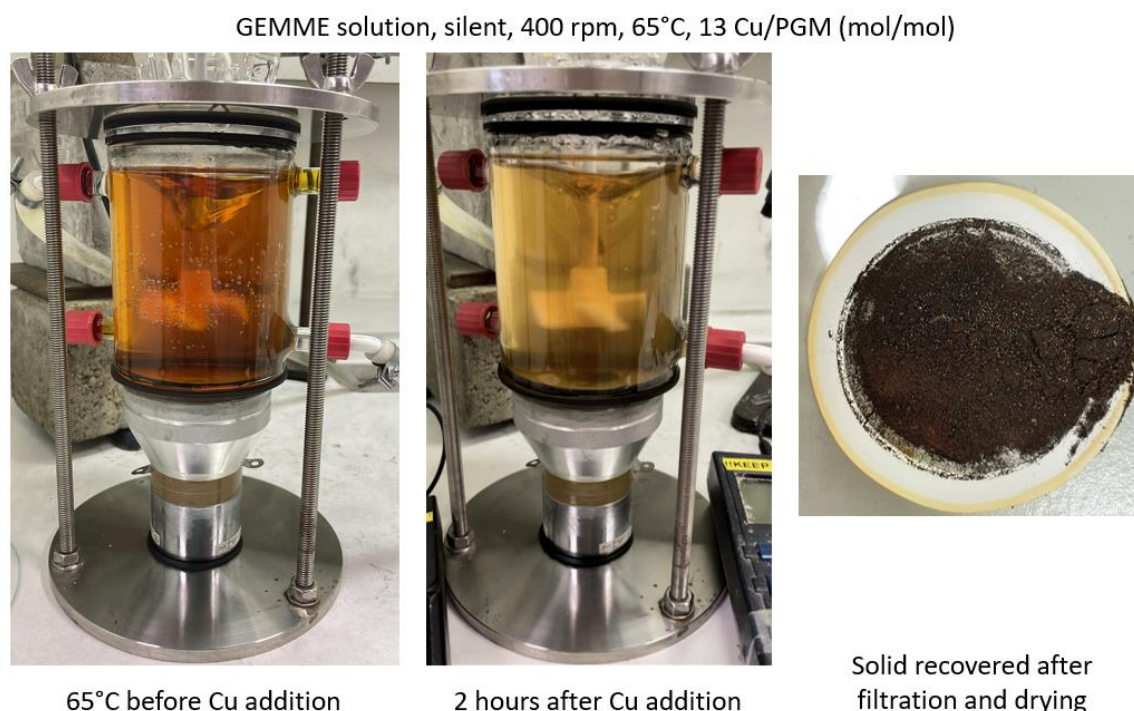


*Figure 26: GEMME solution at 65°C without sonication at 400 rpm with 13 Cu/PGM (mol/mol) with the setup of Liège. The Figure shows the initial solution heated, the solution after 2 hours of experiment and the solid after filtration and drying.*



GEMME solution, 20 kHz, 10W, 400 rpm, 65°C, 13 Cu/PGM (mol/mol)

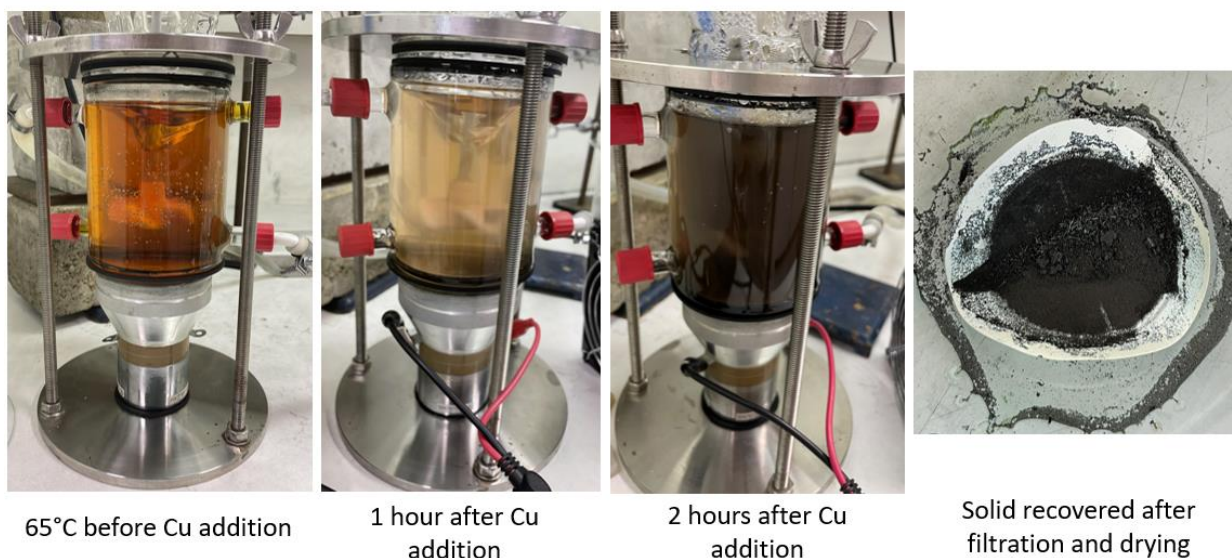


Figure 27: GEMME solution at 65°C with ultrasounds at 20kHz, 10W, at 400 rpm with 13 Cu/PGM (mol/mol) with the setup of Liège. The figure shows the initial solution heated, the solution after 2 hours of experiment and the solid after filtration and drying.

#### 10.5.2 Presence of iron and aluminium in the GEMME solution

When the GEMME solution was originally created one year ago, it contained 3921 ppm of Fe and 1125 ppm of Al. However, the solution used in recent experiments showed 3425 ppm of Fe and 1000 ppm of Al, indicating that some of the aluminium and iron have precipitated over time, despite being stored in a closed container without light. Before each experiment, the solution was thoroughly homogenized to ensure a representative sample. This change in composition suggests that certain elements, including aluminium and iron, may have precipitated, and others may have changed their oxidation states, potentially complicating the removal of PGMs. Despite the aging of the solution, significant amounts of iron and aluminium remain present. The initial redox potential of the solution, measured at 750 mV vs. SHE, along with the presence of  $\text{H}_2\text{O}_2$ , further supports the likelihood of  $\text{Fe}^{3+}$  being present, as these factors indicate an oxidative environment that favours the existence of iron in its ferric state.

The iron present in the solution is likely to react with the copper added to the system, as  $\text{Fe}^{3+}$  can be reduced by metallic copper, leading to the consumption of copper in side reactions. In contrast, aluminium is less reactive under the conditions of the experiments and is less likely to consume significant amounts of copper. The protective oxide layer on aluminium generally prevents it from reacting readily with copper in the acidic solution. Therefore, the presence of aluminium in the solution poses less risk of copper consumption compared to iron.

The behaviour of iron in the solution can be analysed using Pourbaix diagrams, as shown in Figures 28 and 29. The first diagram, a simplified Pourbaix diagram, illustrates the stability regions of iron species in an aqueous system at 25°C at a pressure of 1 atm (Fioravante et al., 2019), while the second diagram, constructed in the laboratory at Liège, represents the iron behaviour in a hydrochloric acid system at 85°C and 1 atm with a molality of  $1\text{E-}6$  for the Fe and Cl. This customized diagram provides insights into the behaviour of iron under elevated temperature conditions but the concentration of the elements in the solution does not correctly copy the GEMME solution. These diagrams even if they do not represent exactly the conditions of the system are still interesting because these gave a global idea of the behaviour of the iron under high temperatures.

The pH of the GEMME solution during reactions fluctuates between 1.4 and 2, with an initial redox potential around 750 mV vs. SHE, which decreases to 400–500 mV vs. SHE as the reaction progresses. According to the Pourbaix diagrams of the iron, iron hydrolysis typically begins at a pH higher than 2 at 25°C. However, at 85°C, hydrolysis can occur at pH levels above 1, a condition commonly observed during the experiments. The general tendency for iron hydrolysis is to occur at lower pH levels as the system is heated. To minimize iron precipitation, the pH must be reduced below 1, which would require significant amounts of HCl and approach the operational limits of the pH meter.

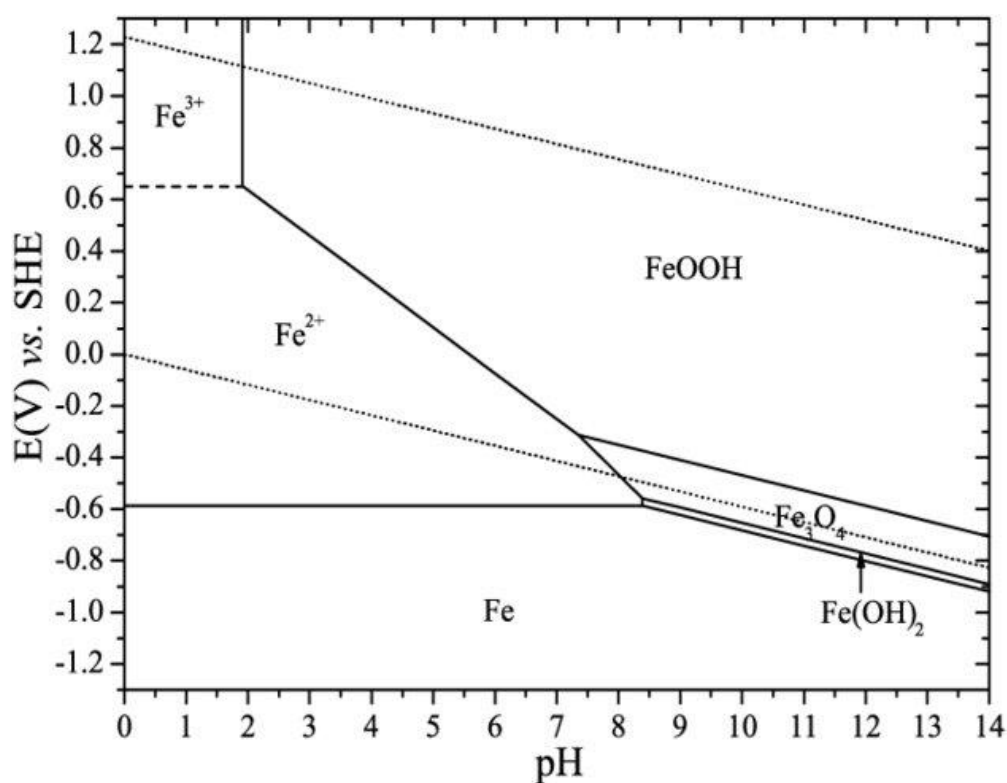


Figure 28: Simplified Pourbaix diagram for the Fe-H<sub>2</sub>O system at 25°C, 1 atm (Fioravante et al., 2019).

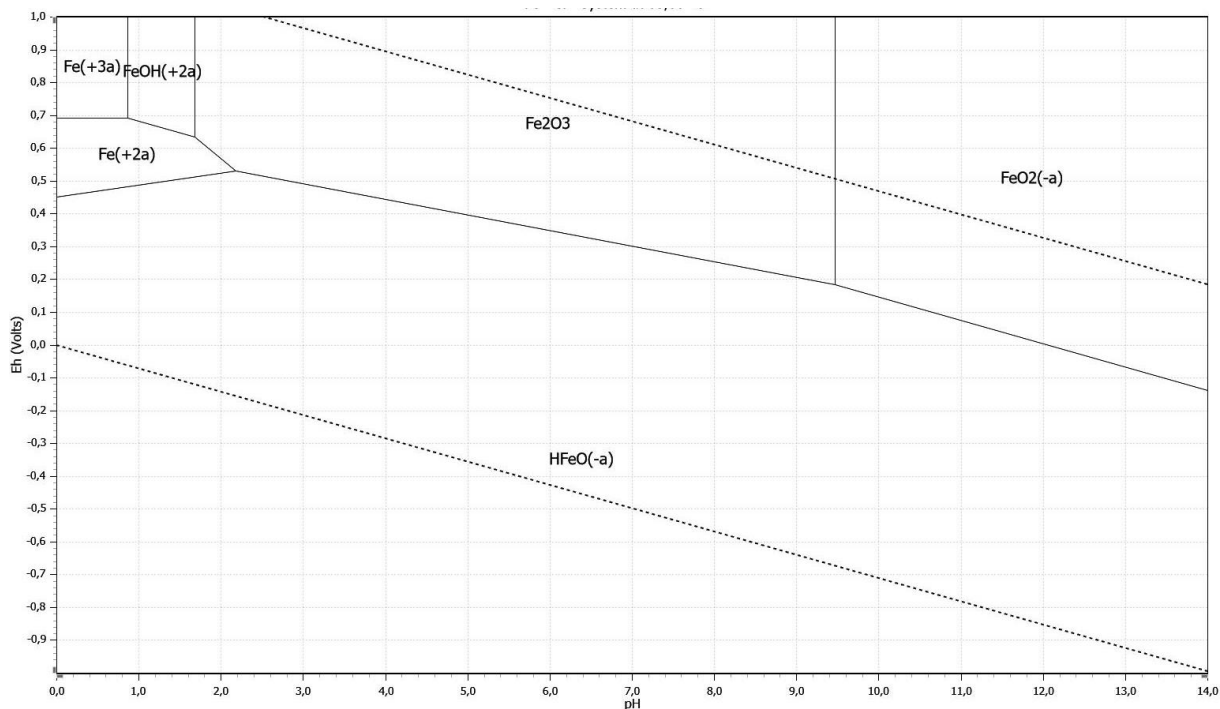
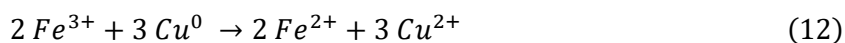


Figure 29: Simplified Pourbaix diagram for the Fe – Cl – H<sub>2</sub>O system at 85°C, 1 atm and a molality of Fe of 10<sup>-6</sup>.

Monolithos Catalysts & Recycling Ltd. has indicated that the presence of iron or other metals in the cement is not considered an impurity. What is important is the ratio between PGMs and these metals; therefore, if the iron content in the solid is too high, fresh PGMs can be added to achieve the desired ratio. This implies that it may not be necessary to minimize iron precipitation, allowing for a reduction in copper consumption. The interaction between Fe<sup>3+</sup> and metallic copper, as described by the reaction:



illustrates that Fe<sup>3+</sup> consumes copper during the reaction. To minimize this side reaction and reduce copper consumption, one strategy could be to precipitate Fe<sup>3+</sup> from the solution before adding copper powder. Heating the solution to 85°C promotes this precipitation, but it also risks the formation of jarosite, which poses challenges in industrial processes. Although this approach could enhance the efficiency of copper use, managing jarosite formation remains a significant challenge in the process.

The formation of jarosite and alunite has been considered and studied, but since the reaction environment is HCl, it is not possible to obtain them. Indeed, these minerals require a sulphate environment to form and precipitate (Cruells & Roca, 2022; Rodriguez-Clemente & Hidalgo-Lopez, 1985).

Given that aluminium is present in our system, it is useful to examine its Pourbaix diagram, shown in Figure 30. Aluminium is unlikely to react with copper, so it is useful to understand the final state of this element in the system without needing to trace it explicitly. According to its Pourbaix diagram, below a pH of 4 and for potentials more negative than -1500 mV vs SHE, aluminium exists in an ionic form in solution. Under the conditions of our experiments, aluminium should predominantly be in solution rather than in the solid phase. It would be interesting to plot the Pourbaix diagram for aluminium at higher temperatures (65°C or 85°C) to see if this remains the case. However, since aluminium does not react with copper and, according to Monolithos Catalyst & Recycling Ltd., it is not an impurity in the cement, its final state in the system provides limited additional information.

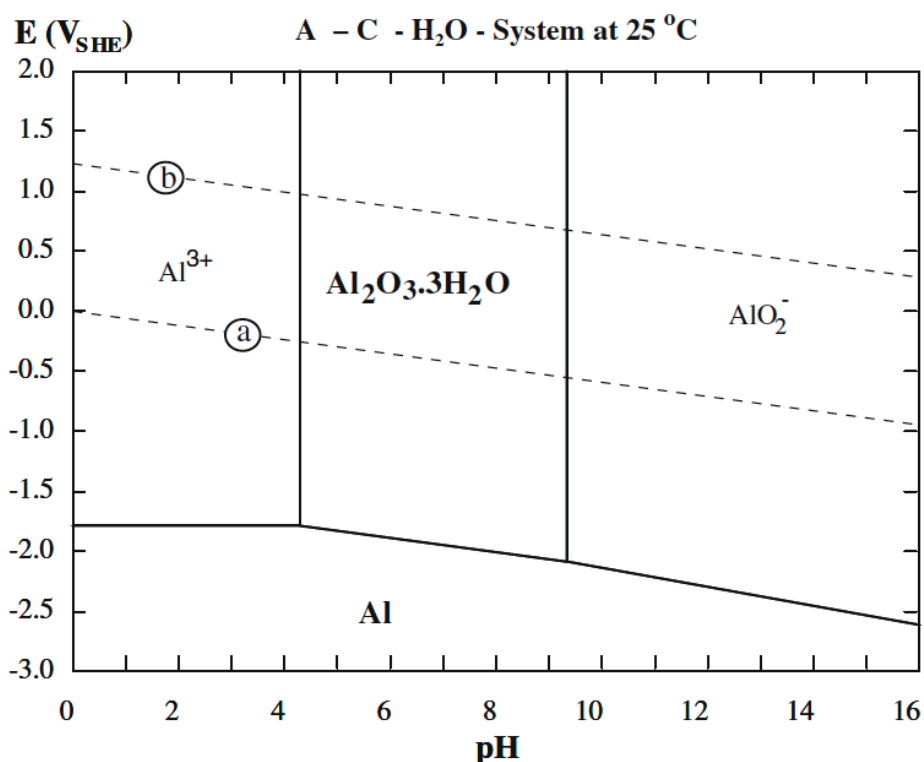


Figure 30: Pourbaix diagram for aluminium at 25 °C (McCafferty, 2009).

### 10.5.3 Results of the experiments without sonication

Various parameters are investigated here to understand their impact on the system and to gain insight into the behaviour of PGM cementation from different leachates onto copper. Each parameter is examined individually to identify the optimal set of conditions that maximize PGM removal efficiency while ensuring cement composition. This section will discuss the influence of temperature, agitation, and the amount of copper powder added to the GEMME solution.

Graphs illustrate the removal percentages of palladium, platinum, and rhodium separately, with multiple experiments displayed on a single graph to facilitate comparison of each parameter's influence on removal efficiency. The optimal value for each parameter is then presented alongside the precipitant factor for the three elements, providing a comprehensive overview of the system's behaviour. Each element has a specific colour to facilitate the reading of the graphs.

#### 10.5.3.1 Repeatability of the results

During an experimental campaign, assessing the repeatability of data is important. Repeatability pertains to the consistency of experimental outcomes when the same test is performed multiple times under identical conditions within a single laboratory, using the same equipment and operators. In contrast, reproducibility evaluates whether consistent results can be obtained when the same experiment is conducted under varying conditions, such as in different laboratories, with different operators, or using different equipment. While repeatability ensures precision within a controlled environment, reproducibility confirms the reliability and generalizability of results across diverse settings (Friedland, 2023).

Proving reproducibility is often challenging in studies with limited budgets, as it requires replication of experiments in different laboratories with new setups and operators. Conversely, repeatability can be demonstrated within the same lab, even though it demands additional tests and analyses. Typically, research protocols include performing tests in triplicate to confirm repeatability. However,

due to time constraints and limited resources, I was unable to conduct triplicates. Instead, I noticed that the analysis of three experiments with identical parameters done to investigate the effect of pH on the system could be an alternative to have a general idea of the repeatability of the results. The first experiment was conducted without pH adjustment, while the subsequent two experiments involved adjusting the pH to 1.4 and 1.7 by adding 37% HCl. This adjustment aimed to prevent iron hydrolysis in the system.

After discussions with Monolithos Catalysts and Recycling Ltd., it was confirmed that iron in the cement is not considered an impurity; only the ratio between PGMs and other metals is critical. If necessary, additional PGMs can be added to achieve the desired ratio. Additionally, at 85°C, research and Pourbaix diagrams indicated that iron hydrolysis can be avoided at pH levels lower than 0.7, which is too close to the limit of applications of the pH-meter I used to be performed. At room temperature (25°C), iron hydrolysis typically begins at a pH around 2. That is why I initially did two tests to see the impact of the adjustment of the pH level on the system but afterward, I discovered that these experiments were not relevant. These experiments can still be analysed to know if there is a tendency of repeatability of the data.

The following figures illustrate the removal percentages of palladium, platinum, and rhodium over time at 85°C, without ultrasound, with agitation set at 200 rpm, and a Cu/PGM molar ratio of 13. The experiments were conducted using the same setup and operator, with pH adjustment being the only variable. Although triplicates would provide a more definitive measure of repeatability, the results from these three experiments suggest a general trend of repeatability. The data show consistent patterns, except for palladium removal, which is notably higher without pH adjustment. Nonetheless, the results from the pH-adjusted experiments are closely aligned. These observations provide an indication of the data's repeatability, although additional experiments are necessary to confirm this with greater certainty.

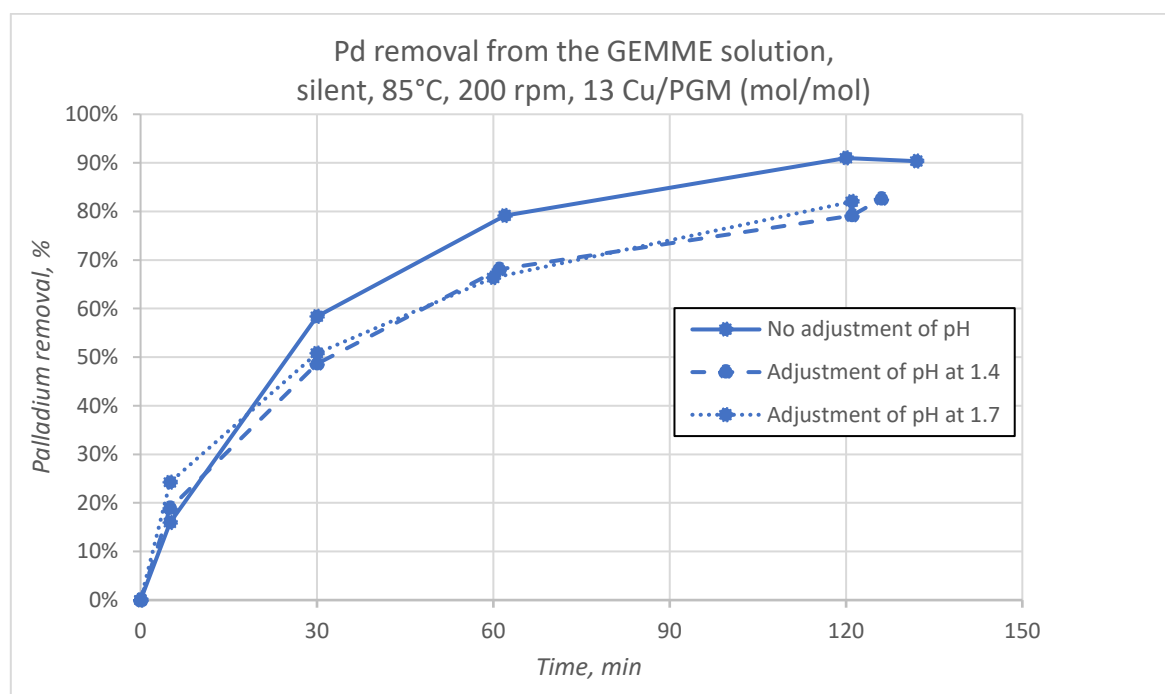


Figure 31: Palladium removal over time from the GEMME solution under silent conditions at 85°C with a 200 rpm agitation speed and a Cu/PGM molar ratio of 13. The graph compares palladium removal efficiency without the adjustment of the pH and with an adjustment at 1.4 and 1.7.

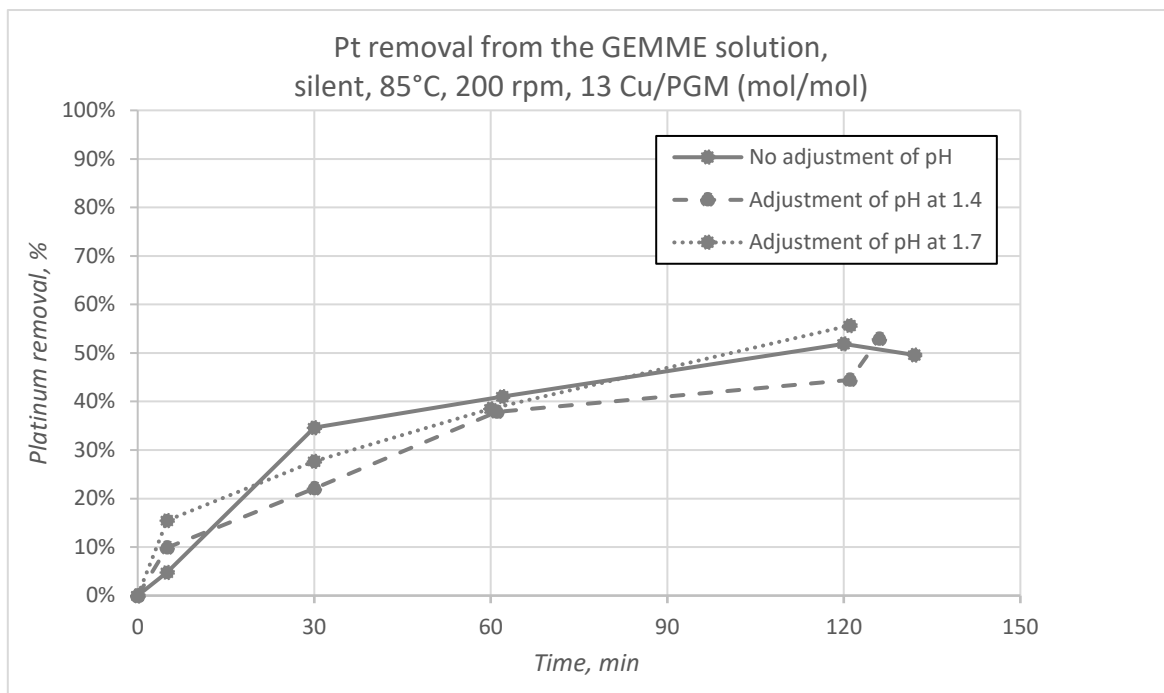


Figure 32: Platinum removal over time from the GEMME solution under silent conditions at 85°C with a 200 rpm agitation speed and a Cu/PGM molar ratio of 13. The graph compares platinum removal efficiency without the adjustment of the pH and with an adjustment at

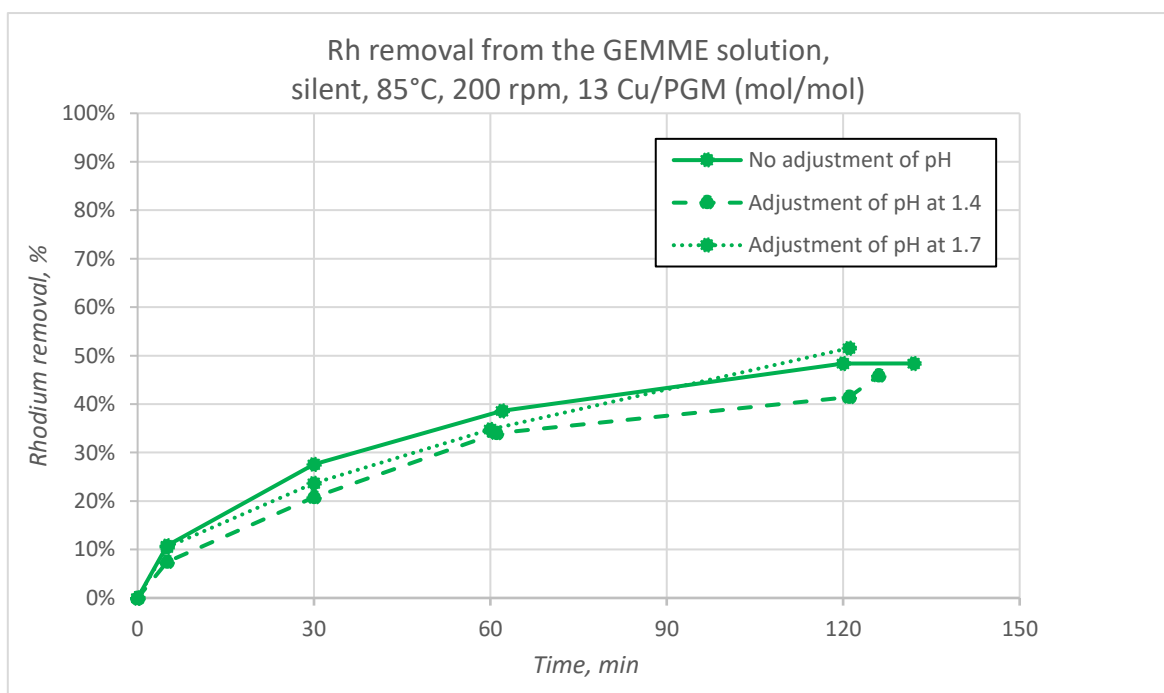


Figure 33: Rhodium removal over time from the GEMME solution under silent conditions at 85°C with a 200 rpm agitation speed and a Cu/PGM molar ratio of 13. The graph compares rhodium removal efficiency without the adjustment of the pH and with an adjustment at

#### 10.5.3.2 Influence of the temperature

The first parameter analysed is the influence of temperature on the system. Other parameters were set at values that, based on literature and previous experiments with the Pt-DOC solution, should not act as limiting factors in the cementation of PGMs. The solution is agitated with an excess of copper powder, equivalent to 15 times the molar ratio of copper to PGMs, similar to the 16 times molar ratio



used in Pt-DOC experiments that achieved high removal rates. This excess of copper should therefore not be a limiting factor.

The following figures depict the removal percentages of platinum, palladium, and rhodium in the GEMME solution after the addition of copper powder. Previous experiments on the Pt-DOC solution demonstrated a clear dependence on temperature, where heating the solution significantly facilitated platinum extraction. A similar trend is observed in these experiments, but with a noticeable distinction between solutions heated above 65°C and those below 45°C. Heating the solution to 45°C results in only minimal PGM removal, and there is a marked difference in removal efficiency, particularly for palladium, when comparing the results at 65°C and 85°C. Therefore, heating the solution to 45°C is insufficient for the GEMME solution containing all three PGMs.

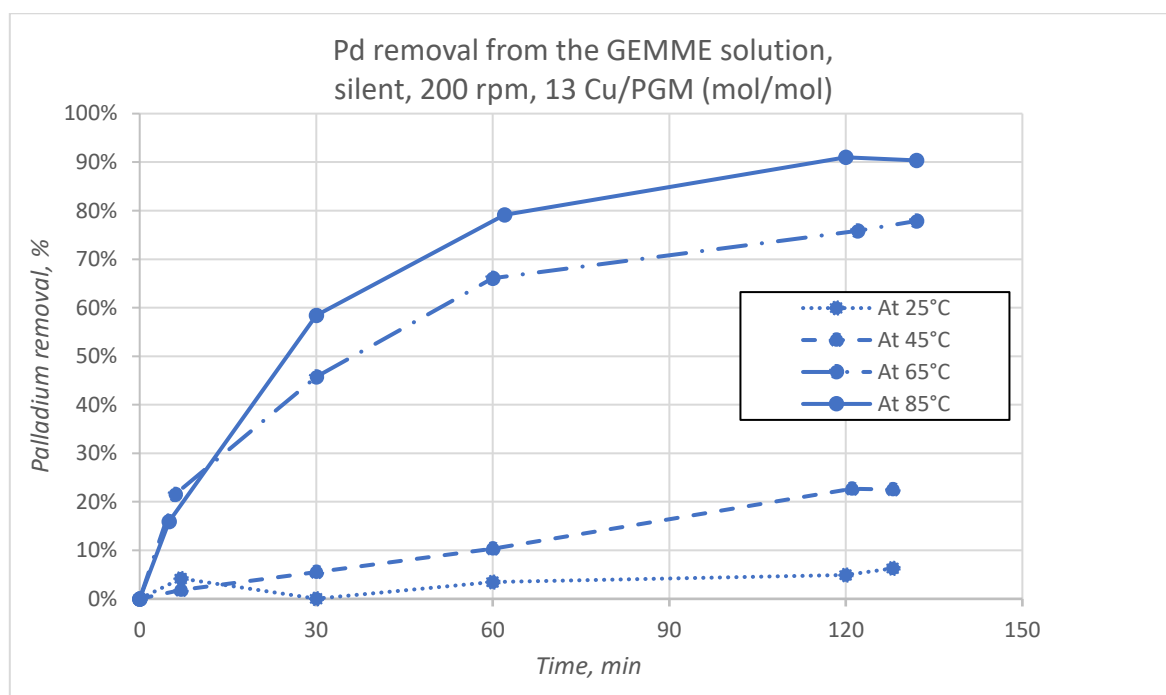


Figure 34: Palladium removal over time from the GEMME solution under silent conditions at 200 rpm and a Cu/PGM molar ratio of 13. The graph compares palladium removal efficiency at four different temperatures: 25°C, 45°C, 65°C, and 85°C.

Palladium removal efficiency reaches up to 90% after two hours at 85°C. At 65°C, the removal rate is approximately 80%, while at 45°C, only 20% of the palladium is removed. At 25°C, a mere 5% removal is observed, indicating that sufficient heating is required to effectively initiate the cementation reaction. After 30 minutes at 85°C, 60% of the palladium is already removed, and at 65°C, 45% is removed within the same period. In contrast, at 45°C and 25°C, palladium removal remains below 5% after 30 minutes. These observations highlight the significant enhancement of reaction kinetics with increasing temperature. Within the first 5 minutes of the experiment, palladium removal at 85°C and 65°C reaches 20%, equivalent to the total removal achieved after two hours at 45°C.

While extending the experiment beyond two hours could potentially increase palladium removal to approximately 95% at 65°C and 85°C, the reaction appears to approach a plateau. Given that extending the duration would require maintaining the same conditions (heating and agitation), which are both costly and time-consuming, the efficiency of this approach is questionable. Subsequent

analysis will explore the optimization of other parameters within the two-hour experimental timeframe to maximize removal percentages.

Platinum and rhodium exhibited similar trends in the experiments which could be due to their lower initial concentrations and multiple oxidation states. That complicates their reduction to a metallic form.

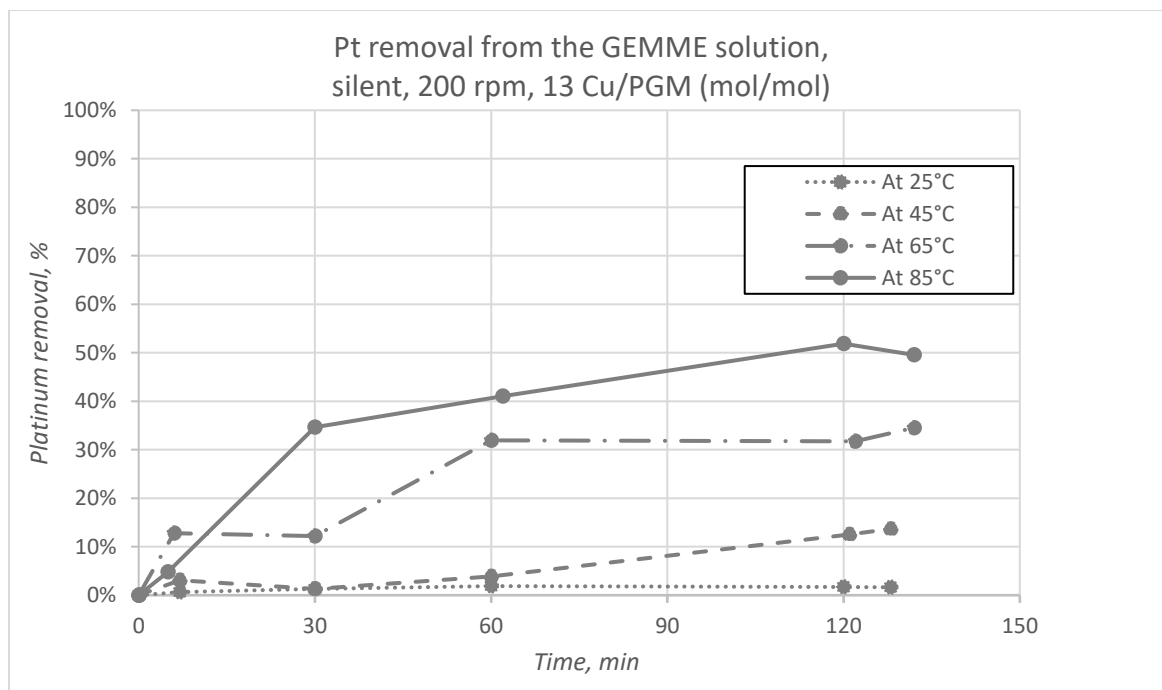


Figure 35: Platinum removal over time from the GEMME solution under silent conditions at 200 rpm and a Cu/PGM molar ratio of 13. The graph compares platinum removal efficiency at four different temperatures: 25°C, 45°C, 65°C, and 85°C.

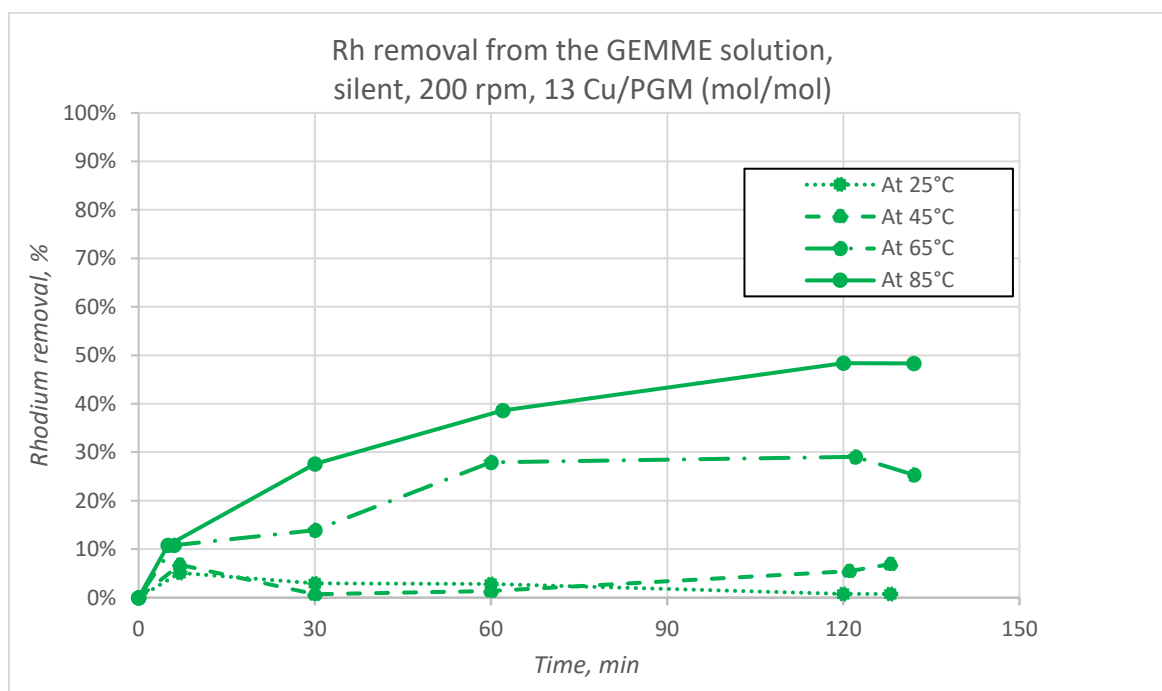


Figure 36: Rhodium removal over time from the GEMME solution under silent conditions at 200 rpm and a Cu/PGM molar ratio of 13. The graph compares rhodium removal efficiency at four different temperatures: 25°C, 45°C, 65°C, and 85°C.



The behaviour of platinum and rhodium, as shown in the Figures 35 and 36, closely mirrors each other. Temperature significantly impacts their removal percentages, with effective recovery requiring heating above 45°C. After two hours at 85°C, 50% of the platinum and rhodium is recovered and at 65°C, approximately 30% of both metals are removed. When the solution is at 25°C or 45°C, the removal percentages are negligible, falling below 10%. The reaction kinetics for platinum and rhodium are slower compared to palladium; within the first five minutes at 85°C and 65°C, only 10% of platinum and rhodium are removed, whereas palladium removal reaches 20% under the same conditions.

Although 85°C proves to be the optimal temperature for this set of parameters, future experiments will be conducted at 65°C. The filtration process posed challenges due to the formation of a fine yellow precipitate on the cement, as visible in Figure 37, which should be the result of the hydrolysis of the iron. The hydrolysis of the iron normally starts for pH higher than 2 but at 85°C, it starts with pH higher than 0.8 which is the case in this experiment. Indeed, the pH of the solution starts at 1.4 to end at 2. This precipitate is not considered as impurities but the filtration is longer and more challenging due to its small granulometry. The hydrolysis of the iron is discussed in the section 10.5.2. Next experiments will then be conducted at 65°C to minimise the creation of this precipitate.

GEMME solution, silent, 200 rpm, 85°C, 13 Cu/PGM (mol/mol)

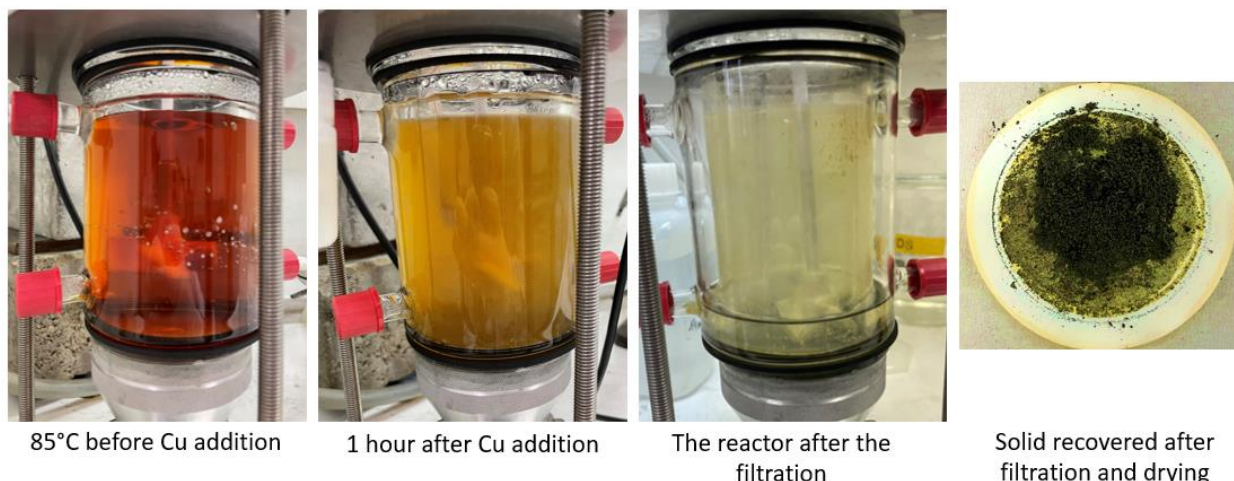


Figure 37: GEMME solution at 85°C without sonication at 200 rpm with a Cu/PGM molar ratio of 13, using the Liège setup. The figure depicts the initial heated solution, the solution after 1 hour of experimentation, the reactor post-filtration, and the solid after filtration and drying. A fine yellowish solid layer is visible in the last two images, indicating challenges in the filtration process.

The results of the experiment conducted at 85°C are shown in Figure 38, where the precipitant factor remains stable and relatively low. Palladium achieves a high removal percentage, while platinum and rhodium each reach 50% recovery. To further improve these recovery rates, adjustments to the parameters will be made in future experiments. Due to the filtration difficulties encountered at 85°C,

subsequent experiments will be carried out at 65°C. Although the removal percentages at 65°C follow the same trend as those observed at 85°C, they are slightly lower.

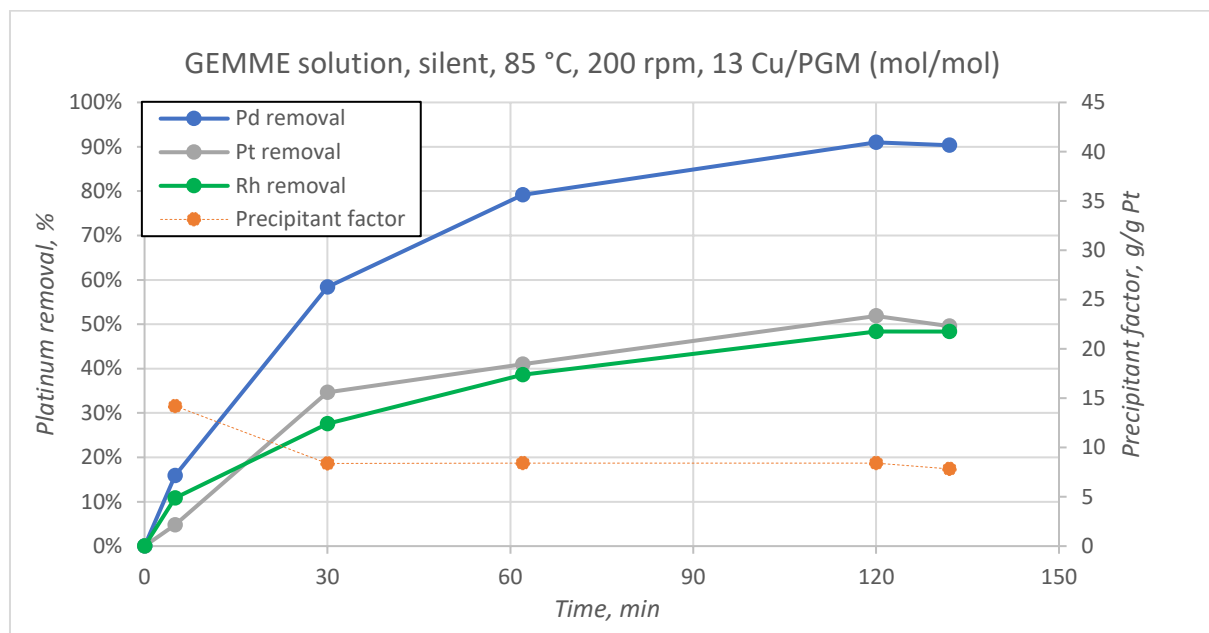


Figure 38: Best temperature to achieve high PGMs removal percentage over time from the GEMME solution under silent conditions at 200 rpm and a Cu/PGM molar ratio of 13.

#### 10.5.3.3 Influence of the agitation

Agitation plays an important role in the cementation reaction, as it directly influences the surface area of the solid in contact with the solution. Increased agitation enhances the interaction between the solid particles and the solution, which, in theory, should accelerate the cementation process by improving the transfer of PGMs from the solution onto the copper surface. However, this increased availability of copper powder can also lead to side reactions, as the copper becomes more accessible for other reactions within the solution.

In the case of the Pt-DOC solution, agitation was essential to initiate the cementation process. However, due to the solution's low pH—indicative of its corrosivity and the presence of excess reactants from the leaching step—a moderate level of agitation was found to be more effective. In this scenario, a barely agitated solid, as opposed to a moving solution, reduced the amount of copper powder required for effective cementation. This approach minimizes the exposure of copper to side reactions while still promoting sufficient contact between the PGMs and the copper surface.

Given these observations, the role of agitation in the cementation process is complex and must be carefully optimized. Agitation is a critical parameter that requires detailed study to balance the enhancement of cementation with the minimization of side reactions, particularly in solutions with challenging properties like low pH.

At Monolithos Catalyst & Recycling Ltd., agitation was performed using a magnetic stir bar controlled by a hot plate, set at 500 rpm. This method is less effective than an overhead stirrer, so to achieve a "barely agitated" solid, the mechanical agitation was adjusted to 200 rpm. At 400 rpm, the solid was more mobile but still somewhat concentrated at the bottom of the reactor. Increasing the agitation beyond this level created a vortex inside the reactor that was too large, hindering accurate sampling and data collection. Consequently, agitation speeds of 0 rpm, 200 rpm, and 400 rpm were selected as parameters to study to understand the impact of agitation on this system. The other conditions were

set at 65°C, without ultrasound, and with a copper amount 13 times the molar ratio relative to the PGM concentration in the GEMME solution.

The following figures illustrate the removal percentages of palladium, platinum, and rhodium for these three agitation levels. It is evident that agitation is essential for successful cementation. Without agitation, the removal percentages after two hours reach only 10% for platinum and palladium, while the rhodium removal remains near 0%. Therefore, cementing rhodium is not feasible without agitation, as other parameters have been optimized to ensure they are not the limiting factors.

Among the agitation speeds, 400 rpm results in the highest removal percentages, though 200 rpm also achieves substantial results. After two hours, palladium removal reaches 90% at 400 rpm and 80% at 200 rpm, as shown in Figure 39. Platinum removal ranges from 45% to 50% at 400 rpm and 35% at 200 rpm, and a similar trend is observed for rhodium, with removal rates between 40% and 45% at 400 rpm and 25% to 30% at 200 rpm. Comparing these results with those in Figure 38, which also shows 50% removal of platinum and rhodium at 200 rpm at 85°C, it appears that increasing agitation can compensate for a lower solution temperature during a two-hour experiment.

If the experiment is stopped after 30 minutes to 1 hour, no significant differences between the two agitation levels are observed. After 1 hour, the palladium removal percentages range between 65% and 75% for 200 rpm and 400 rpm, respectively, while platinum removal is around 35% and rhodium around 30%.

A notable behaviour observed in this set of experiments, which was not evident in previous experiments, is the lower removal percentage after 5 minutes of reaction at 400 rpm compared to 200 rpm. For all three metals, the removal percentage is initially lower at 400 rpm but then surpasses the 200 rpm setup in subsequent samples. This initial lower removal rate at 400 rpm could be attributed to the redissolution of PGMs that have already cemented on the copper, driven by excess reactants after the leaching step. Another possible explanation is that the kinetics of side reactions with copper are initially faster than those of cementation. However, the overall concentration of dissolved copper in the solution is relatively low, less than 1000 ppm (compared to 4000 ppm at the end of the experiment), suggesting that if this hypothesis is correct, the copper might dissolve initially and then precipitate later.

It is essential to maintain some agitation in the solution; without it, cementation will not commence. For experiments lasting less than 2 hours, there is no clear preference between the two agitation settings, so 200 rpm should be selected to minimize operational costs. The most critical factor is ensuring that the solution is in motion. However, for experiments lasting two hours or longer, an agitation rate of 400 rpm is more advantageous as it leads to higher removal percentages, especially for valuable metals.

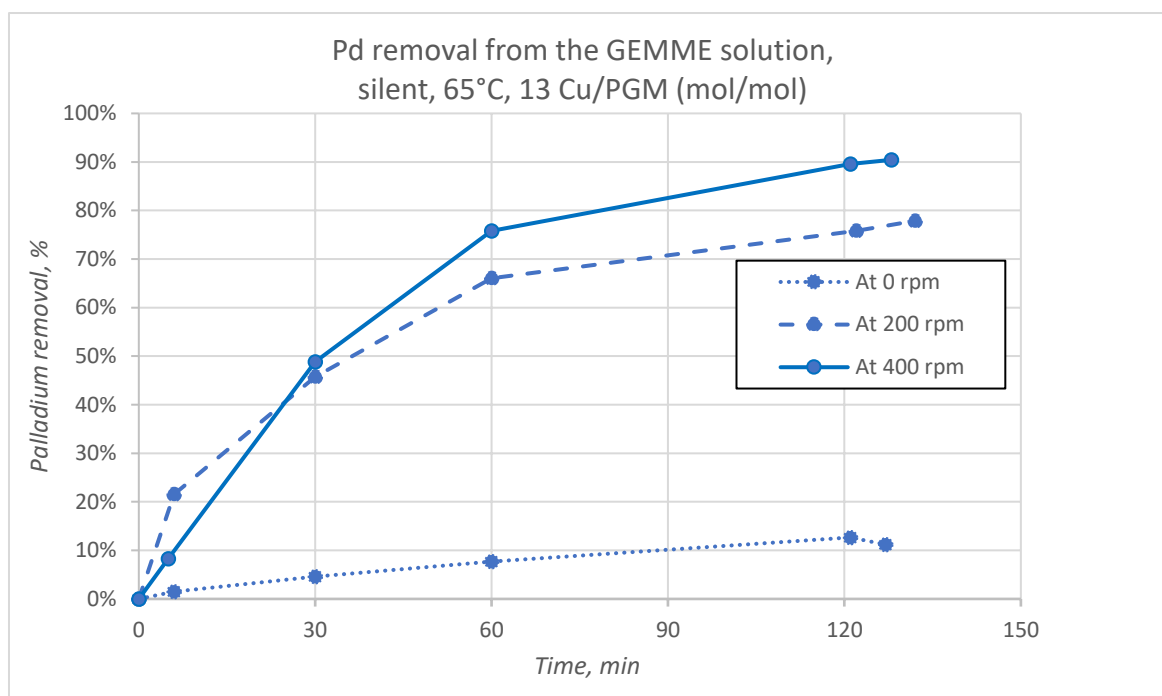


Figure 39: Palladium removal over time from the GEMME solution under silent conditions at 65°C and a Cu/PGM molar ratio of 13. The graph compares palladium removal efficiency at three different agitations by an overhead stirrer: 0 rpm, 200 rpm and 400 rpm.

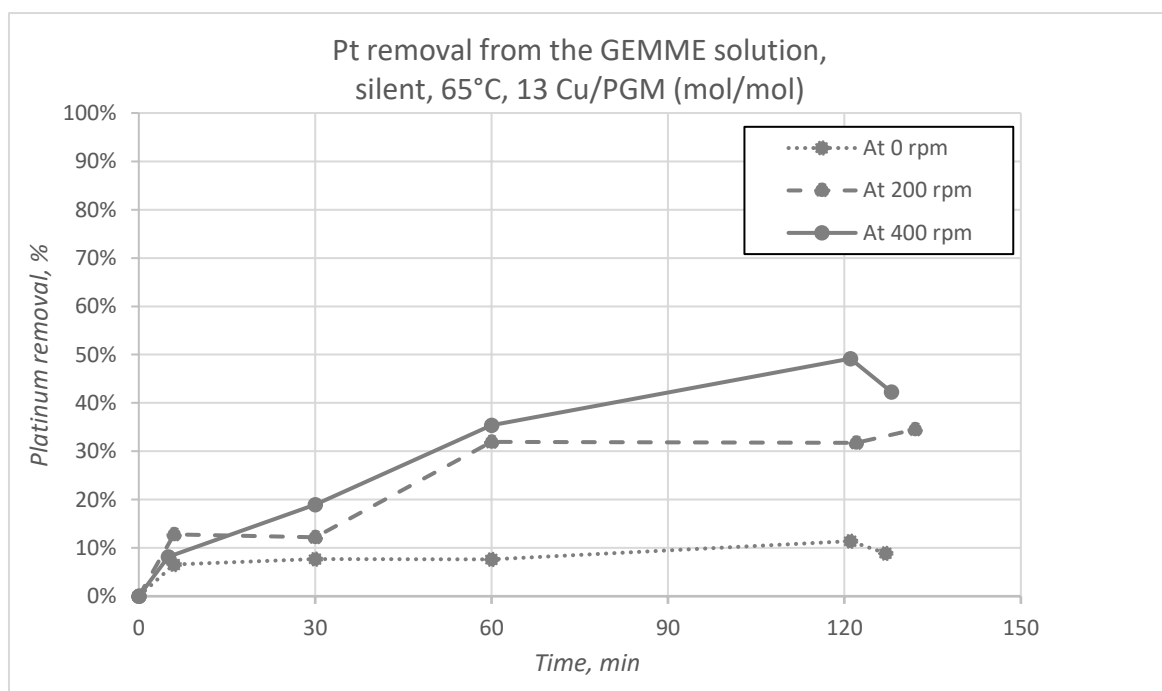


Figure 40: Platinum removal over time from the GEMME solution under silent conditions at 65°C and a Cu/PGM molar ratio of 13. The graph compares platinum removal efficiency at three different agitations by an overhead stirrer: 0 rpm, 200 rpm and 400 rpm.

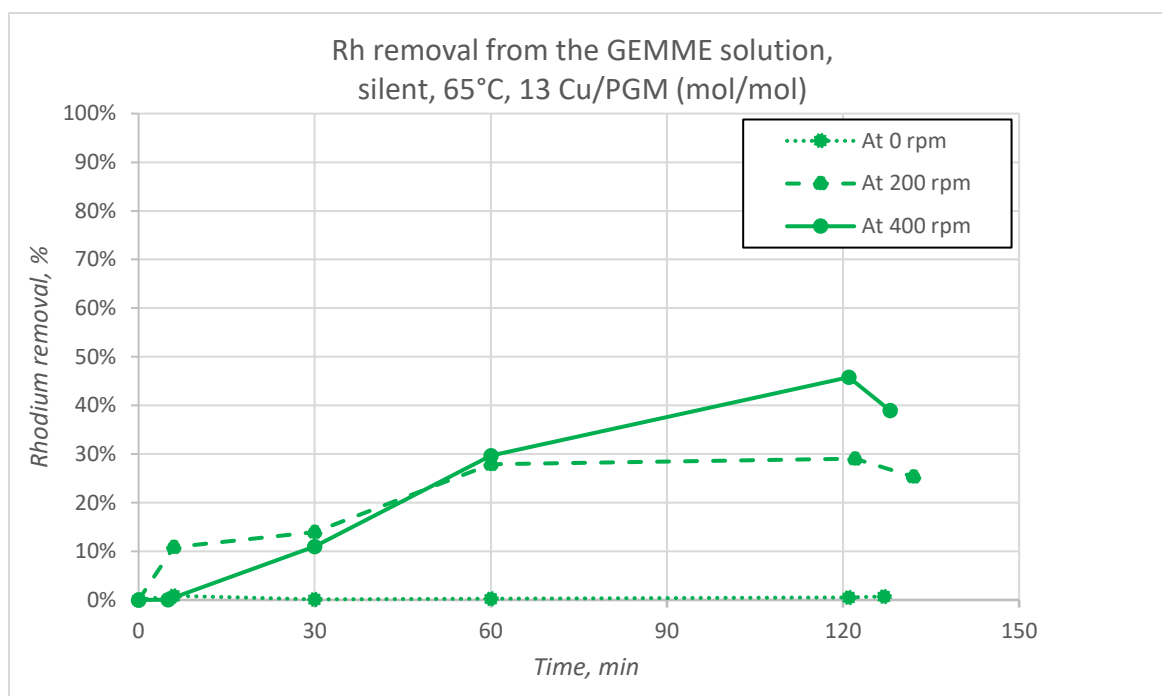


Figure 41: Rhodium removal over time from the GEMME solution under silent conditions at 65°C and a Cu/PGM molar ratio of 13. The graph compares rhodium removal efficiency at three different agitations by an overhead stirrer: 0 rpm, 200 rpm and 400 rpm.

The Figure 42 shows the removal percentages for palladium, platinum, and rhodium from the GEMME solution at an agitation rate of 400 rpm. This represents the optimal choice for the experiments conducted in Liège, which typically last two hours, making 400 rpm the most effective agitation condition. The precipitant factor is also shown in the figure. As observed, it remains generally stable, although it is higher at the beginning of the experiment. This aligns with the hypothesis that either copper is reacting initially or PGMs are being redissolved due to excess reactants, both of which would result in a higher precipitant factor early in the experiment.

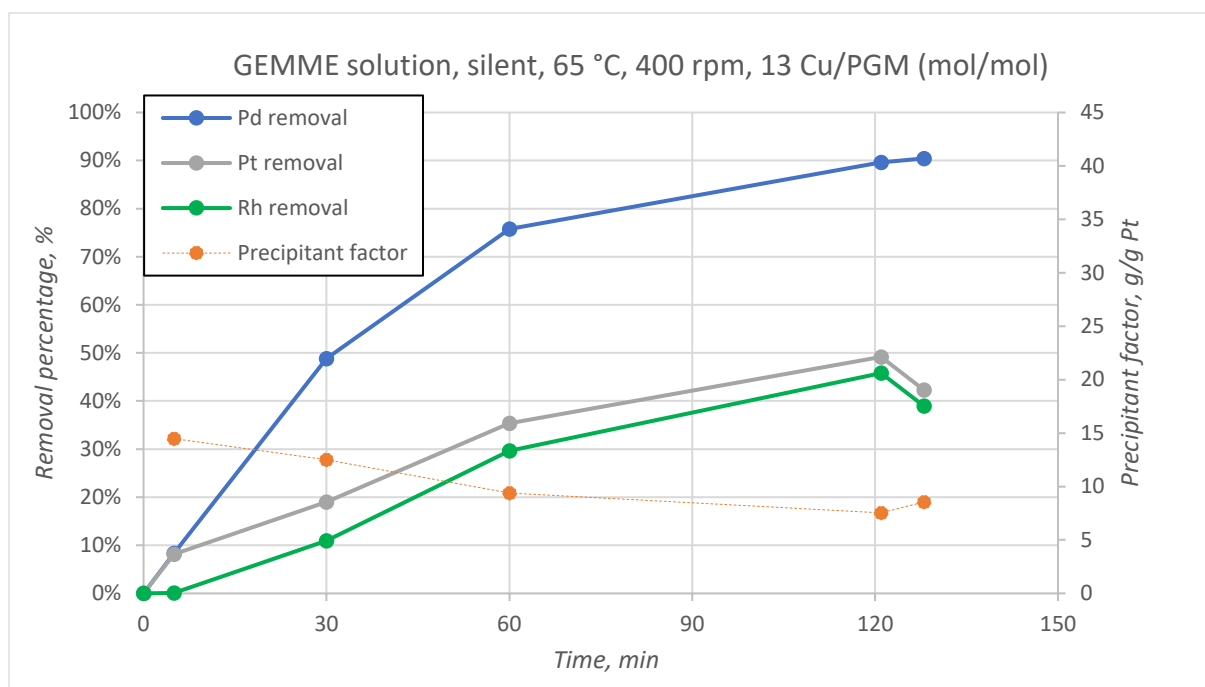


Figure 42: Best agitation with an overhead stirrer to achieve high PGMs removal percentage over time from the GEMME solution under silent conditions at 65°C and a Cu/PGM molar ratio of 13.

#### 10.5.3.4 Influence of the molar ratio of Cu/PGM

The molar ratio of copper to PGMs is a critical factor in the cementation process, influencing the efficiency of PGM recovery from solutions. For effective cementation, the sacrificial metal (copper) must remain in its metallic state to act as an electron donor, facilitating the reduction of PGMs. If the surface of the copper becomes completely covered with a passivation layer, cementation halts. Therefore, an excess of sacrificial metal is necessary to ensure that some copper remains available for continued reaction, despite side reactions or the formation of passivation layers. The required amount of copper depends on the solution's pH, redox potential, and overall composition. For instance, highly acidic solutions, like the Pt-DOC solution, demand a substantial excess of copper to counteract rapid side reactions as copper complex formation and its oxidation. In such environments, the kinetics of side reactions often surpass those of cementation, further emphasizing the need for a surplus of sacrificial metal.

Moreover, since the PGMs are derived from a leaching process where reagents are typically used in excess to maximize recovery, it is important that sufficient copper is present to prevent the dissolution of PGMs or the oxidation of metallic copper by residual leaching agents. Indeed,  $H_2O_2$  is often used as oxidizing agent in leaching so if it is in excess in the solution, it will oxidate either the copper or the PGMs. The cementation efficiency also depends on the likelihood of contact between PGMs and copper in solution; a higher copper concentration increases this probability, leading to better recovery rates. Additionally, the surface area of the sacrificial metal plays a significant role—larger surface areas, as provided by copper powder rather than larger copper pieces, significantly enhance cementation efficiency.

For the Pt-DOC solution, experiments were conducted with Cu/Pt molar ratios of 53, 16, and 1.6. High removal percentages of PGMs were achieved with the first two ratios, even under highly acidic and corrosive conditions, while a ratio of 1.6 resulted in inadequate recovery. Based on these findings, further experiments were planned on the GEMME solution with molar ratios of 5, 10, and 15, but due to solution aging and storage, the actual ratios used were 5, 9, and 13 Cu/PGM. The

results showed that a molar ratio of 13 was sufficient, with palladium removal reaching 90% after 2 hours, and platinum and rhodium reaching 45-50%. Lower ratios resulted in significantly reduced PGM removal, with ratios of 5 leading to negligible recovery rates below 10%.

Initially, the copper effectively cemented palladium, followed by platinum and rhodium. However, a large portion of the copper remained in the solid phase, suggesting either the formation of a passivation layer that hindered further cementation or precipitation of copper in another form. Over time, the copper concentration in the solution increased, indicating ongoing dissolution of copper. These results highlight the importance of using a sufficiently high molar ratio of Cu/PGM to achieve better recovery rates. Future experiments could explore even higher Cu/PGM ratios to determine their impact on platinum and rhodium removal. The optimal conditions align with findings from the previous section and the results of the removal percentages of the three metals under these conditions is shown on the Figure 42.

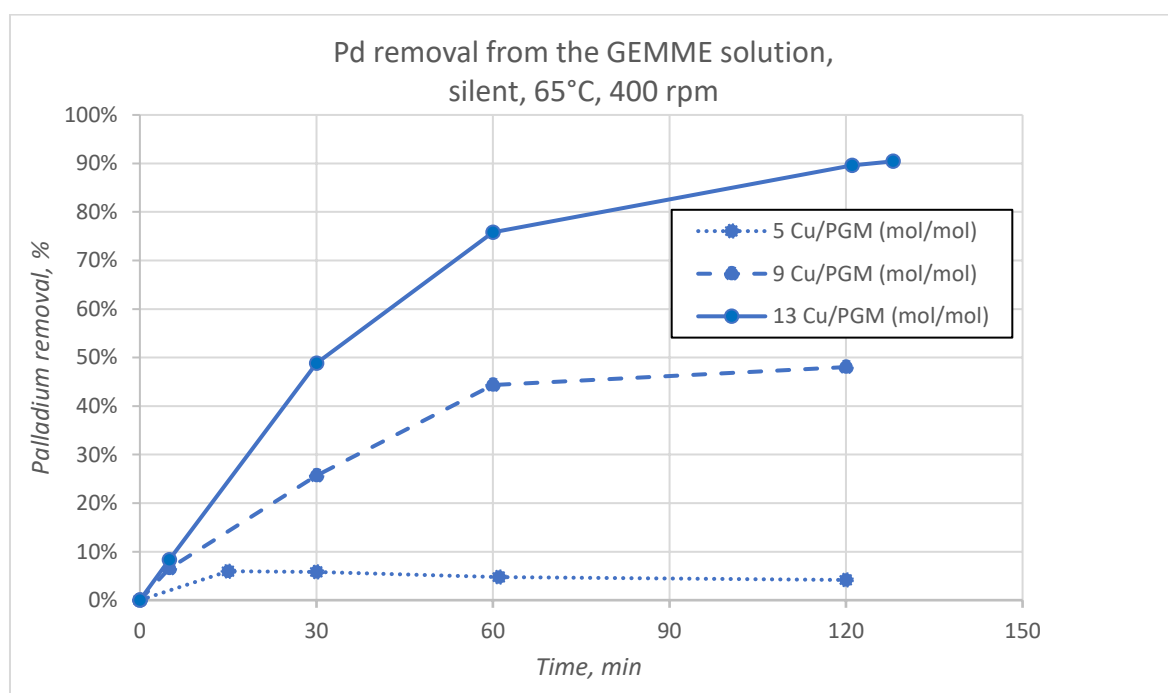


Figure 43: Palladium removal over time from the GEMME solution under silent conditions at 65°C and with an overhead stirrer at 400 rpm. The graph compares palladium removal efficiency with three different Cu/PGM molar ratios: 5 times, 9 times and 13 times.

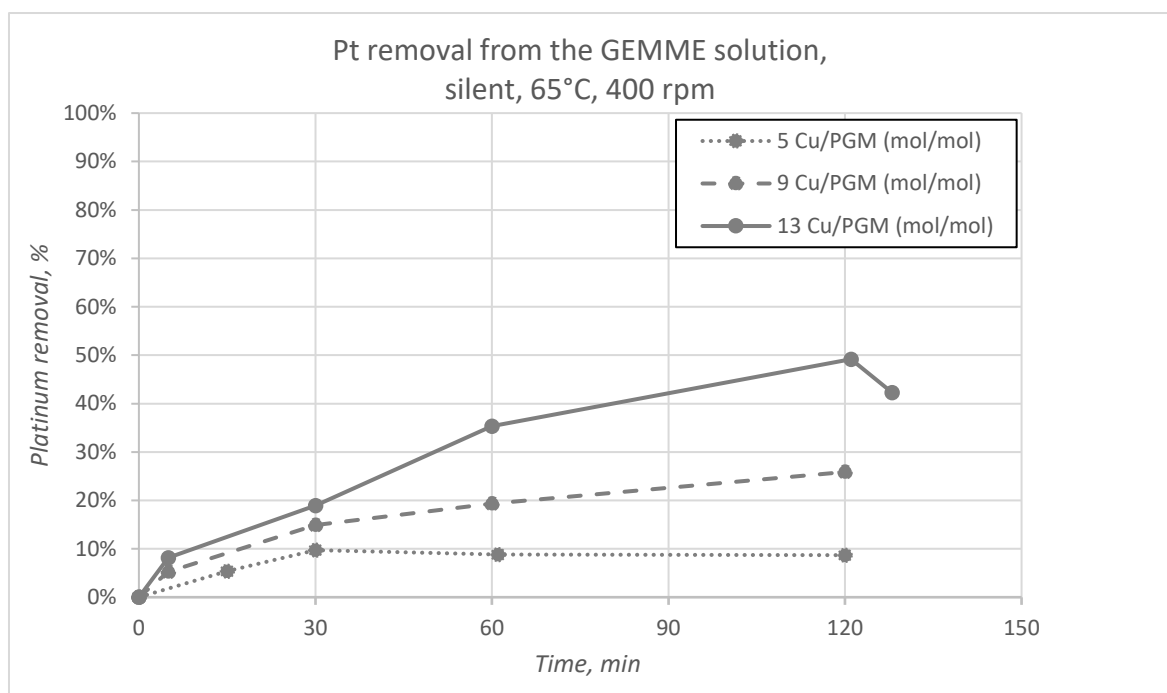


Figure 44: Platinum removal over time from the GEMME solution under silent conditions at 65°C and with an overhead stirrer at 400 rpm. The graph compares platinum removal efficiency with three different Cu/PGM molar ratios: 5 times, 9 times and 13 times.

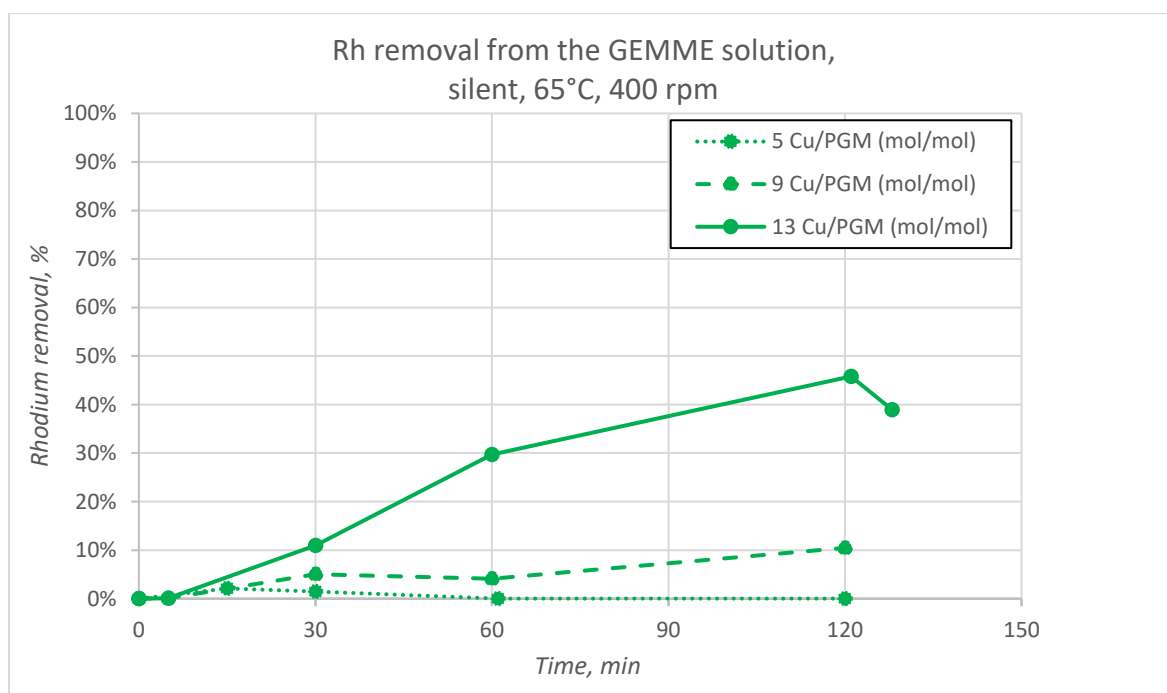


Figure 45: Rhodium removal over time from the GEMME solution under silent conditions at 65°C and with an overhead stirrer at 400 rpm. The graph compares rhodium removal efficiency with three different Cu/PGM molar ratios: 5 times, 9 times and 13 times.

#### 10.5.3.5 Conclusion of the experiments without ultrasounds on the GEMME solution

The experiments conducted without ultrasound on the GEMME solution explored the influence of temperature (25°C, 45°C, 65°C, and 85°C), agitation speed (0 rpm, 200 rpm, and 400 rpm), and the molar ratio of Cu/PGM (5 times, 9 times, and 13 times) on the efficiency of palladium, platinum and rhodium removal. The results indicate that the most effective combination of parameters is the



highest temperature, agitation speed, and molar ratio, specifically at 85°C, 400 rpm, and a Cu/PGM ratio of 13.

However, operating at 85°C presents significant challenges due to the hydrolysis of iron, which complicates filtration at the end of the experiment because of the fine granulometry of the precipitate. Although pH regulation could theoretically mitigate this issue, it is impractical due to its high cost and proximity to the pH meter's operational limits. Additionally, the precipitation of the iron at the beginning of the experiment could lower the copper consumption and iron is not considered as impurities for the cement. Therefore, a balance must be struck between effective filtration and minimizing copper usage. Based on these considerations, the recommended optimal conditions for future experiments are a temperature of 65°C, agitation at 400 rpm, and a Cu/PGM molar ratio of 13:1. These parameters provide a compromise that maximizes palladium removal efficiency while minimizing the complications associated with iron hydrolysis.

#### 10.5.4 Results of the experiments with ultrasounds

The same setup from the previous experiments in the GEMME lab, without ultrasound, was used again; however, this time, the ultrasound generator was activated and a ventilator was used to cool down the transducer.

The ultrasound generator works by sending an alternating electrical current to the Langevin-type transducer, which converts the electrical energy into mechanical vibrations. The transducer consists of piezoelectric elements that expand and contract when subjected to the alternating current, creating high-frequency sound waves that are transmitted into the system. The frequency of the signal refers to the number of vibrations or cycles per second, measured in Hertz (Hz), and it determines the penetration depth and resolution of the ultrasound. The amplitude is the magnitude of these vibrations, which affects the intensity of the sound waves generated. The power transmitted to the system is a product of both the frequency and amplitude and represents the total energy delivered by the ultrasound, influencing the efficiency of processes. The power being studied is the power consumed by the system, which is the total power transmitted to the system minus the power returned by it.

In these experiments, the effects of ultrasound frequency and power on the system were initially examined to determine the system's response and to optimize these parameters for the cementation process. Once these ultrasound parameters were established, further experiments were conducted to study the influence of other variables previously examined, including temperature, agitation, and the molar ratio of Cu/PGM.

For clarity, the results are presented with each metal individually represented, using a consistent colour code to easily identify the specific element being analysed. To facilitate comparison between experiments conducted with and without ultrasound, the corresponding results from the previous, silent experiments are also included in the graphs. In these figures, the data from ultrasound-assisted experiments are depicted in black, while the results from silent experiments are shown in blue for palladium, grey for platinum, and green for rhodium. To summarize the findings, the parameter that yielded the most effective recovery for all three metals is highlighted at the end of each section. These summary graphs present the results for all elements simultaneously, with the precipitant factor indicated as a key metric of comparison.

##### 10.5.4.1 Impacts of the ultrasounds on the particle size of the solid

During the experiments under ultrasounds, the solution could turn completely dark, as shown in Figure 37. This darkening is attributed to the reduction in the size of the solid particles in the

solution, driven by the energy released during the collapse of cavitation bubbles. Although the initial solid added to the system was a powder with a particle size of 58  $\mu\text{m}$ , the application of ultrasounds reduced its size, producing particles smaller than 8  $\mu\text{m}$  in diameter. This conclusion is supported by filtration results: samples from silent experiments were effectively filtered through 8  $\mu\text{m}$  mesh filters, while samples from ultrasound experiments were not, indicating the presence of finer particles. The persistence of these small particles in the samples means that reactions continued, as the solid was still present, potentially leading to an overestimation of the ultrasound effects. However, at the end of the experiments, the solution passed through 0.47  $\mu\text{m}$  filters with no solid particles detected in the filtrate so these results are more accurate and give a general idea of the preciseness of the results.

A white precipitate visible in Figure 46 may correspond to sodium chloride crystals. This hypothesis is supported by the presence of sodium in the solution. During experiments conducted in Athens, a similar white crystal precipitate formed during filtration, which was linked to significant evaporation and easily dissolved during washing. These observations, combined with the presence of sodium, suggest that these crystals are likely sodium chloride. Additionally, the yellowish-brownish precipitate observed could be due to iron hydrolysis. This fine deposit, with a particle size smaller than 8  $\mu\text{m}$ , aligns with the expected conditions for iron hydrolysis.

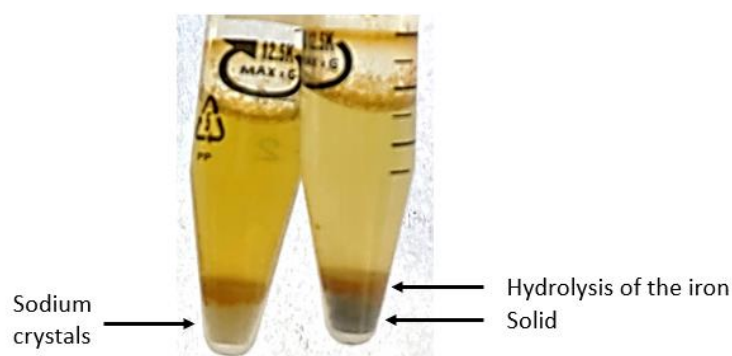


Figure 46: Image of the residues obtained after filtering the samples through an 8  $\mu\text{m}$  mesh size filter. These samples were associated with an experiment conducted at 65°C with stirring at 400 rpm, using a Cu/PGM molar ratio of 13, and subjected to ultrasound at 20 kHz and 4 W. The sample on the left was taken after 5 minutes and the second sample on the right was taken after 30 minutes.

#### 10.5.4.2 Influence of the frequency

The comparison between 20 kHz and 40 kHz ultrasound frequencies in the literature reveals significant differences in their impact on the solution. The 20 kHz ultrasound generates more intense cavitation, resulting in higher shear forces and agitation. This increased cavitation energy leads to more forceful bubble collapse, which in turn produces greater shear forces and finer particle sizes. Consequently, the 20 kHz frequency is effective in enhancing mixing, disrupting particles, and accelerating reactions. In contrast, the 40 kHz ultrasound induces less intense cavitation with smaller bubbles and a more localized effect. The energy released at bubble collapse is lower compared to 20 kHz, leading to less aggressive particle size reduction and milder mixing (Dong et al., 2020; Fargassa & Ippoliti, 2016; Capote & De Castro, 2007).

These two frequencies were studied to see which one gave higher results. The following figures show the palladium, platinum, and rhodium removal percentage over time and compare the results with ultrasounds at 20 kHz and 40 kHz with the results in the same conditions but without ultrasound. These silent conditions are the most optimal set of parameters as discussed in the previous section.

Platinum removal follows a similar trend with 20 kHz ultrasound, though the effect is less pronounced. After 3 hours, 20 kHz ultrasound achieves a 65% removal rate, compared to 40% without ultrasound. However, experiments with 40 kHz ultrasound result in lower removal rates than those observed in silent conditions. Ultrasound is known to enhance reaction kinetics, but it can also intensify side reactions. The initial boost in palladium cementation within the first 5 minutes is not observed for platinum, where results are similar with or without sonication. However, after 1 hour of 20 kHz ultrasound, the removal percentage matches that of the 3-hour silent experiment, indicating that ultrasound can reduce experimental duration.

The removal of rhodium is also significantly impacted by ultrasound. The 40 kHz ultrasound produces lower removal rates than silent conditions, while 20 kHz ultrasound achieves much higher removal percentages. After 3 hours, the 20 kHz treatment removes 75% of rhodium, compared to 40% without ultrasound. Although the initial kinetic advantage of 20 kHz ultrasound is not evident in the first few minutes, it becomes apparent within 1 hour, where over 40% of rhodium is removed—a percentage that the other two experiments only achieve after 3 hours. This demonstrates that ultrasound, particularly at 20 kHz, significantly enhances the cementation of rhodium.

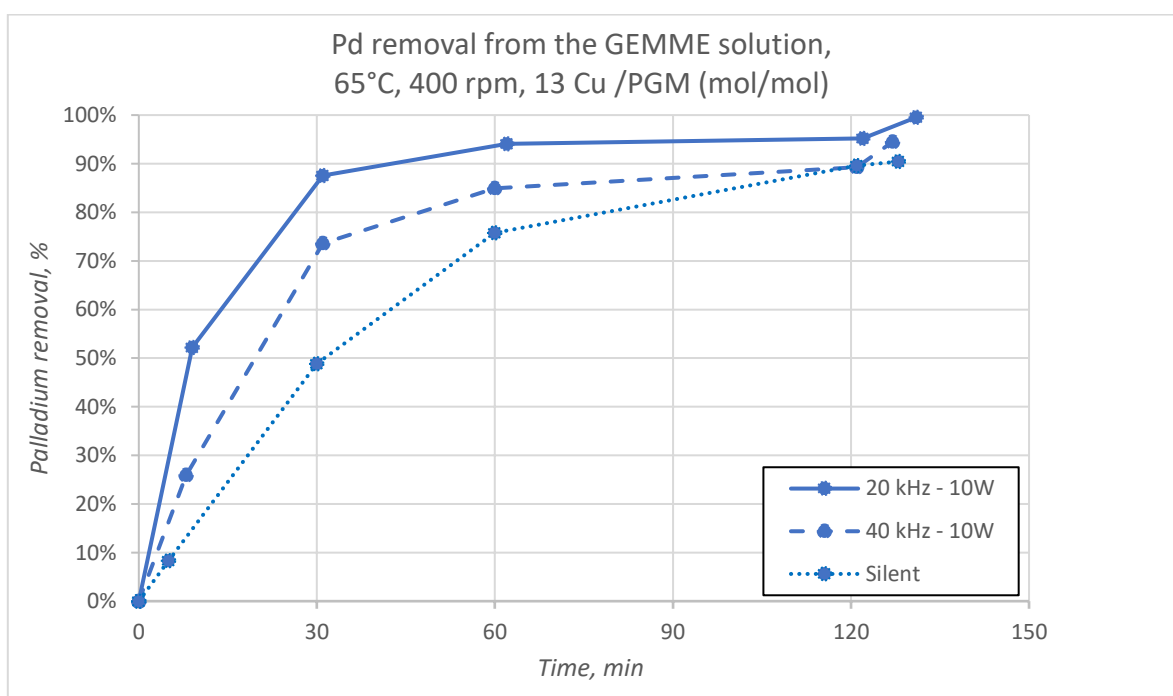


Figure 47: Palladium removal over time from the GEMME solution heated at 65°C at 400 rpm and a Cu/PGM molar ratio of 13. The graph compares palladium removal efficiency under silent conditions and with ultrasound at two different frequencies: 20 kHz and 40 kHz with a power consumed by the system of 10 W.

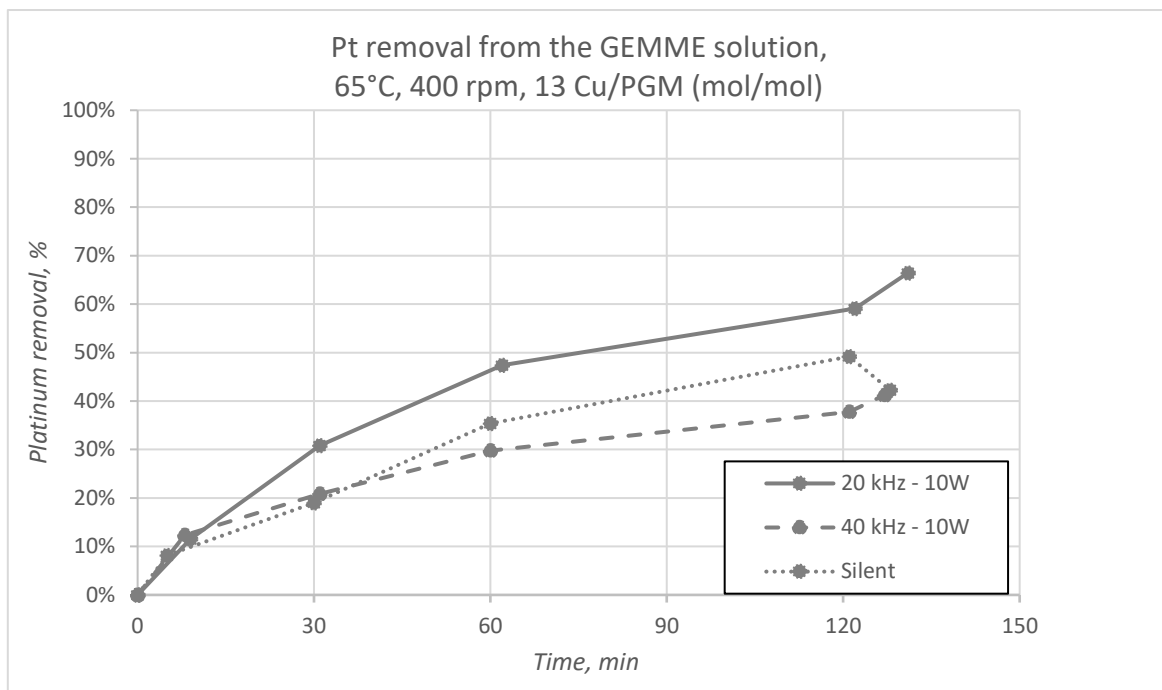


Figure 48: Platinum removal over time from the GEMME solution heated at 65°C at 400 rpm and a Cu/PGM molar ratio of 13. The graph compares platinum removal efficiency under silent conditions and with ultrasound at two different frequencies: 20 kHz and 40 kHz with a power consumed by the system of 10 W.

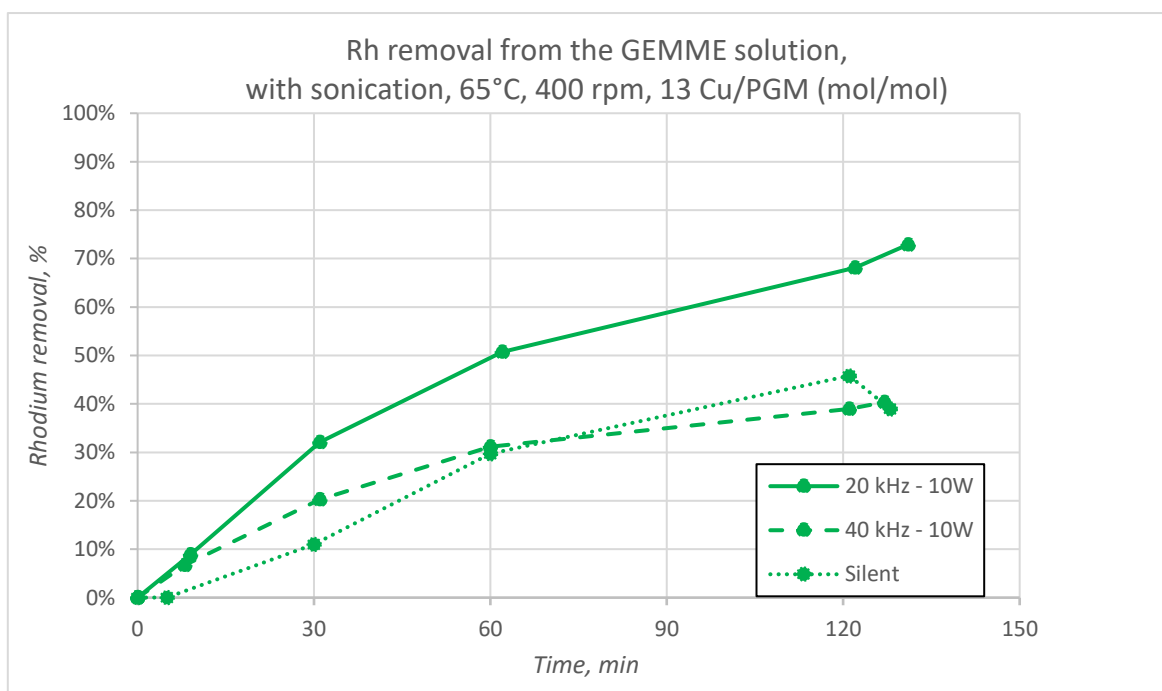


Figure 49: Rhodium removal over time from the GEMME solution heated at 65°C at 400 rpm and a Cu/PGM molar ratio of 13. The graph compares rhodium removal efficiency under silent conditions and with ultrasound at two different frequencies: 20 kHz and 40 kHz with a power consumed by the system of 10 W.

The optimal frequency for the recovery of platinum and rhodium is unequivocally 20 kHz. The overall results, as illustrated in Figure 50, indicate that this frequency enables the recovery of nearly 100% of palladium, 75% of rhodium, and 70% of platinum. The system appears to prioritize the cementation of palladium during the first 30 minutes, achieving 90% removal before the other two metals begin to

cement, following a quasi-linear trend. Extending the reaction time beyond 2 hours could provide valuable insights into whether the plateau observed in the removal of rhodium and platinum can be reached, potentially achieving 100% recovery.

The precipitation factor remains stable at approximately 7 throughout the experiment. Notably, copper continues to be present in the solution even after 90% of the palladium has been removed. This persistence is likely due to the reduction in particle size during the experiment, which increases the available surface area for cementation while preventing the formation of a passivation layer. This suggests that the process is efficient in maintaining active cementation sites, thereby enhancing the overall recovery of the targeted metals.

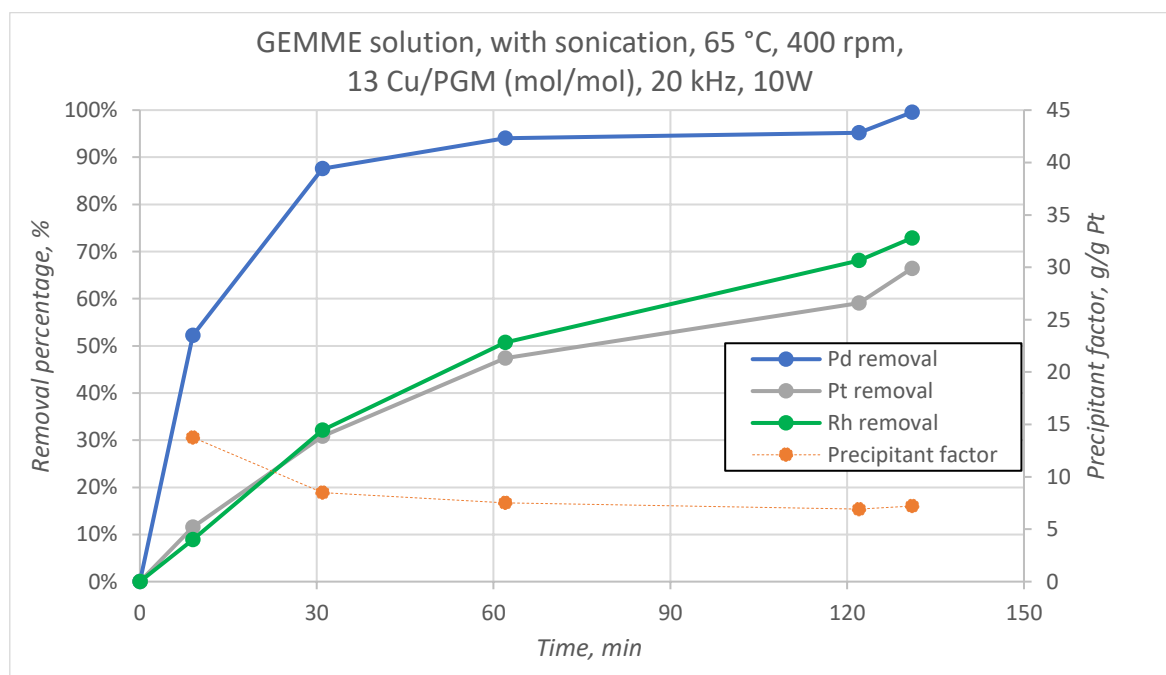


Figure 50: Best frequency of ultrasounds transmitted to the system to achieve high PGMs removal percentage over time from the GEMME solution at 65°C, with an agitation of 400 rpm, a Cu/PGM molar ratio of 13 and a power consumed by the system of 10 W.

#### 10.5.4.3 Influence of the power consumed by the system

The net power transmitted to the system during an experiment involving ultrasound refers to the power delivered to the solution which is calculated by the difference of the power emitted to the system and its respond. The losses due to inefficiencies such as absorption by reactor walls, heat dissipation, and wave reflection are also part of this number so it is really important to try to minimise these losses. The power consumed is a direct respond of the system to the ultrasounds.

In these experiments, powers studied are 4 W and 10 W. An experiment done with a frequency of 40 kHz trying to maximise the power consumed by the system (up to 40 W) was realised but the results are not available before the deadline of this work. This experiment was really noisy and painful for researchers in the lab.

The palladium, platinum, and rhodium removal percentages are showed on the three following figures and these results can be easily compared with the experiments without ultrasounds which is also represented on the graphs. The impact of ultrasounds on the system have already been discussed in the last section so the removal percentage of palladium with and without ultrasound is much higher with ultrasounds. The plateau is quickly reached, after 30 minutes 85% of palladium is removed and after one hour, 90% is reached. The difference between power consumed by the

system is not especially noticeable on the palladium removal but with 10W, 5 more percents is gained for the 5- and 30-minutes samples. After 1 hour, the plateau of 95% is reached and the experiment with 4 W or 10 W have the same results.

The platinum and rhodium removal percentages are quite similar. The use of ultrasounds boosts the kinetic of cementation especially for the rhodium removal. Within one hour of experiment, the results with ultrasounds equals the experiment of two hours without. The power consumed by the system gives the same results during the first hour but for the last hour of the experiment, the power of 10 W gives higher removal percentages. It goes from 50% with power of 4 W to 60% with a power of 10 W for the platinum while the rhodium is removed from 60% to 75% with the power of 4W and 10 W respectively.

The best value of the power consumed by the system is therefore 10 W so the graph with this set of parameters is represented on the Figure 50 which is represented in the last section.

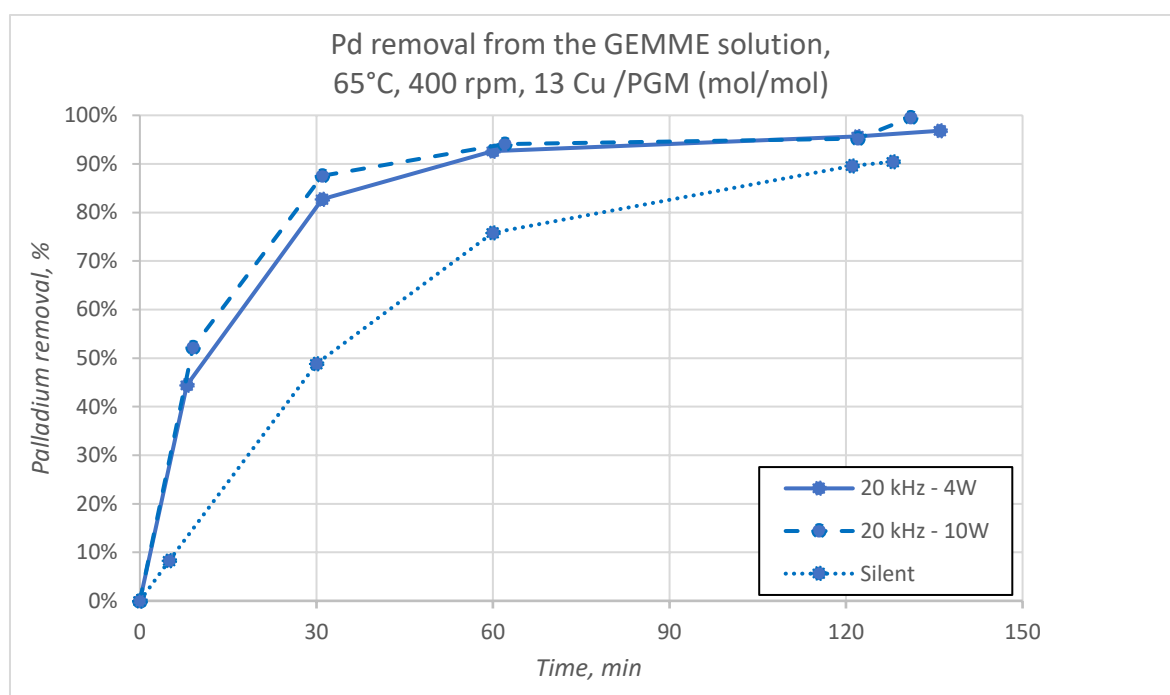


Figure 51: Palladium removal over time from the GEMME solution heated at 65°C at 400 rpm and a Cu/PGM molar ratio of 13. The graph compares palladium removal efficiency under silent conditions and with ultrasound at 20 kHz with two different powers consumed by the system: 4 W and 10 W.

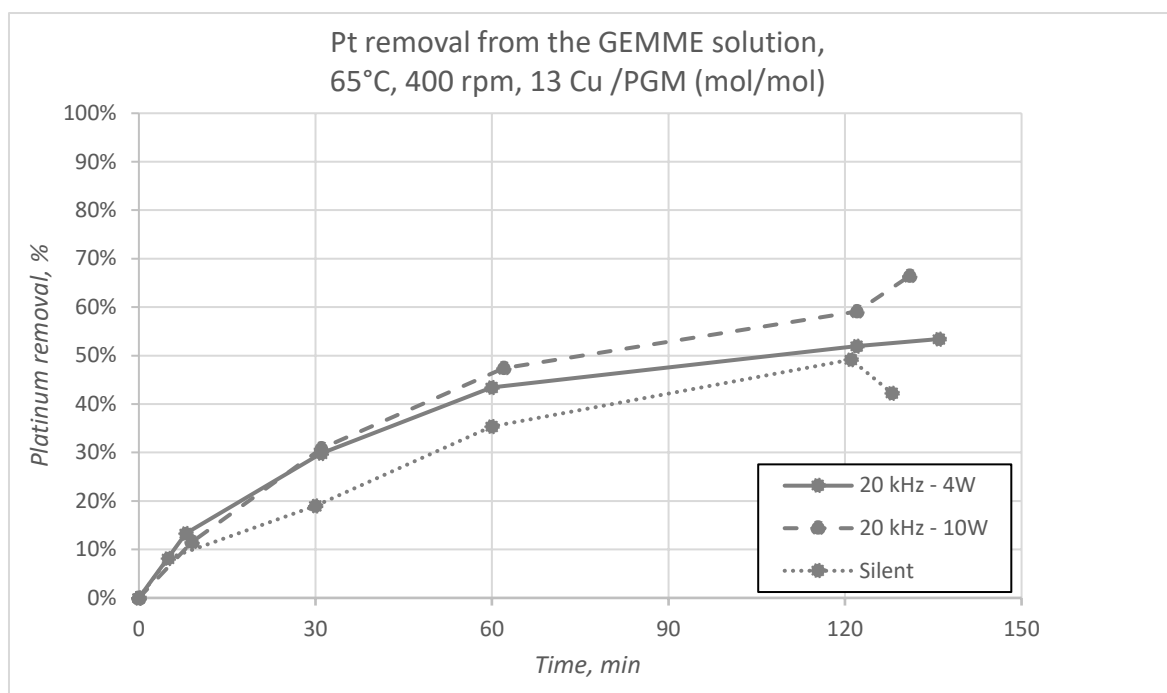


Figure 52: Platinum removal over time from the GEMME solution heated at 65°C at 400 rpm and a Cu/PGM molar ratio of 13. The graph compares platinum removal efficiency under silent conditions and with ultrasound at 20 kHz with two different powers consumed by the system: 4W and 10 W.

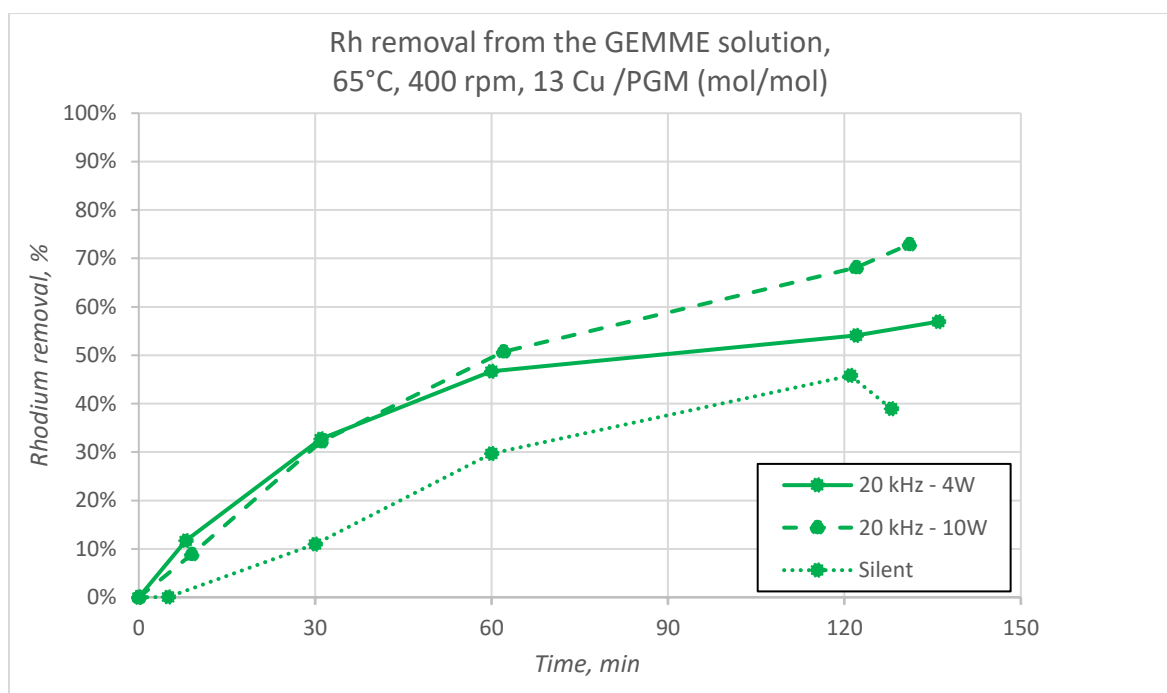


Figure 53: Rhodium removal over time from the GEMME solution heated at 65°C at 400 rpm and a Cu/PGM molar ratio of 13. The graph compares rhodium removal efficiency under silent conditions and with ultrasound at 20 kHz with two different powers consumed by the system: 4 W and 10 W.

#### 10.5.4.4 Influence of the temperature

The temperature was a key factor in the previous experiments on the Pt-DOC solution and on the GEMME solution without ultrasound. The general behaviour is the higher the temperature, the higher the removal percentage. The impact of the temperature on the reactions of cementation with ultrasound of 20 kHz with a power consumed of 10 W is studied in this section. To have a better



general point of view of the influence of the temperature with and without ultrasound, the different curves are represented on the same graph. The results with ultrasounds are represented in black while the results without ultrasounds are represented in the same colour code as in the rest of the document.

Based on the following graphs, temperature has a significant impact on the cementation of PGMs in the solution. The observed trend is consistent with expectations: higher temperatures lead to higher removal percentages, a pattern that persists even when ultrasound is applied. The combination of elevated temperature and ultrasound (20 kHz, 10W) yields the most efficient palladium removal, with complete extraction achieved at 85°C. After just 1 hour at this temperature, a plateau is reached, and remarkably, within 30 minutes, 90% of the palladium is removed. Ultrasound further accelerates this process, with 60% of the palladium removed after only 5 minutes at 85°C. The results at 65°C follow a similar trend, although there is a slight 5% gap in removal efficiency compared to 85°C. Interestingly, heating the solution to 85°C or 65°C without ultrasound proves more effective than using ultrasound at 45°C. Initially, during the first 30 minutes, the removal efficiency at 65°C under silent conditions closely matches that at 45°C with ultrasound, but after 1 hour, the 45°C ultrasound condition becomes less effective. At lower temperatures, such as 25°C, ultrasound still enhances palladium removal compared to silent conditions. Specifically, ultrasound facilitates 40% removal at 25°C, 60% at 45°C, and 100% at 65°C and 85°C after 2 hours. These findings highlight the substantial role of ultrasound in accelerating palladium cementation, particularly at higher temperatures, while also demonstrating its utility even at lower temperatures where it significantly improves the reaction kinetics.

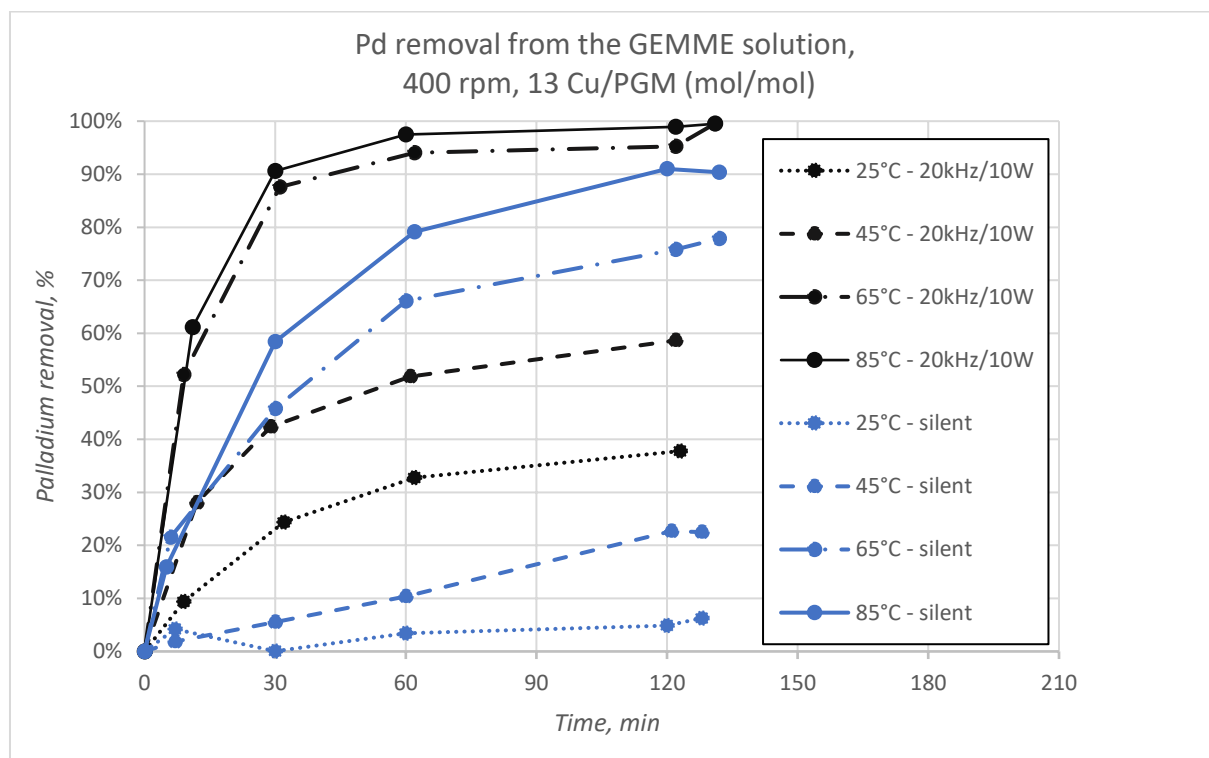


Figure 54: Palladium removal over time from the GEMME at an agitation of 400 rpm and a Cu/PGM molar ratio of 13. The graph compares palladium removal efficiency under silent conditions and with ultrasound at 20 kHz with a power consumed of 10 W at four different temperatures: 25°C, 45°C, 65°C and 85°C.

The Figure 55 illustrates the impact of temperature and ultrasound (20 kHz, 10W) on the efficiency of platinum removal from the GEMME solution. The experiments were conducted at 400 rpm with a

Cu/PGM molar ratio of 13. The data reveal a clear relationship between temperature, ultrasound application, and the effectiveness of platinum cementation.

At 85°C, the combination of ultrasound and high temperature results in the most significant removal efficiency, with approximately 75% of the platinum removed after 2 hours. This outcome highlights the strong influence of both temperature and ultrasound on enhancing the cementation process. The removal percentage at 85°C with ultrasound after 30 minutes is equal to the removal percentage of the same experiment without ultrasound after 2 hours. The kinetic of the reaction is enhanced by ultrasound. A similar trend is observed at 65°C with ultrasound, where the final removal percentage reaches 65%. In contrast, at 45°C and 25°C, the platinum removal percentages are significantly lower, reaching only about 15% in the best case, regardless of ultrasound application. Without ultrasound, the removal efficiency at 85°C reaches 50%, and at 65°C, it only achieves 35%, which is roughly half of what can be recovered with ultrasound at the same temperature.

The experiments do not appear to have reached a plateau, indicating that extending the duration with the optimal set of parameters could provide valuable insights into the cementation behaviour of platinum over a longer period and potentially achieve removal percentages higher than 75%.

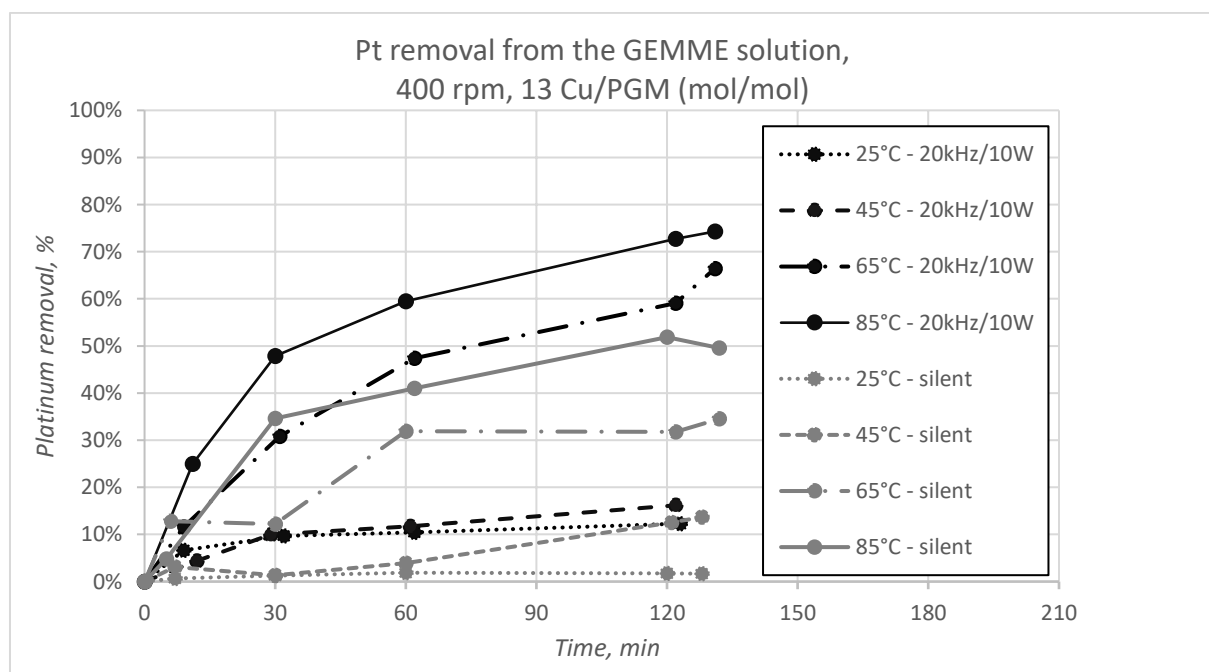


Figure 55: Platinum removal over time from the GEMME at an agitation of 400 rpm and a Cu/PGM molar ratio of 13. The graph compares platinum removal efficiency under silent conditions and with ultrasound at 20 kHz with a power consumed of 10 W at four different temperatures: 25°C, 45°C, 65°C and 85°C.

The Figure 56 presents the rhodium removal percentage over time at four different temperatures, comparing experiments conducted without sonication to those using ultrasound at 20 kHz and 10W. The most effective set of parameters is 85°C with ultrasound, achieving an 85% removal rate. Experiments conducted at 65°C with ultrasound recover 75% of the rhodium from the initial solution. These results are significant as they demonstrate that high recovery rates of rhodium are achievable through cementation onto copper under optimal conditions.

In contrast, without ultrasound, the removal percentages are lower, with 50% rhodium removal at 85°C and 25% at 65°C. This highlights the substantial impact of ultrasound on enhancing rhodium

recovery during the cementation process. Experiments performed at 45°C and 25°C, both with and without ultrasound, yield low removal percentages, around 10%. Therefore, to effectively recover rhodium, it is essential to heat the solution and apply ultrasound.

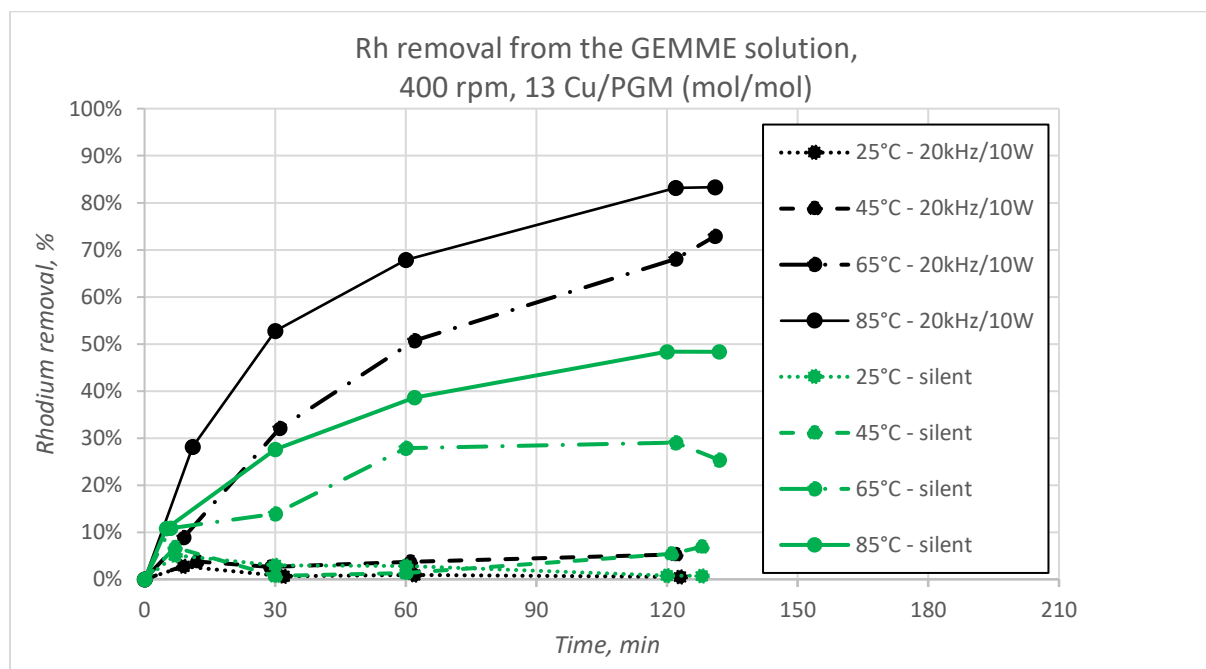


Figure 56: Rhodium removal over time from the GEMME at an agitation of 400 rpm and a Cu/PGM molar ratio of 13. The graph compares rhodium removal efficiency under silent conditions and with ultrasound at 20 kHz with a power consumed of 10 W at four different temperatures: 25°C, 45°C, 65°C and 85°C.

The optimal temperature for the process is 85°C, though 65°C also yields high removal rates. The Figure 57 displays the removal percentages of the three metals at 85°C, under agitation at 400 rpm, with a Cu/PGM molar ratio of 13, and ultrasound applied at 20 kHz and 10W. The precipitant factor remains constant, indicating a stable copper-to-PGM consumption ratio of approximately 7. This suggests that copper is not excessively consumed at any point during the process.

The continuous removal of metals after 2 hours implies that copper is still available and has not developed a passivation layer around its grains, which would otherwise inhibit the reaction. However, the hydrolysis of iron is a potential issue at 85°C with ultrasound, complicating filtration. Therefore, subsequent experiments were conducted at 65°C to facilitate easier filtration while maintaining effective metal removal.

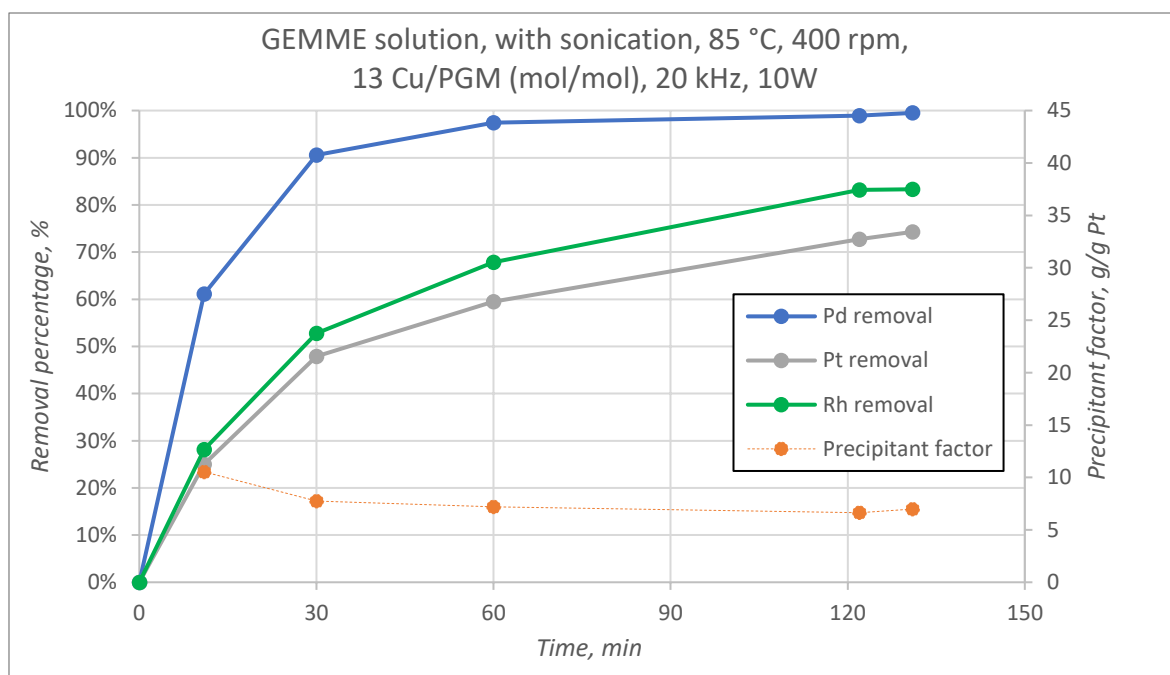


Figure 57: Best temperature to achieve high PGMs removal percentage over time from the GEMME solution at 65°C, at 400 rpm, a Cu/PGM molar ratio of 13 with ultrasound set at 20 kHz and a power consumed by the system of 10 W.

#### 10.5.4.5 Influence of the agitation

Agitation plays a critical role in the efficiency and effectiveness of cementation reactions, particularly in systems where side reactions may occur. The cementation is a process that is influenced by various factors including the surface area of the solid metal, mass transfer rates, and the interaction of reactants within the solution. However, agitation must be carefully controlled, as excessive turbulence can introduce unwanted side reactions

The impact of agitation will be studied in the following figures by comparing the results with and without ultrasound (20 kHz, 10 W) for palladium, platinum, and rhodium separately. This comparison will help determine how ultrasound influences the efficiency of metal recovery in the cementation process for each of these precious metals.

The recovery percentages for palladium are higher than those for platinum and rhodium, but the overall trends are consistent across all three metals. The influence of agitation on the system is well-known. For a solution with a very low pH, such as the Pt-DOC, it is preferable to keep the solid relatively immobile compared to the solution to avoid side reactions with the sacrificial metal, which in this case is copper. In contrast, for the GEMME solution, higher agitation levels result in better recovery outcomes. This trend is also observed when ultrasounds are applied.

Interestingly, the effect of ultrasound on the system is most beneficial when the agitation is set to 400 rpm. However, when the agitation is reduced to 200 rpm, the tests without ultrasound become more favourable. Without agitation, whether ultrasound is applied or not, the results are below 10%, rendering them negligible.

Palladium reaches a 100% recovery rate with ultrasound at 400 rpm and 90% at 200 rpm. Although the reaction kinetics at 200 rpm with ultrasound were slower, satisfactory results were still achieved after 2 hours. Without ultrasound, at 400 rpm, 90% of palladium is recovered, and 80% at 200 rpm. For platinum and rhodium, similar recovery percentages are observed. With ultrasound at 400 rpm and 200 rpm, 65% and 50% of platinum and rhodium are recovered, respectively. Without

ultrasound, at 400 rpm and 200 rpm, recovery rates of 45% and 30% are achieved. Therefore, it is preferable to agitate the solution at 400 rpm with ultrasound. The complete results for the three metals, along with the precipitant factor, are shown in Figure 57.

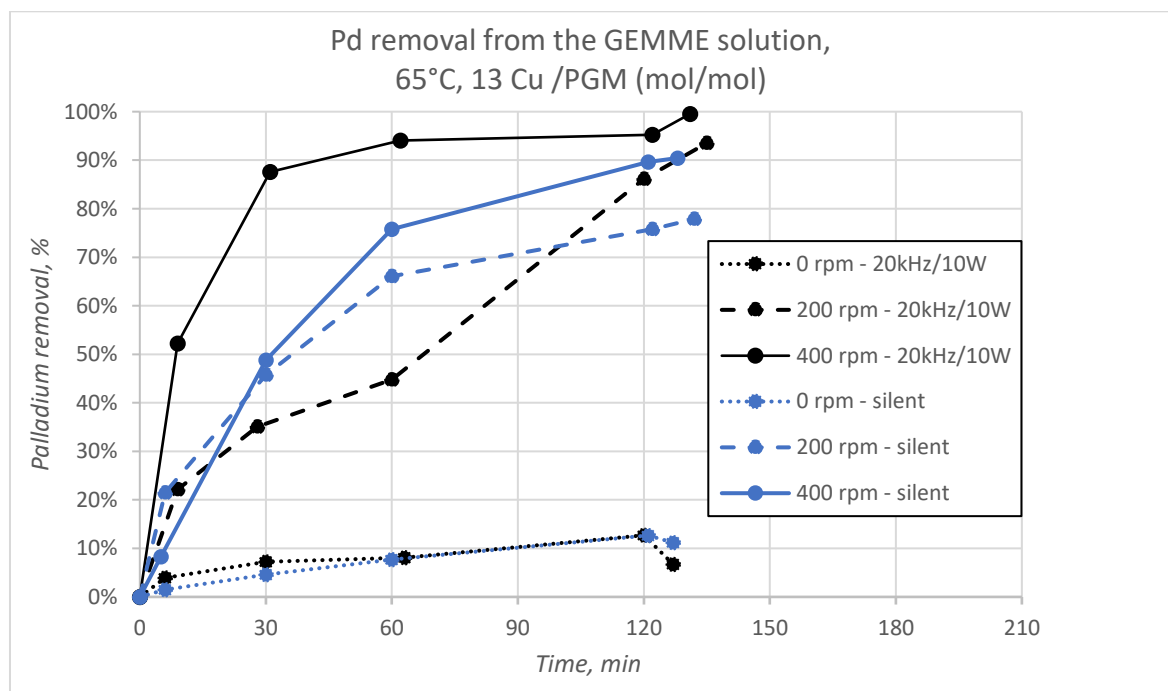


Figure 58: Palladium removal over time from the GEMME at 65°C and a Cu/PGM molar ratio of 13. The graph compares palladium removal efficiency under silent conditions and with ultrasound at 20 kHz with a power consumed of 10 W at three different agitations: 0 rpm, 200 rpm and 400 rpm.

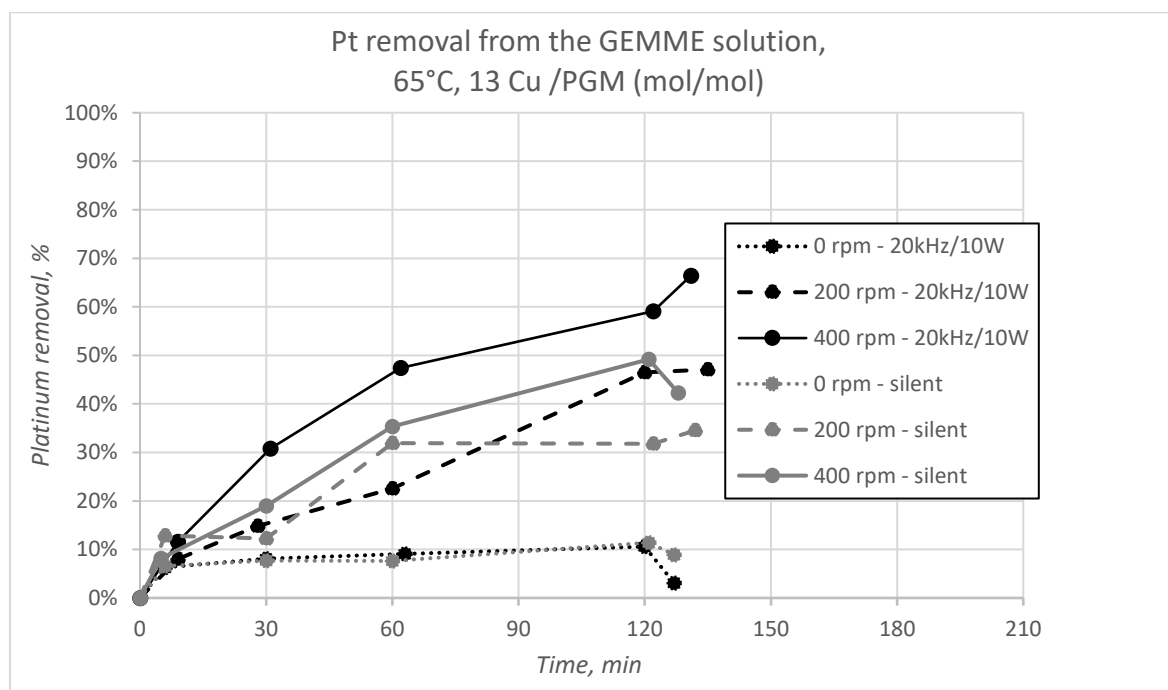


Figure 59: Platinum removal over time from the GEMME at 65°C and a Cu/PGM molar ratio of 13. The graph compares platinum removal efficiency under silent conditions and with ultrasound at 20 kHz with a power consumed of 10 W at three different agitations: 0 rpm, 200 rpm and 400 rpm.

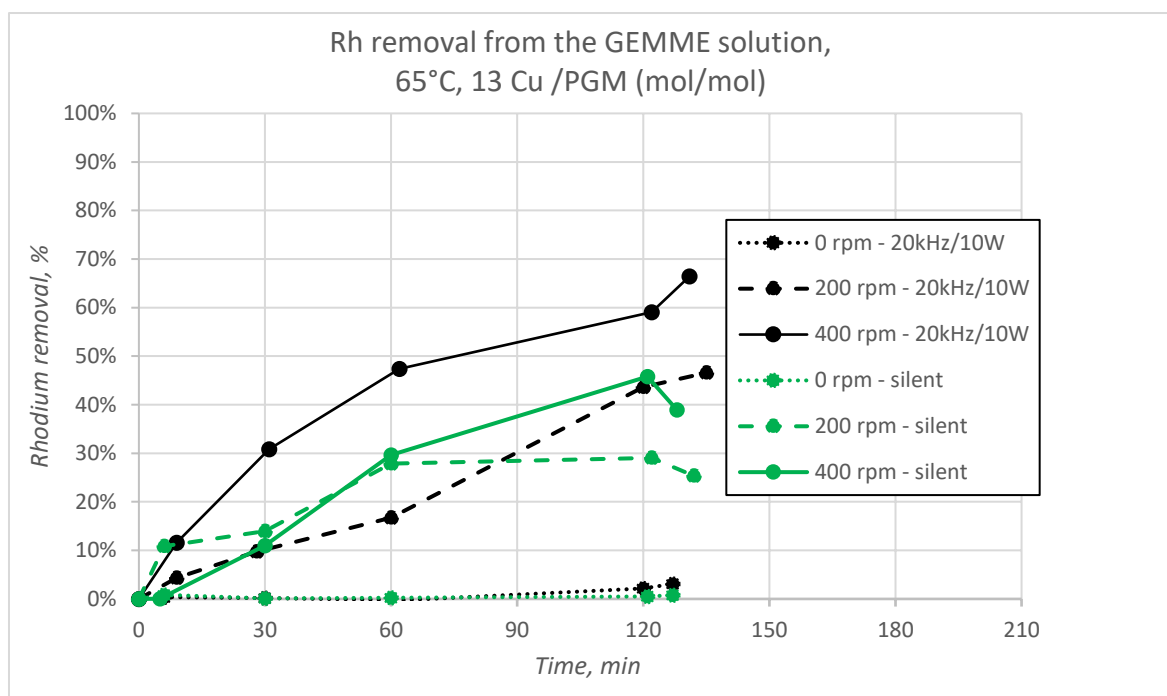


Figure 60: Rhodium removal over time from the GEMME at 65°C and a Cu/PGM molar ratio of 13. The graph compares rhodium removal efficiency under silent conditions and with ultrasound at 20 kHz with a power consumed of 10 W at three different agitations: 0 rpm, 200 rpm and 400 rpm.

#### 10.5.4.6 Influence of the Cu/PGM molar ratio

In cementation processes, the presence of the sacrificial metal in excess is crucial for maintaining its availability in the metallic state, which is necessary for the ongoing reduction of the target metal ions. This excess ensures that even as some of the sacrificial metal undergoes side reactions—inevitable in any reactive system—there remains a sufficient quantity in its elemental form to drive the cementation forward effectively. By maintaining an excess of the sacrificial metal, the system can accommodate these side reactions without compromising the efficiency and completeness of the cementation process.

In Athens, the Pt-DOC solution exhibited a negative pH, indicating that oxidant reactants from the leaching step were still present in the solution. This necessitated the addition of copper in significant excess to ensure complete cementation of the platinum. Specifically, using 53 times and 16 times the stoichiometric molar amount of copper resulted in high recovery rates with nearly complete platinum cementation. Tests conducted with only 1.6 times the molar ratio of copper yielded very low recovery rates. Given this context, and considering that the current solution is less acidic, implying fewer excess reactants from the leaching step, the Cu/PGM molar ratios under consideration have been adjusted to 13 times, 9 times, and 5 times.

The following figures present the results for the three elements—palladium, platinum, and rhodium—studied separately with and without ultrasound (20 kHz, 10W), each after 2 hours of experimentation. The recovery of palladium has consistently been high since the initial ultrasound results. With 13 times Cu/PGM, 100% of the palladium can be recovered with ultrasound, and 90% without ultrasound, compared to 50% recovery with and without ultrasound at 10 times Cu/PGM, and only 5% at 5 times Cu/PGM. The results with and without ultrasound follow the same trend when the Cu/PGM ratio is the same, with ultrasound yielding higher recoveries.

For platinum recovery, using 13 times Cu/PGM yields 65% recovery with ultrasound and 45% without, whereas with only 9 times Cu/PGM, both experiments result in 25% recovery, and with 5

times Cu/PGM, only 10% is recovered. In the case of rhodium, with 13 times Cu/PGM, the results show 75% recovery with ultrasound compared to 40% without, indicating a more significant gap than with the other two metals. For 9 and 5 times Cu/PGM, the amount of copper added is too low, resulting in recoveries below 10%. Therefore, it is important to add at least 13 times Cu/PGM to the system to achieve sufficiently high recovery rates, and an experiment could be conducted with even more copper to see if it would further improve these results.

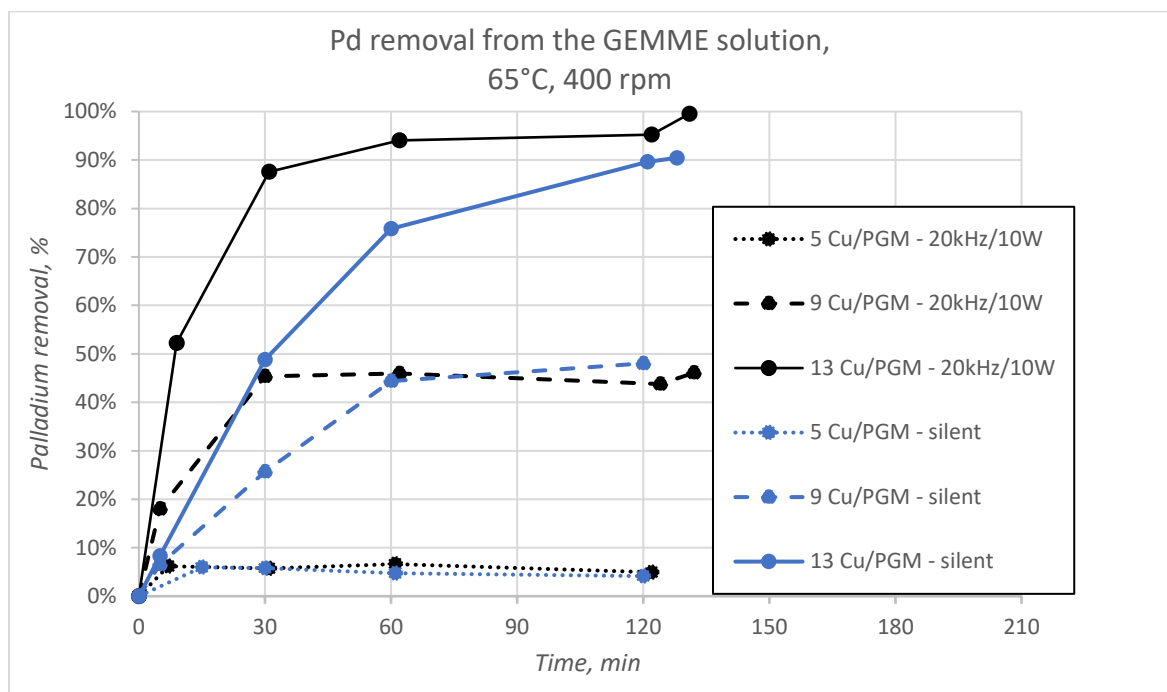


Figure 61: Palladium removal over time from the GEMME at 65°C and 400 rpm. The graph compares rhodium removal efficiency under silent conditions and with ultrasound at 20 kHz with a power consumed of 10 W at three different Cu/PGM molar ratio: 5 times, 9 times and 13 times.

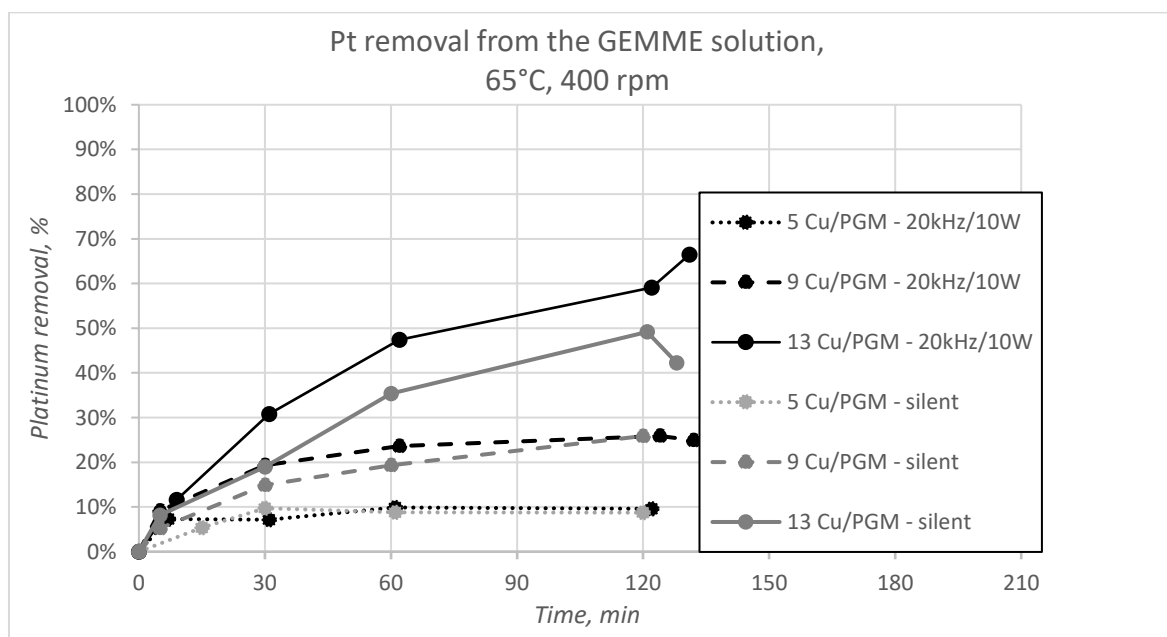


Figure 62: Platinum removal over time from the GEMME at 65°C and 400 rpm. The graph compares platinum removal efficiency under silent conditions and with ultrasound at 20 kHz with a power consumed of 10 W at three different Cu/PGM molar ratio: 5 times, 9 times and 13 times.



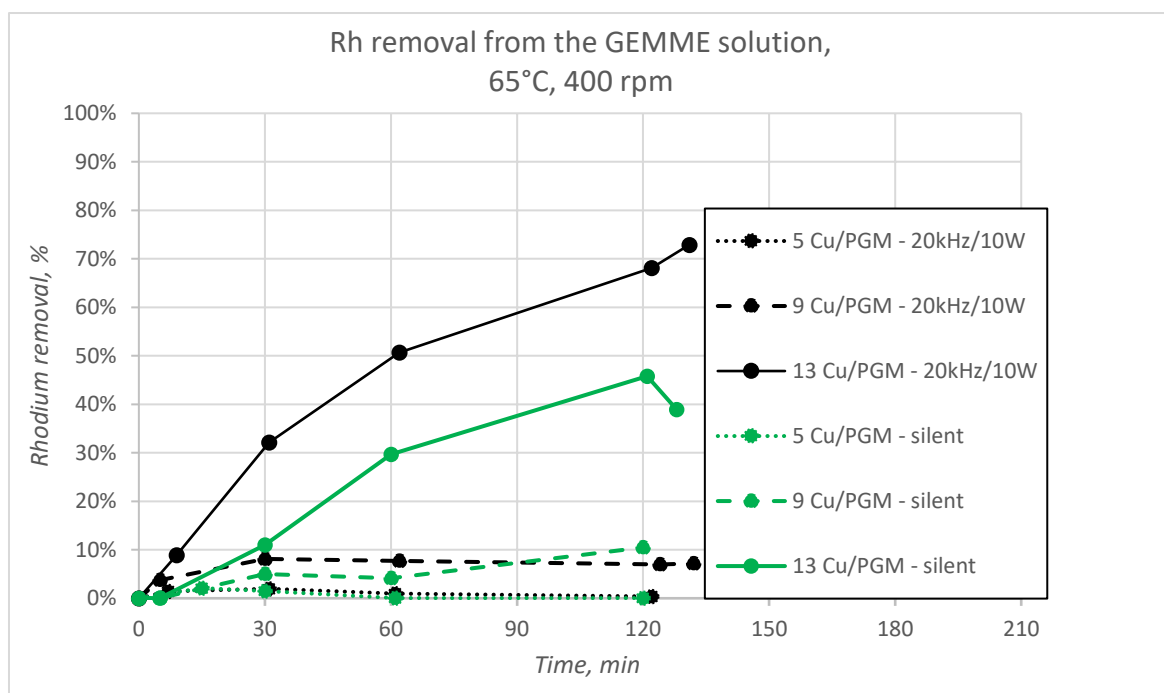


Figure 63: Rhodium removal over time from the GEMME at 65°C and 400 rpm. The graph compares rhodium removal efficiency under silent conditions and with ultrasound at 20 kHz with a power consumed of 10 W at three different Cu/PGM molar ratio: 5 times, 9 times and 13 times.

#### 10.5.5 Conclusion of the experiments with ultrasounds on the GEMME solution

The experiments conducted on the GEMME solution with the application of ultrasound have provided significant insights into optimizing the cementation of platinum group metals onto copper. The use of ultrasound has led to high removal efficiencies, achieving approximately 100% for palladium, 75% for platinum, and 85% for rhodium. In contrast, without ultrasound, the removal efficiencies decrease to 90% for palladium and 50% for both platinum and rhodium.

The impact of ultrasound on the solid particle size is probably one of the key factors. Sonication generates high-energy bubble collapse, which fragments the solid particles, thereby increasing the surface area of copper available for cementation. The availability of the sacrificial material in its metallic state is a critical parameter to have a cementation reaction. Consequently, the amount of copper added to the system is a parameter that had to be studied expressed as Cu/PGM molar ratio. Based on these results, with and without ultrasound, it is necessary to add at least 13 times the stoichiometric amount of copper to achieve optimal cementation. When the molar ratio of Cu/PGM is reduced to 9, the removal percentages decrease by half, indicating that this lower ratio is insufficient for effective cementation, even with ultrasound. To assess whether the limiting factor in cementation is the availability of surface area or the probability of molecular interactions, further experiments could be conducted. These experiments might involve increasing the initial amount of copper in the system with the habitual setup or employing a closed-circuit system to circulate the solution. This new setup would involve a larger overall solution volume, maintaining the same Cu/PGM molar ratio. However, the solid would interact with a smaller, localized volume of solution, as the remainder circulates. This approach allows for testing the probability of molecular interactions without altering the Cu/PGM molar ratio.

To optimize the cementation of PGMs onto copper from the GEMME solution, various parameters must be studied. Among these, the frequency and power of the ultrasound system are essential for achieving optimal conditions. While different frequencies and power levels were tested, the most

effective configuration was found to be a frequency of 20 kHz with a power consumed by the system of 10 W. This specific frequency generates more intense cavitation, leading to stronger shear forces and more effective disruption of solid particles, which in turn enhances the overall reaction kinetics. Although varying the frequency yields different results, making its optimization a priority, changes in power consumption had a lesser impact on the system's performance. The choice of 10 W was made because it provided a 5% improvement in PGM removal efficiency, although a power level of 4 W also achieved reasonable results.

Once the ultrasound parameters are optimized, another critical factor to consider is temperature, which significantly influences the removal efficiency of PGMs, both with and without ultrasound. Higher temperatures generally lead to better results, with the most effective temperature identified as 85°C among the temperatures studied: 25°C, 45°C, 65°C, and 85°C. However, maintaining a temperature of 85°C poses challenges, particularly with filtration. At this temperature, iron hydrolysis occurs at a lower pH compared to reactions at 25°C, making iron hydrolysis unavoidable under the experimental conditions. The precipitation of the iron at the beginning of the experiment is a way to reduce the copper consumption of the system. Although the presence of iron in the cement is not considered an impurity by Monolithos Catalysts & Recycling Ltd., since the key factor is its ratio relative to the PGM grade, the main issue lies in filtration. The fine particles produced by iron hydrolysis complicate the filtration process. Therefore, a temperature of 65°C was selected as a compromise, allowing for smoother filtration while avoiding the complications associated with iron hydrolysis at higher temperatures. This trade-off must be carefully considered when selecting the optimal temperature.

Agitation was the final parameter studied. Previous experiments conducted on the Pt-DOC solution in Athens, a highly acidic solution with a negative pH, demonstrated that minimal agitation of the solid relative to the solution's movement is optimal for recovering platinum without excessive copper consumption. This approach minimizes side reactions while still achieving high removal percentages. In contrast, for the GEMME solution, increased agitation correlated with higher removal percentages. This effect is likely due to the enhanced probability of molecular interactions, which improves with greater agitation. Even with the application of ultrasound, higher agitation yielded better results. Consequently, an agitation speed of 400 rpm using an overhead stirrer was determined to be the most effective parameter.

In conclusion, the combination of ultrasound at 20 kHz and 10W, with high temperatures (65°C – not 85°C because of the challenging filtration), vigorous agitation (400 rpm), and an adequate Cu/PGM molar ratio (13 times), provides the most efficient conditions for the cementation process in the GEMME solution.

## 11 Kinetic study of the cementation reactions

A kinetic study is essential for gaining a deeper understanding of a system's behaviour, enabling researchers to predict how it will respond under various conditions. This understanding is crucial, particularly when scaling up a process, as it allows for more accurate control and optimization of the system. The study of kinetics helps determine whether the system is controlled by chemical reactions, diffusion, or a combination of both, as highlighted in previous research (Aâtach et al., 2024; Casado, 2018; Khudenko, 1984; Power & Ritchie, 1976). Achieving a comprehensive understanding of these processes makes the system more predictable, which is a key goal in research and development.

A kinetic study typically involves several steps. The first step is to obtain precise data on the concentration of the element under study in the solution at various specific times. Conducting experiments at different temperatures is important for making accurate approximations of the system's behaviour. The more data points available—such as concentrations and temperatures—the more precise the study will be. Once the different concentrations are known and sufficient data points are collected, the rate constant  $k$  can be determined. Following this, the activation energy of the process can be calculated, providing further insights into the system's kinetics.

### 11.1 Theoretical background

This section elucidates the fundamental mechanisms involved in kinetic studies. Although kinetic analysis can encompass a wide range of complex reactions, this study specifically addresses a well-characterized, simpler reaction system. While existing data provide a foundation, additional experimental work is essential to expand the dataset, thereby reducing experimental variability and enhancing the accuracy of empirical model fitting. This investigation represents an initial exploration of the reaction kinetics, with the potential for further detailed analysis in subsequent studies.

An irreversible reaction can be summarized by the following equation:



Assuming the reaction is essentially irreversible (i.e., any intermediates formed are reactive and do not accumulate), the reaction rate is related to the rate of disappearance of reactants or the formation of products by the following equation, which is based on the stoichiometry of the reaction:

$$Rate = -\frac{1}{a} \frac{d[A]}{dt} = -\frac{1}{b} \frac{d[B]}{dt} = \frac{1}{p} \frac{d[P]}{dt} = \frac{1}{q} \frac{d[Q]}{dt} \quad (14)$$

where the symbols within the brackets denote concentrations, and (a, b, p, q) are the stoichiometric coefficients (Farcas & Aubert, 2016).

The reaction rate generally depends on factors such as temperature, pressure, concentration of species, and the phases in which the reaction occurs. However, an empirical relation known as the rate law can be experimentally determined, which expresses the rate of reaction in terms of the concentrations of chemical species:

$$Rate = k[A]^m[B]^n \quad (15)$$

where  $k$  is the rate constant, and the exponents  $m$  and  $n$  are determined experimentally. These exponents can be whole numbers (positive or negative) or, in complex reactions, fractions. Importantly, these exponents are independent of concentration and time, meaning they are not directly linked to the stoichiometric coefficients  $a$  and  $b$ . The order of the reaction is the sum of the exponents in the rate law, i.e., the sum of the partial orders with respect to individual reagents ( $m + n$ ) in Equation 15 (Farcas & Aubert, 2016).

The concentration expressed in Equation 3 can also be represented in terms of the conversion rate, symbolized as  $X_A$ . This represents the initial amount of  $A$  in the solution minus what is present at time  $t$ , divided by the initial amount of  $A$ . It is often more accurate to use  $X_A$  when the volume of the solution does not remain constant (Levenspiel, 1998). In this study, while the volume has some variations, these can sometimes be neglected. Therefore, it may be more appropriate to use the conversion ratio instead of the concentration of the element in the solution.

### 11.1.1 Determination of the rate constant

The rate constant,  $k$ , is the proportionality constant that relates the reaction rate to the concentrations of the reactants. Notably,  $k$  cannot be directly compared between reactions of different orders due to the differing units involved (Farcas & Aubert, 2016). The value of  $k$  is highly dependent on temperature, typically increasing rapidly as temperature rises. It is also influenced by the presence of catalysts (Havlík, 2008).

For this study, the rate equation can be simplified by focusing exclusively on reactant A, as reactant B—copper in this case—is maintained in excess throughout the experiments to ensure sufficient availability for the cementation of PGMs. Under these conditions, the rate equation reduces to:

$$\text{Rate} = k[A]^n = -\frac{d[A]}{dt} \quad (16)$$

$$\frac{d[A]}{[A]^n} = k dt \quad (17)$$

To determine the value of the rate constant,  $k$ , integration of the above equation yields:

$$\text{Zero order: } [A] = [A]_0 - kt \quad (18)$$

$$\text{First order: } \ln[A] = \ln[A]_0 - kt \quad (19)$$

$$\text{Second order: } \frac{1}{[A]} = \frac{1}{[A]_0} + kt \quad (20)$$

In a zero-order reaction, the rate is independent of the reactant concentration. A first-order reaction is characterized by a rate directly proportional to the concentration of a single species, while a second-order reaction has a rate proportional to the square of that concentration (Farcas & Aubert, 2016).

To determine the reaction order, various plots can be generated—such as  $[A]$ ,  $\ln[A]$ , and  $\frac{1}{[A]}$  versus time. The plot that yields a linear relationship indicates the reaction order, and the slope of this plot corresponds to the rate constant,  $k$ . Once  $k$  is known, the activation energy can be studied, as direct comparisons of rate constants across reactions of different orders are not valid (Havlík, 2008).

In this study, the concentration of A should be replaced by the conversion of A, expressed as the unconverted fraction,  $1-X_A$  (Levenspiel, 1998).

### 11.1.2 Determination of the activation energy of a reaction

Activation energy is the minimum amount of energy required for a chemical reaction to proceed, acting as an energy barrier that reactants must overcome to be transformed into products. In chemistry, the significance of activation energy lies in its direct impact on the reaction rate: a lower activation energy facilitates a faster reaction, whereas a higher activation energy results in a slower reaction. Understanding activation energy is essential for controlling reaction conditions and designing catalysts that lower this energy barrier, thereby enhancing reaction efficiency.

The Arrhenius activation energy is determined by measuring the rate constants at different temperatures, a method applicable to most homogeneous elementary and complex reactions. The Arrhenius rate law, derived empirically prior to the development of transition state theory, is based on the observation that reaction rates increase exponentially with an increase in absolute temperature:

$$k = Ae^{-\frac{E_a}{RT}} \quad (21)$$

where  $A$  is the Arrhenius pre-exponential factor,  $E_a$  the Arrhenius activation energy,  $R$  the gas constant ( $1.987 \text{ cal mol}^{-1} \text{ K}^{-1}$  or  $8.314 \text{ J mol}^{-1} \text{ K}^{-1}$ ), and  $T$  the absolute temperature. To find the energy of activation, the Equation 21 can be rearranged as:

$$\ln(k) = \ln(A) - \frac{E_a}{R} \frac{1}{T} \quad (22)$$

To calculate the activation energy, a graph of  $\ln(k)$  versus  $1/T$  is plotted. The slope of the resulting linear function equals  $-\frac{E_a}{R}$ , from which  $E_a$  can be directly calculated. Reactions with high activation energies are highly sensitive to temperature changes, whereas those with low activation energies are relatively temperature-insensitive (Levenspiel, 1998).

### 11.1.3 Diffusion coefficient

Nernst's theory is foundational in mass transfer theory, particularly in systems where chemical reactions at interfaces are involved. Nernst postulated that chemical processes occurring at the interface are significantly faster than the mass transfer steps, making the overall reaction rate controlled by mass transfer. In the simplest scenario, the reaction between a reactant ion and a solid surface occurs so rapidly that equilibrium is achieved almost instantaneously. As a result, the concentration of the reactant at the interface, denoted as  $c_1$ , remains negligible. The rate-limiting step in this process is thus determined by the rate at which the reactant reaches the reaction surface (Havlík, 2008).

In a well-mixed solution, the concentration  $c$  within the bulk of the solution is uniform, and the concentration gradient between the bulk concentration  $c$  and the interfacial concentration  $c_1$  is determined by the difference in concentration across a thin stationary liquid layer of thickness  $\delta$  adjacent to the leached surface. If the reaction surface area is  $A$  Fick's law can be applied, stating that the number of molecules  $dN$  transferring from the bulk solution to the solid surface over time  $dt$  is proportional to the concentration gradient normal to the surface,  $dc/dy$ :

$$dN = -DA \left( \frac{dc}{dy} \right) dt \quad (23)$$

The proportionality coefficient  $D$  is the diffusion coefficient with the dimension  $[(\text{length})^2/\text{time}]$ . For a solid substance in contact with the solution, the volume  $V$  is also considered. a linear concentration gradient, expressed as  $\frac{c-c_1}{V\delta}$  (Havlík, 2008).

Consequently, the equation becomes:

$$-\frac{dc}{dt} = \frac{DA(c - c_1)}{V\delta} \quad (24)$$

When simplifying particles as spheres, the diffusion coefficient  $D$  can be derived using the Stokes-Einstein relation, which relates the velocity associated with the kinetic energy of particles to the viscous drag experienced as they move within a fluid of viscosity  $\mu$ :

$$D = \frac{kT}{6\pi\mu r} \quad (25)$$

where  $k$  is the Boltzmann constant ( $\text{J/K}$ ) also known as the rate constant of first-order reaction,  $T$  is the absolute temperature ( $\text{K}$ ),  $\mu$  is the dynamic viscosity ( $\text{Pas}$ ) and  $r$  is the particles radius ( $\text{m}$ ) (Hamada & De Anna, 2021). This relationship underscores the role of temperature, viscosity, and particle size in the diffusion process, integral to understanding mass transfer in reactive systems.

#### 11.1.4 Chemically controlled or diffusion-controlled reactions

The activation energy of a reaction provides insights into whether the reaction is controlled by chemical kinetics, diffusion, or a combination of both. Understanding this behaviour is important for predicting how various parameters will impact the system.

Reactions that are diffusion-controlled generally exhibit low activation energies, typically ranging from 4 to 15 kJ/mol (Zhu et al, 2012; Havlík, 2008). These processes are governed by the movement of reactants through a medium to the reaction site. Consequently, the rate of diffusion-controlled reactions is less sensitive to temperature changes because the activation energy is relatively low. The diffusion coefficient  $D$ , as described by the Stokes-Einstein equation, increases linearly with temperature. However, since the rate constant  $k$  of chemical reactions increases exponentially with temperature, diffusion-controlled reactions are less influenced by temperature variations compared to chemical kinetics (Levenspiel, 1998; Habashi, 1986).

In contrast, chemically controlled reactions have high activation energies, usually exceeding 40 kJ/mol (Zhu et al., 2012; Havlík, 2008). In these reactions, the rate-determining step is the intrinsic chemical reaction at the molecular level. The reaction rate is highly sensitive to temperature changes, as described by the Arrhenius equation, because the activation energy influences the rate constant  $k$ , which changes exponentially with temperature. Additionally, the reaction order, which represents the dependence on reactant concentrations, plays a significant role in determining the overall rate (Levenspiel, 1998; Habashi, 1986).

Reactions that are governed by a mixed mechanism exhibit activation energies in the range of 20 to 35 kJ/mol (Havlík, 2008). These reactions are influenced by both diffusion and chemical kinetics, reflecting a combination of the characteristics of the above two types. Understanding the activation energy helps in distinguishing between these mechanisms and in optimizing reaction conditions for better performance (Levenspiel, 1998; Habashi, 1986).

#### 11.2 Results for the different experiments

This study involved several kinetic analyses focused on understanding the behaviour of PGMs under different experimental conditions. The initial concentration of PGMs was kept constant, so its influence on the system was not examined. However, the effect of temperature can be studied. For each temperature, four samples were collected during the experiment. Given the small quantities involved, there is a possibility of experimental errors, underscoring the need for more samples to capture a clearer trend in the kinetic data. In this study, the results provide a preliminary analysis of the reaction kinetics to determine the controlling process, but with only four data points per graph, the trends are not definitive.

The experiments were conducted at four different temperatures: 25°C, 45°C, 65°C, and 85°C. For each temperature, a rate constant was determined and subsequently used to create an Arrhenius plot ( $\ln(k)$  versus  $1/T$ ) to calculate the activation energy of the reaction. The order of the reaction, which is directly related to the choice of the rate constant, was selected based on the best fit to the data, with the coefficient of determination ( $R^2$ ) guiding the decision when the best fit was not immediately obvious. In these models,  $R^2$  values ranged from 0.75 to 0.99, which is generally acceptable.

The coefficient of determination,  $R^2$ , is a key metric in statistical modelling and data analysis, particularly in reaction kinetics. It measures the goodness-of-fit of a model to the experimental data, indicating how well a proposed kinetic model, such as zero-order, first-order, or second-order, represents the observed reaction rates or concentration changes over time.  $R^2$  is calculated as the

ratio of variance explained by the model to the total variance in the data, with values ranging from 0 to 1. A higher  $R^2$  indicates a better fit, meaning the model more accurately describes the relationship between variables. Therefore,  $R^2$  is essential for validating kinetic models and ensuring accurate predictions of reaction rates.

A kinetic analysis was conducted using the Monolithos Catalyst and Recycling Ltd. solution, with magnetic stirring at 500 rpm, and an excess of copper powder at temperatures of 25°C, 45°C, 65°C, and 85°C. The cementation times were 30 minutes, 1 hour, 2 hours, and 3 hours. Platinum was the only PGM analysed, as it was the only one present in the solution.

Two additional kinetic studies were conducted in the laboratory at Liège using the GEMME leachate to assess the impact of ultrasound on the system. The first study involved "silent" experiments with excess copper powder and an overhead stirrer set to 200 rpm. The second study involved experiments with ultrasound at a frequency of 20 kHz and a power of 10W, with excess copper powder and an overhead stirrer set to 400 rpm. The difference in agitation affects the system, but the impact of ultrasound on the system is more pronounced. Comparing the activation energies across these experiments provides a comprehensive understanding of the mechanisms controlling these reactions and highlights the extent to which ultrasound reduces activation energy. The study was conducted on three metals: platinum, palladium, and rhodium, with samples taken at 5 minutes, 30 minutes, 1 hour, and 2 hours.

	Pt-DOC without sonication	GEMME solution without sonication	GEMME solution with sonication
Palladium	-	238 kJ/mol	22 kJ/mol
Platinum	89 kJ/mol	303 kJ/mol	68 kJ/mol
Rhodium	-	305 kJ/mol	56 kJ/mol

*Table 1: Table presenting the activation energy values for the cementation reactions of Palladium, Platinum, and Rhodium across different initial solutions and setups: Pt-DOC solution, GEMME solution without sonication, and GEMME solution with sonication (20kHz - 10W). These values highlight the impact of sonication and solution type on the energy barriers for the cementation of these metals.*

The exact values of activation energies could not be independently verified, yet the kinetic models in the absence of ultrasound appear more intricate than the three reaction orders discussed in this section, potentially accounting for the observed higher activation energy values. Nevertheless, these findings distinctly highlight the differing behaviour of the system with and without ultrasound application. To enhance the robustness of this analysis, further experiments should be conducted to increase the dataset, which would enable the fitting of more sophisticated models to the experimental data.

Based on Havlík's (2008) activation energy thresholds for determining whether a reaction is controlled by chemistry, diffusion, or a combination of both, the cementation process without sonication is primarily controlled by chemical reactions. When sonication is applied, the cementation of palladium and rhodium continues to be controlled by chemistry, while the cementation of platinum exhibits characteristics of a mixed mechanism involving both chemical and diffusion-controlled processes. The application of ultrasound significantly reduces the activation energy, thereby enhancing the reaction rate. This reduction in activation energy due to sonication effectively accelerates the cementation process, as evidenced by the kinetic studies.



## 12 Conclusion

The objective of this study was to investigate the cementation of platinum group metals onto copper using different real-life solutions from leachates of old catalytic converters. Three distinct solutions were examined: a synthetic solution to assess the feasibility of the reaction, and two real-life solutions, referred to as the Pt-DOC and GEMME solutions.

The synthetic solution was prepared in the GEMME laboratory at the University of Liège by dissolving  $\text{PtCl}_4$  in a 37% HCl solution, resulting in a pH of 1.5 and a redox potential of 800 mV vs SHE. The platinum concentration in this solution was 175 ppm. This solution served as a controlled environment to evaluate the basic cementation reaction of platinum onto copper. The second solution, the Pt-DOC solution, is a leachate derived from Diesel Oxidation Catalytic converters (DOC) and was produced at Monolithos Catalyst & Recycling Ltd. in Athens. The experiments on this solution were conducted in their laboratory during my internship. This solution is highly concentrated in platinum, ranging from 400 ppm to 1300 ppm, depending on the container used for storage and the aging of the solution, which led to fluctuations in concentration inherent to the experimental conditions. The Pt-DOC solution is highly acidic, with a negative pH and an initial redox potential of 750 mV vs SHE.

The third solution was the GEMME solution which is produced in the laboratory of the university of Liège with catalytic converters containing the three PGMs: palladium, platinum, and rhodium. The concentration of the solution is 410 ppm of Pd, 220 ppm of Pt and 60 ppm of Rh and its pH reaches 1.5 while its potential redox reached 750 mV vs SHE. In the two real-life solutions, reactants of the leaching process are possibly in excess so  $\text{H}_2\text{O}_2$  and sodium are present in the solutions. The GEMME solution also contains iron (4000 ppm) and aluminium (1000 ppm). The third solution, the GEMME solution, was produced in the laboratory at the University of Liège from catalytic converters containing palladium, platinum, and rhodium. The concentrations of these metals were 410 ppm of Pd, 220 ppm of Pt, and 60 ppm of Rh. The pH of this solution was 1.5, with a redox potential of 750 mV vs SHE. Additionally, the GEMME solution contained iron (4000 ppm) and aluminium (1000 ppm). Both solutions contain residual leaching agents such as  $\text{H}_2\text{O}_2$  and sodium.

This study aimed to optimize the cementation of PGMs onto copper from these various solutions by evaluating key parameters including temperature, agitation, the stoichiometric amount of copper required (expressed as the Cu/PGM molar ratio), and the impact of ultrasound on the system. Experiments on the synthetic and GEMME solutions were conducted using the same experimental setup, while those on the Pt-DOC solution were performed using a different setup.

The initial experiments on the synthetic solution focused on determining the feasibility of platinum cementation onto copper in a simplified system. Following analysis of the results, it was found that complete cementation occurred at 65°C, 200 rpm, and a 16 Cu/PGM molar ratio. These findings provided a basis for subsequent studies on the real-life solutions.

The first real-life solution was studied in Athens, where various parameters, including temperature, cementation time, agitation, and copper addition, were optimized. The optimal conditions identified were 85°C, 500 rpm using a magnetic stirrer achieving minimal agitation of the solid, a Cu/PGM molar ratio of 16, and a 2-hour cementation time. While the results generally aligned with trends reported in the literature, the effect of agitation was unexpected. Typically, increased agitation leads to higher removal percentages, but in this highly acidic solution, agitation enhanced side reactions rather than cementation, leading to greater consumption of the sacrificial copper. Although agitation was necessary to initiate cementation, the best results were obtained when the solid was barely agitated. Additionally, the presence of sodium in the solution, particularly when evaporation was

significant, led to the formation of white precipitates that redissolved during washing. This precipitate, likely sodium chloride, posed challenges for filtration, indicating that evaporation should be minimized to avoid sodium chloride precipitation.

Following these experiments, the GEMME solution was studied to understand the behaviour of palladium, platinum, and rhodium in a single solution. The same parameters were evaluated, with cementation time capped at 2 hours, using a new setup that offered improved control over agitation (via an overhead stirrer), temperature (using a thermostatic bath), minimized evaporation (in a closed vessel), and enabled the transmission of ultrasound to the solution. Without ultrasound, the best removal percentages were achieved at high temperature (85°C), high agitation speed (400 rpm), and a high Cu/PGM molar ratio (13 times). However, at these high temperatures with this pH and  $E_h$  conditions, iron hydrolysis occurred, leading to precipitation. Although iron precipitation is not considered an impurity according to Monolithos Catalyst & Recycling Ltd., and may reduce copper consumption, it complicates filtration due to the formation of fine solids that impede the process. A balance must be struck to address this issue, and in this study, a temperature of 65°C is recommended to facilitate filtration, despite potentially increasing copper consumption.

Subsequently, the impact of ultrasound on the GEMME solution was explored. The first step was to optimize the ultrasound conditions, determining that a frequency of 20 kHz with a power of 10W was most effective, although 4W also produced comparable results. The other parameters were then examined, revealing consistent trends: higher temperatures (with attention to iron hydrolysis), increased agitation, and higher Cu/PGM molar ratios yielded better results. The impact of ultrasound was significant, often doubling the removal rates and accelerating the reaction kinetics. For instance, results typically achieved after a 2-hour experiment were obtained within the first hour when ultrasound was applied. The recovery of rhodium and platinum also improved significantly, reaching high removal rates compared to previous experiments. Under optimal conditions, palladium removal was complete with ultrasound and reached 90% without it. Platinum and rhodium removal reached 75% and 85%, respectively, with ultrasound, compared to only 50% without it.

The influence of ultrasound on the cementation reaction was further demonstrated in the kinetic study, which showed a clear decrease in activation energy with the application of ultrasound, indicating that PGM removal was easier under these conditions. The study also revealed that, without ultrasound, the cementation reaction was primarily controlled by chemical processes. However, with ultrasound, some cementation reactions were governed by a combination of diffusion and chemical processes. Although further refinement of the study is needed for precise results, these findings are consistent with the experimental trends observed.

During the experiments, a general trend was observed: the kinetics of palladium cementation was faster, leading to higher removal percentages compared to platinum and rhodium, which exhibited similar behaviours. Three hypotheses might explain this phenomenon. First, the initial concentration of palladium was twice that of platinum and six times that of rhodium, making the likelihood of palladium ions encountering copper higher, thus enhancing palladium removal rates. Second, palladium has fewer oxidation states compared to platinum and rhodium, which makes its reduction to a metallic state easier, whereas platinum and rhodium may undergo transformations into other forms before achieving their metallic state, complicating their cementation. Third, the aging of the solution could have significantly altered the PGMs' oxidation states, particularly for platinum and rhodium, leading to the formation of new, more difficult-to-cement molecules or ions.

For future studies, several experiments could be valuable. First, it is essential to further investigate the relationship between the Cu/PGM molar ratio and cementation efficiency. Experiments with a

higher amount of copper should be conducted to determine whether the limiting factor is the availability of the copper surface or the probability of encounters between the PGMs and copper. To test this hypothesis, a new setup could be designed where a larger volume of solution circulates in a closed circuit with the same Cu/PGM molar ratio. This increased volume would mean more copper overall, but the portion of the solution interacting with the solid copper would remain constant. This experiment could provide interesting insights into whether surface availability or molecular interactions are the limiting factors in Cu/PGM cementation in this system.

Additionally, a SEM (Scanning Electron Microscopy) analysis of the cement could be conducted to obtain a detailed understanding of particle size and morphology, as well as to identify any potential passivation layers on the sacrificial copper that might hinder the cementation reaction. To assess whether any copper remains available for further cementation, the existing cement could be reused as the sacrificial metal in subsequent experiments. Moreover, a Synthetic Gas Bench (SGB) analysis could be performed in Athens to evaluate the cement's properties as a catalyst after undergoing the impregnation process.

It would also be prudent to conduct triplicate experiments to ensure the repeatability of the results. Based on these outcomes, a more detailed kinetic study using complex models could be undertaken to gain a deeper understanding of the cementation reactions in the system. Additionally, the use of pulsed, sweeping, or bi-modal ultrasound signals, which have been shown to enhance active cavitation more effectively than continuous wave output, could be explored. Continuous wave ultrasound tends to lose efficiency due to limited spatial distribution, coalescence-induced loss of applied pressure amplitude, and bubble growth beyond the active cavitation region (Wood et al., 2017). Modifying the ultrasound signal type could potentially lead to higher removal percentages.

## 13 References

- Aâtach, M., Simão, M. A., & Gaydardzhiev, S. (2024). Effects of ultrasound on the electrochemical cementation of copper onto iron. *Minerals Engineering*, 213, 108750. <https://doi.org/10.1016/j.mineng.2024.108750>
- Aktas, S. (2011). Rhodium recovery from rhodium-containing waste rinsing water via cementation using zinc powder. *Hydrometallurgy* 106, 71–75. <https://doi.org/10.1016/j.hydromet.2010.12.005>
- Aktas, S. (2012). Cementation of rhodium from waste chloride solutions using copper powder. *International Journal of Mineral Processing*, 114–117, 100–105. <https://doi.org/10.1016/j.minpro.2012.07.006>
- Aktas, S., Morcali, M. H., & Yucel, O. (2010). Silver Recovery from Waste Radiographic Films by Cementation and Reduction. *Canadian Metallurgical Quarterly*, 49(2), 147–153. <https://doi.org/10.1179/cmqr.2010.49.2.147>
- Aleman, C., Aurousseau, M., Lapique, F., & Ozil, P. (2002). Cementation and corrosion at a RDE: changes in flow and transfer phenomena induced by surface roughness. *Journal of Applied Electrochemistry*, 32(11), 1269–1278. <https://doi.org/10.1023/a:1021642327507>
- Capote, F. P., & De Castro, M. L. (2007). Analytical applications of ultrasound (Vol. 26). *Elsevier Science*.
- Casado, J. (2018). Revisiting the mechanism of cementation: The role of hydrogen species in acidic aqueous media. *Minerals & Metallurgical Processing*, 35(2), 55–60. <https://doi.org/10.19150/mmp.8286>
- Chidunchi, I., Kulikov, M., Safarov, R., & Kopishev, E. (2024). Extraction of platinum group metals from catalytic converters. *Heliyon*, 10(3), e25283. <https://doi.org/10.1016/j.heliyon.2024.e25283>
- Choi, J., & Son, Y. (2022). Quantification of sonochemical and sonophysical effects in a 20 kHz probe-type sonoreactor: Enhancing sonophysical effects in heterogeneous systems with milli-sized particles. *Ultrasonics Sonochemistry*, 82, 105888. <https://doi.org/10.1016/j.ultsonch.2021.105888>
- Cruells, M., & Roca, A. (2022). Jarosites: Formation, Structure, Reactivity and Environmental. *Metals*, 12(5), 802. <https://doi.org/10.3390/met12050802>
- Dey, S., & Mehta, N. (2020). Automobile pollution control using catalysis. *Resources, Environment and Sustainability*, 2, 100006. <https://doi.org/10.1016/j.resenv.2020.100006>
- Dong, Z., Delacour, C., Carogher, K. M., Udepurkar, A. P., & Kuhn, S. (2020). Continuous ultrasonic reactors: design, mechanism and application. *Materials*, 13(2), 344. <https://doi.org/10.3390/ma13020344>
- Dong, H., Zhao, J., Chen, J., Wu, Y., & Li, B. (2015). Recovery of platinum group metals from spent catalysts: A review. *International Journal of Mineral Processing*, 145, 108–113. <https://doi.org/10.1016/j.minpro.2015.06.009>

- Dragulovic, S., Dimitrijevic, M., Kostov, A., & Jakovljevic, S. (2008). Recovery of platinum group metals from spent automotive catalyst. *Trends in the Development of Machinery and Associated Technology, Istanbul*.
- Environment Agency. (2023). Air pollution in Europe: 2023 reporting status under the National Emission reduction Commitments Directive. <https://doi.org/10.2800/149724>
- European Commission. (2023). Study on the Critical Raw Materials for the EU. <https://doi.org/10.2873/725585>
- Farcas, A., & Aubert, P. (2016). Encyclopedia of Physical Organic Chemistry, 5 volume set. In *John Wiley & Sons, Inc. eBooks*. <https://doi.org/10.1002/9781118468586>
- Farrauto, R. J., & Heck, R. M. (1999). Catalytic converters: state of the art and perspectives. *Catalysis Today*, 51(3–4), 351–360. [https://doi.org/10.1016/s0920-5861\(99\)00024-3](https://doi.org/10.1016/s0920-5861(99)00024-3)
- Fioravante, I., Nunes, R., Acciari, H., & Codaro, E. (2019). Films formed on carbon Steel in Sweet Environments - a review. *Journal of the Brazilian Chemical Society*. <https://doi.org/10.21577/0103-5053.20190055>
- Fragassa, C., & Ippoliti, M. (2016). FAILURE MODE EFFECTS AND CRITICALITY ANALYSIS (FMECA) AS a QUALITY TOOL TO PLAN IMPROVEMENTS IN ULTRASONIC MOULD CLEANING SYSTEMS. *DOAJ (DOAJ: Directory of Open Access Journals)*. <https://doi.org/10.18421/ijqr10.04-14>
- Friedland, G. (2023). Repeatability and reproducibility. In *Springer eBooks (pp. 201–208)*. [https://doi.org/10.1007/978-3-031-39477-5\\_15](https://doi.org/10.1007/978-3-031-39477-5_15)
- Gao, J., Tian, G., Sornioti, A., Karci, A. E., & Di Palo, R. (2019). Review of thermal management of catalytic converters to decrease engine emissions during cold start and warm up. *Applied Thermal Engineering*, 147, 177–187. <https://doi.org/10.1016/j.applthermaleng.2018.10.037>
- Ghodrat, M., Sharafi, P., & Samali, B. (2018). Recovery of platinum group metals out of automotive Catalytic Converters Scrap: A review on Australian trends and challenges. *The Minerals, Metals & Materials Series*, 149–161. [https://doi.org/10.1007/978-3-319-72131-6\\_13](https://doi.org/10.1007/978-3-319-72131-6_13)
- Gould, J. P. (1982). The kinetics of hexavalent chromium reduction by metallic iron. *Water Research*, 16(6), 871–877.
- Gould, J. P., Masingale, M. Y., & Miller, M. (1984). Recovery of silver and mercury from COD samples by iron cementation. *Journal (Water Pollution Control Federation)*, 280–286.
- Grilli, M. L., Slobozeanu, A. E., Larosa, C., Paneva, D., Yakoumis, I., & Cherkezova-Zheleva, Z. (2023). Platinum Group Metals: Green Recovery from Spent Auto-Catalysts and Reuse in New Catalysts—A Review. *Crystals*, 13(4), 550. <https://doi.org/10.3390/cryst13040550>
- Habashi, F. (1986). Principles of Extractive Metallurgy (1st ed.). *Routledge*. <https://doi.org/10.1201/9780203742112>
- Hamada, M., & De Anna, P. (2021). A method to measure the diffusion coefficient in liquids. *Transport in Porous Media*, 146(1–2), 463–474. <https://doi.org/10.1007/s11242-021-01704-0>
- Havlík, T. (2008). Kinetics of heterogeneous reactions of leaching processes. In *Elsevier eBooks (pp. 184–241)*. <https://doi.org/10.1533/9781845694616.184>

- Hosseinzadeh, M., & Petersen, J. (2024). Recovery of Pt, Pd, and Rh from spent automotive catalysts through combined chloride leaching and ion exchange: A review. *Hydrometallurgy*, 228, 106360. <https://doi.org/10.1016/j.hydromet.2024.106360>
- IPA - International Platinum Group Metals Association. (n.d.). <https://ipa-news.com/index/about-us/>
- Izatt, S. R., Izatt, R. M., Bruening, R. L., Krakowiak, K. E., & Navarro, L. (2023). Platinum Group Metals: Highly selective separation by MRT (molecular recognition technology) -- Review of individual separations of palladium, platinum, rhodium, iridium and ruthenium from industrial feedstocks and comparison with classical PGM separation processes. *The IPMI Journal - a Publication of the International Precious Metals Educational and Scientific Foundation*, 4, 78–115. <https://www.researchgate.net/publication/380375723>
- Izatt, R. M. (2007). Charles J. Pedersen: Innovator in macrocyclic chemistry and co-recipient of the 1987 Nobel Prize in chemistry. *Chemical Society Reviews*, 36(2), 143–147. <https://doi.org/10.1039/b613448n>
- Khudenko, B. M. (1984). Mechanism and kinetics of cementation processes. *Water Science and Technology*, 17, 719–731. <https://doi.org/10.2166/wst.1985.0174>
- Kim, M., Kim, B., Kim, E., Kim, S., Ryu, J., & Lee, J. (2011). Recovery of Platinum Group Metals from the Leach Solution of Spent Automotive Catalysts by Cementation. *Journal of the Korean Institute of Resources Recycling*, 20(4), 36–45. <https://doi.org/10.7844/kirr.2011.20.4.036>
- Kinas, S., Jermakowicz-Bartkowiak, D., Pohl, P., Dzimitrowicz, A., & Cyganowski, P. (2024). On the path of recovering platinum-group metals and rhenium: A review on the recent advances in secondary-source and waste materials processing. *Hydrometallurgy*, 223, 106222. <https://doi.org/10.1016/j.hydromet.2023.106222>
- Kritsanaviparkporn, E., Baena-Moreno, F. M., & Reina, T. R. (2021). Catalytic Converters for Vehicle Exhaust: Fundamental aspects and technology Overview for newcomers to the field. *Chemistry*, 3(2), 630–646. <https://doi.org/10.3390/chemistry3020044>
- Konsowa, A. (2010). Intensification of the rate of heavy metal removal from wastewater by cementation in a jet reactor. *Desalination*, 254(1–3), 29–34. <https://doi.org/10.1016/j.desal.2009.12.0188>
- Leighton, T. (2012). The acoustic bubble. *Academic press*.
- Levenspiel, O. (1998). Chemical Reaction Engineering. *John Wiley & Sons*.
- Liu, C., Sun, S., Zhu, X., & Tu, G. (2020). Metals smelting-collection method for recycling of platinum group metals from waste catalysts: A mini review. *Waste Management & Research*, 39(1), 43–52. <https://doi.org/10.1177/0734242x20969795>
- Luna-Sánchez, R. M., Gonzalez, I., & Lapidus, G. T. (2003). Limitations for the Use of Evans' Diagrams to Describe Hydrometallurgical Redox Phenomena. *Electrometallurgy and Environmental Hydrometallurgy, Volume 2*, 1141-1150. <https://doi.org/10.13140/2.1.5106.3048>
- Makua, L., Langa, K., Saguru, C., & Ndlovu, S. (2019). PGM recovery from a pregnant leach solution using solvent extraction and cloud point extraction: a preliminary comparison. *Journal of the Southern African Institute of Mining and Metallurgy*, 119(5). <https://doi.org/10.17159/2411-9717/17/484/2019>

- Margulis, I. M., & Margulis, M. A. (2005). Measurement of acoustic power in studying cavitation processes. *Acoustical Physics*, 51(6), 695–704. <https://doi.org/10.1134/1.2130901>
- McCafferty, E. (2009). Thermodynamics of Corrosion: Pourbaix diagrams. In *Springer eBooks* (pp. 95–117). [https://doi.org/10.1007/978-1-4419-0455-3\\_6](https://doi.org/10.1007/978-1-4419-0455-3_6)
- Moreno, E., Acevedo, P., Fuentes, M., Sotomayor, A., Borroto, L., Villafuerte, M., & Leija, L. (2005). Design and Construction of a Bolt-Clamped Langevin Transducer. <https://doi.org/10.1109/iceee.2005.1529652>
- Mortada, W. I. (2020). Recent developments and applications of cloud point extraction: A critical review. *Microchemical Journal*, 157, 105055. <https://doi.org/10.1016/j.microc.2020.105055>
- Nguyen, T. H., Kumar, B. N., & Lee, M. S. (2016). Selective recovery of Fe(III), Pd(II), Pt(IV), Rh(III) and Ce(III) from simulated leach liquors of spent automobile catalyst by solvent extraction and cementation. *Korean Journal of Chemical Engineering*, 33(9), 2684–2690. <https://doi.org/10.1007/s11814-016-0123-5>
- Nguyen, T. N. H., & Lee, M. S. (2023). Recovery of Au and Pd from the etching solution of printed circuit boards by cementation, solvent extraction, reduction, and precipitation. *Journal of Industrial and Engineering Chemistry/Journal of Industrial and Engineering Chemistry - Korean Society of Industrial and Engineering Chemistry*, 126, 214–223. <https://doi.org/10.1016/j.jiec.2023.06.011>
- Panda, R., Jha, M. K., & Pathak, D. D. (2018). Commercial processes for the extraction of platinum Group metals (PGMs). In *The minerals, metals & materials series* (pp. 119–130). [https://doi.org/10.1007/978-3-319-72350-1\\_11](https://doi.org/10.1007/978-3-319-72350-1_11)
- Patel, K. D., Subedar, D., & Patel, F. (2022). Design and development of automotive catalytic converter using non-nobel catalyst for the reduction of exhaust emission: A review. *Materials Today: Proceedings*, 57, 2465–2472. <https://doi.org/10.1016/j.matpr.2022.03.350>
- Pflieger, R., Nikitenko, S. I., Cairos, C., & Mettin, R. (2019). Characterization of cavitation bubbles and sonoluminescence. In *Springer briefs in molecular science*. <https://doi.org/10.1007/978-3-030-11717-7>
- Pocurull, E., Fontanals, N., Calull, M., & Aguilar, C. (2020). Environmental applications. In *Elsevier eBooks*, 591–641. <https://doi.org/10.1016/b978-0-12-816911-7.00020-7>
- Power, G., & Ritchie, I. (1976). A contribution to the theory of cementation (metal displacement) reactions. *Australian Journal of Chemistry*, 29(4), 699. <https://doi.org/10.1071/ch9760699>
- Reis, M., & Carvalho, J. (1994). Recovery of heavy metals by a combination of two processes: Cementation and liquid membrane permeation. *Minerals Engineering*, 7(10), 1301–1311. [https://doi.org/10.1016/0892-6875\(94\)90119-8](https://doi.org/10.1016/0892-6875(94)90119-8)
- Rodriguez-Clemente, R., & Hidalgo-Lopez, A. (1985). Physical conditions in alunite precipitation as a secondary mineral. In *Springer eBooks* (pp. 121–141). [https://doi.org/10.1007/978-94-009-5333-8\\_8](https://doi.org/10.1007/978-94-009-5333-8_8)
- Rumpold, R., & Antrekowitsch, J. (2012). Recycling of platinum group metals from automotive catalysts by an acidic leaching process. *The Southern African Institute of mining and metallurgy platinum*, 2012, 695–714.



- Safarzadeh, M. S., Moradkhani, D., & Ilkhchi, M. O. (2007). Determination of the optimum conditions for the cementation of cadmium with zinc powder in sulfate medium. *Chemical Engineering and Processing*, 46(12), 1332–1340. <https://doi.org/10.1016/j.cep.2006.10.014>
- Saguru, C., Ndlovu, S., & Moropeng, D. (2018). A review of recent studies into hydrometallurgical methods for recovering PGMs from used catalytic converters. *Hydrometallurgy*, 182, 44–56. <https://doi.org/10.1016/j.hydromet.2018.10.012>
- Samaddar, P., & Sen, K. (2014). Cloud point extraction: A sustainable method of elemental preconcentration and speciation. *Journal of Industrial and Engineering Chemistry*, 20(4), 1209–1219. <https://doi.org/10.1016/j.jiec.2013.10.033>
- Sharma, S. K., Goyal, P., Maheshwari, S., & Chandra, A. (2015). A technical review of automobile catalytic converter: current status and perspectives. *Strategic Technologies of Complex Environmental Issues-A Sustainable Approach*, 1, 171-179.
- Sharma, S., Goyal, P., & Tyagi, R. (2016). Conversion efficiency of catalytic converter. *International Journal of Ambient Energy*, 37(5), 507–512. <https://doi.org/10.1080/01430750.2015.1020567>
- Sędzimir, J. (2002). Precipitation of metals by metals (cementation)—kinetics, equilibria. *Hydrometallurgy*, 64(3), 161–167. [https://doi.org/10.1016/s0304-386x\(02\)00033-6](https://doi.org/10.1016/s0304-386x(02)00033-6)
- Stefanowicz, T., Osińska, M., & Napieralska-Zagózdza, S. (1997). Copper recovery by the cementation method. *Hydrometallurgy*, 47(1), 69–90. [https://doi.org/10.1016/s0304-386x\(97\)00036-4](https://doi.org/10.1016/s0304-386x(97)00036-4)
- Steinlechner, S., & Antrekowitsch, J. (2015). Potential of a hydrometallurgical recycling process for catalysts to cover the demand for critical metals, like PGMs and cerium. *JOM*, 67(2), 406–411. <https://doi.org/10.1007/s11837-014-1263-x>
- Stole-Hansen, K., Wregget, D. A., Gowanlock, D., & Thwaites, P. E. (1997). Model based analysis and control of a cementation process. *Computers & chemical engineering*, 21, S1099-S1103.
- Sulka, G., & Jaskuła, M. (2002). Study of the kinetics of the cementation of silver ions onto copper in a rotating cylinder system from acidic sulphate solutions. *Hydrometallurgy*, 64(1), 13–33. [https://doi.org/10.1016/s0304-386x\(02\)00002-6](https://doi.org/10.1016/s0304-386x(02)00002-6)
- Suoranta, T., Zugazua, O., Niemelä, M., & Perämäki, P. (2015). Recovery of palladium, platinum, rhodium and ruthenium from catalyst materials using microwave-assisted leaching and cloud point extraction. *Hydrometallurgy*, 154, 56–62. <https://doi.org/10.1016/j.hydromet.2015.03.014>
- Trinh, H. B., Lee, J., Srivastava, R. R., & Kim, S. (2019). Total recycling of all the components from spent auto-catalyst by NaOH roasting-assisted hydrometallurgical route. *Journal of Hazardous Materials*, 379, 120772. <https://doi.org/10.1016/j.jhazmat.2019.120772>
- Trinh, H. B., Lee, J., Suh, Y., & Lee, J. (2020). A review on the recycling processes of spent auto-catalysts: Towards the development of sustainable metallurgy. *Waste Management*, 114, 148–165. <https://doi.org/10.1016/j.wasman.2020.06.030>
- Umicore. (2024). Metals prices / Umicore Precious Metals Management. <https://pmm.umicore.com/en/prices>
- Votsmeier, M., Kreuzer, T., Gieshoff, J., Lepperhoff, G., & Elvers, B. (2019). Automobile Exhaust control. *Ullmann's Encyclopedia of Industrial Chemistry*, 1–19. [https://doi.org/10.1002/14356007.a03\\_189.pub3](https://doi.org/10.1002/14356007.a03_189.pub3)



- Wood, R. J., Lee, J., & Bussemaker, M. J. (2017). A parametric review of sonochemistry: Control and augmentation of sonochemical activity in aqueous solutions. *Ultrasonics Sonochemistry*, 38, 351–370. <https://doi.org/10.1016/j.ultsonch.2017.03.030>
- Yakoumis, I. (2021). PROMETHEUS: a Copper-Based polymetallic catalyst for automotive applications. Part I: Synthesis and Characterization. *Materials*, 14(3), 622. <https://doi.org/10.3390/ma14030622>
- Yakoumis, I., Panou, M., Moschovi, A. M., & Papias, D. (2021). Recovery of platinum group metals from spent automotive catalysts: A review. *Cleaner Engineering and Technology*, 3, 100112. <https://doi.org/10.1016/j.clet.2021.100112>
- Zupanc, A., Install, J., Jereb, M., & Repo, T. (2022). Sustainable and selective modern methods of noble metal recycling. *Angewandte Chemie*, 62(5). <https://doi.org/10.1002/anie.202214453>
- Rooze, J., Rebrov, E. V., Schouten, J. C., & Keurentjes, J. T. (2011). Effect of resonance frequency, power input, and saturation gas type on the oxidation efficiency of an ultrasound horn. *Ultrasonics Sonochemistry*, 18(1), 209–215. <https://doi.org/10.1016/j.ultsonch.2010.05.007>
- Zhu, P., Zhang, X., Li, K., Qian, G., & Zhou, M. (2012). Kinetics of leaching refractory gold ores by ultrasonic-assisted electro-chlorination. *International Journal of Minerals Metallurgy and Materials*, 19(6), 473–477. <https://doi.org/10.1007/s12613-012-0582-6>